

11. SITE 818¹

Shipboard Scientific Party²

HOLE 818A

Date occupied: 8 September 1990
Date departed: 8 September 1990
Time on hole: 4 hr, 56 min
Position: 18°3.767'S, 150°2.533'E
Bottom felt (rig floor; m, drill-pipe measurement): 759.9
Distance between rig floor and sea level (m): 11.26
Water depth (drill-pipe measurement from sea level, m): 748.7
Total depth (rig floor; m): 769.5
Penetration (m): 9.6
Number of cores (including cores with no recovery): 1
Total length of cored section (m): 9.5
Total core recovered (m): 9.6
Core recovery (%): 101.0
Oldest sediment recovered:
Depth (mbsf): 9.6
Nature: foraminifer micrite ooze with bioclasts
Age: Pleistocene

HOLE 818B

Date occupied: 8 September 1990
Date departed: 9 September 1990
Time on hole: 15 hr, 54 min
Position: 18°3.767'S, 150°2.533'E
Bottom felt (rig floor; m, drill-pipe measurement): 756.1
Distance between rig floor and sea level (m): 11.26
Water depth (drill-pipe measurement from sea level, m): 744.8
Total depth (rig floor, m): 1059.0
Penetration (m): 302.9
Number of cores (including cores with no recovery): 32
Total length of cored section (m): 302.9
Total core recovered (m): 314.6
Core recovery (%): 103.9
Oldest sediment recovered:
Depth (mbsf): 302.9
Nature: chalk with bioclasts and foraminifers
Age: late Miocene

Principal results: Site 818 is located on a gently inclined terrace on the upper slope of the Queensland Plateau southwest of the Tregrosse/Lihou/Coringa bank complex. This location was selected to penetrate a uniquely thick pile of upper Neogene sediments that accumulated on the terrace. APC drilling fully

recovered a 303-m-thick sequence of periplatform sediments that range in age from early Pliocene to Pleistocene. Benthic foraminifer assemblages indicate that the depositional environment remained at middle bathyal paleodepths (600–1000 m) throughout this period. The occurrence of platform-derived carbonates throughout the sequence implies that banks were producing and that carbonate has been transported off the Queensland Plateau since the early Pliocene. However, the sequence contains a record of varying flux of bank-derived carbonate to the upper slope that may be associated with either changes in the rate of bank productivity and/or the amount of redeposited sediments that accumulated at the site. Based on sedimentation rates, we identified two periods having significantly modified rates of carbonate accumulation that compared with sedimentation rates for the past 1.5 m.y. (5.7 cm/k.y.): (1) between 1.5 and 2.42 Ma, a decelerated rate of 2.4 cm/k.y. is half as great, and (2) between 2.42 and 2.6 Ma, an accelerated rate of 42 cm/k.y. is more than seven times greater.

One major sedimentary unit was recovered between the seafloor and 293.4 mbsf. A second sedimentary unit was barely penetrated between 293.4 mbsf and the bottom of Hole 818B at 302.9 mbsf. The lithologic units defined are as follows:

1. *Unit I:* depth, 0 to 293.4 mbsf; age, Pleistocene to early Pliocene. Unit I contains white to light gray homogeneous periplatform oozes composed of varying proportions of micrite and nannofossils, with minor amounts of bioclasts, foraminifers, and pteropods. The unit has been divided into four subunits on the basis of compositional changes of pelagic-derived vs. bank-derived carbonates, as defined by nannofossil to micrite ratios that were determined qualitatively from smear-slide descriptions.

Subunit IA: depth, 0 to 65.4 mbsf; age, Pleistocene. Subunit IA consists of periplatform ooze that is characterized by a greater proportion of micritic than nannofossil components and thus is a micrite ooze. The high aragonite content in this interval, with values between 44% and 68%, clearly demonstrates the major contribution of bank-derived carbonate. Near the base, two layers of floatstone with mud clasts and graded foraminifer and lithoclastic packstone, interpreted as calciturbidites, occur in association with slumped sediments.

Subunit IB: depth, 65.4 to 103.4 mbsf; age, late late Pliocene to Pleistocene. The periplatform ooze of Subunit IB contains a visibly greater amount of nannofossils and planktonic foraminifers than the overlying sediments and is predominantly a micrite nannofossil ooze. This indicates that the contribution of pelagic carbonate to the sedimentary deposit during this interval increased relative to the bank-derived carbonate. However, the presence of aragonite in the ooze, as recorded in X-ray diffractograms, implies that the carbonate banks continued to be a source of micrite for transport to the depositional site.

Subunit IC: depth, 103.4 to 198.4 mbsf; age, early late Pliocene. The thick package of sediments comprising Subunit IC contains predominantly micrite ooze. A transition from ooze to chalk occurs between 150 and 180 mbsf that is associated with celestite concretions and burrow fillings.

Subunit ID: depth, 198.4 to 293.4 mbsf; age, early to late Pliocene. Subunit ID contains a mixture of ooze and chalk with a micrite component that gradually decreases with depth. The unit is mainly characterized by the occurrence of gravity-flow deposits, which have been interpreted as calciturbidites, and slumps. Phosphatized benthic and planktonic foraminifers and glauconite grains are scattered throughout the coarser layers.

¹ Davies, P. J., McKenzie, J. A., Palmer-Julson, A., et al., 1991. *Proc. ODP, Init. Repts.*, 133: College Station, TX (Ocean Drilling Program).

² Shipboard Scientific Party is as given in list of participants preceding the contents.

2. *Unit II*: depth, 293.4 to 302.9 mbsf; age, late Miocene. Unit II contains light gray, well-indurated calcareous chalk with bioclasts and foraminifers. The carbonate content of these sediments ranges between 92% and 100%. Throughout Unit II, values show high variability and fluctuate up to 4%, although the mean value remains fairly constant. Between 40 and 80 mbsf, a sharp excursion to decreased values occurs with a minimum centered at 52 mbsf (at about 1.0 Ma). Dilution by noncarbonate material or dissolution might have produced the observed decrease. In the same interval, between 45–50 and 90 mbsf, the sediments are characterized by lower porosity, higher bulk density, and higher velocity than adjacent sediments. Variations in physical properties may be related to the composition of these carbonate components, neritic vs. pelagic. Interestingly, this anomalous interval has considerable overlap with the micrite nannofossil ooze of Subunit IB.

The carbonate mineralogy of the Pleistocene sediments is approximately a 50:50 mixture of calcite and aragonite with detectable amounts of high Mg-calcite only at very shallow depths. The aragonite content can be as high as 68%, but decreases sharply within the upper Pliocene sediments and disappears entirely below about 210 mbsf. Dolomite occurs below 80 mbsf with concentrations less than 3%.

Interstitial water chemistry succinctly reflects the diagenetic reactions occurring within these sediments. With the dissolution of metastable carbonates, aragonite, and high Mg-calcite, concentrations of Sr^{2+} increase steadily, reaching a maximum value at about 70 mbsf. As a consequence, the interstitial water is saturated with respect to celestite (SrSO_4) between 75 and 230 mbsf. Distinctive celestite concretions and burrow fillings were recognized in two cores at about 160 to 170 and 220 mbsf, but microcrystalline celestite may be present elsewhere within the saturated interval. A downward trend toward increasing Ca^{2+} and decreasing Mg^{2+} concentrations relative to that of chloride is apparently controlled by dolomite formation. Concentrations of chloride tend to increase with depth and reach values up to 15% greater than seawater. As at Site 817, interstitial water chemistry indicates the presence of a source of water with elevated salinity at depth below the sampled section.

Total organic carbon contents of the sediments were low, but variable, and ranged from 0.05% to 0.45%. Volatile hydrocarbons having methane concentrations of up to 10 ppm, ethane concentrations of about 1 ppm, and no propane presented no safety problems.

BACKGROUND AND SCIENTIFIC OBJECTIVES

Site 818 is located in a water depth of 748 m on an isolated, gently inclined slope-terrace, 10 km south of the southern edge of the Queensland Plateau, a partially drowned late early to middle Miocene, large (150,000 km²) tropical carbonate platform. The site lies 30 km southwest of Tregrosse Reef, a modern 5100 km² atoll-type platform, which is characterized by a 40- to 60-m-deep lagoon rimmed by a barrier reef at sea level. Tregrosse Reef accounts for one-quarter of the modern Queensland Plateau reef complex near or at sea level today, covers a surface area of about 20,000 km², and represents the protracted remnant of the larger Miocene platform. Site 818 is located on the middle of a slope transect between Sites 814 and 813 on the upper slope and Site 817 on the lower slope, along the southwestern margin of the Queensland Plateau Miocene platform or the modern Tregrosse Reef bank system. Site 818 was expected to have received large volumes of bank-derived material plus pelagic sediments during periods of bank production, as in the early and middle Miocene, and during intervals of highstands of sea level, as in the Pliocene-Pleistocene. On the other hand, more pelagic sedimentary sequences within the slope sediments should correspond to periods during which bank production had substantially decreased or was totally turned off because of either bank drowning or bank exposure in relation to variations in sea level. The Neogene sedimentary sequence in Site 818 thus was expected to include a good record of the evolution through

time of the Queensland Plateau carbonate platform system. Because of the sensitivity in terms of carbonate preservation at the seafloor of the metastable bank-derived aragonite and Mg-calcite carbonates, we expected to recover periplatform oozes in Site 811 that would record variations through time of oceanic carbonate saturation states with respect to aragonite and Mg-calcite in the upper part of the water column that had occurred during the Pliocene-Pleistocene. Because of time constraints, only the upper part of the sedimentary column, and thus only a late Neogene section, was recovered.

Both distribution of site-survey data and the pre-drilling prognosis are shown in Figure 1A, while a seismic section through Site 818 is depicted in Figure 1B.

Our objectives for drilling at Site 818 were as follows:

1. To determine the age and facies of periplatform and fore-reef sequences on the margin of the Miocene, Pliocene-Pleistocene, and modern carbonate bank platform of the Queensland Plateau.
2. To determine the paleoceanographic signal in the periplatform ooze.
3. To establish the relationship between fluctuations in sea level and bank-derived carbonate facies.
4. To determine the diagenetic signal contained within periplatform sediments: in particular, to establish the stability regimes of Mg-calcite and aragonite, the possible occurrence of dolomite, and the chemistry of interstitial waters within the platform margin environment.

OPERATIONS

Transit to Site 818

The sea voyage to Site 818 (proposed Site NEA-9A) began at 0315L (all times given in local time, or L) 8 September 1990 and covered 14 nmi, with an average speed of 9.3 kt. A seismic survey was run over the site that covered 12 nmi in 2.2 hr, at an average speed of 5.5 kt. A Datasonics beacon was dropped at 0550L, 8 September, but we lost the acoustic signal while we were running pipe into the hole with the APC/XCB bottom-hole assembly (BHA). A second beacon, a high-powered Benthos model, was run on taut wire, but this one also gave an erratic signal and was retrieved. We dropped a third beacon, again a high-powered Benthos model, and again received an erratic signal, which led us to suspect that either strong bottom currents were present or that the beacon's power level was too high for the water depth. A fourth beacon, a low-powered Benthos model, was run on taut wire. Although this beacon initially gave an erratic signal, it eventually steadied, and we were finally able to position the ship after more than 4 hr of effort.

Hole 818A

Hole 818A was spudded at 1046L, 8 September at 18°3.767'S, 150°2.533'E. A precision depth recorder (PDR) indicated a water depth of 752.1 m from sea level. We positioned a bit at a water depth of 748.7 m from sea level, where we shot the first core. From Core 133-818A-1H we recovered 9.6 m of sediment, which indicated that we had overshot the mud line at least 0.1 m.

Hole 818B

Hole 818B was spudded at 18°3.767'S, 150°2.533'E, 1112L, 8 September, with the bit positioned at a water depth of 743.7 m from sea level for our first shot. From Core 133-818B-1H we recovered 8.59 m of sediment, which placed the mud line at a water depth of 744.8 m from sea level.

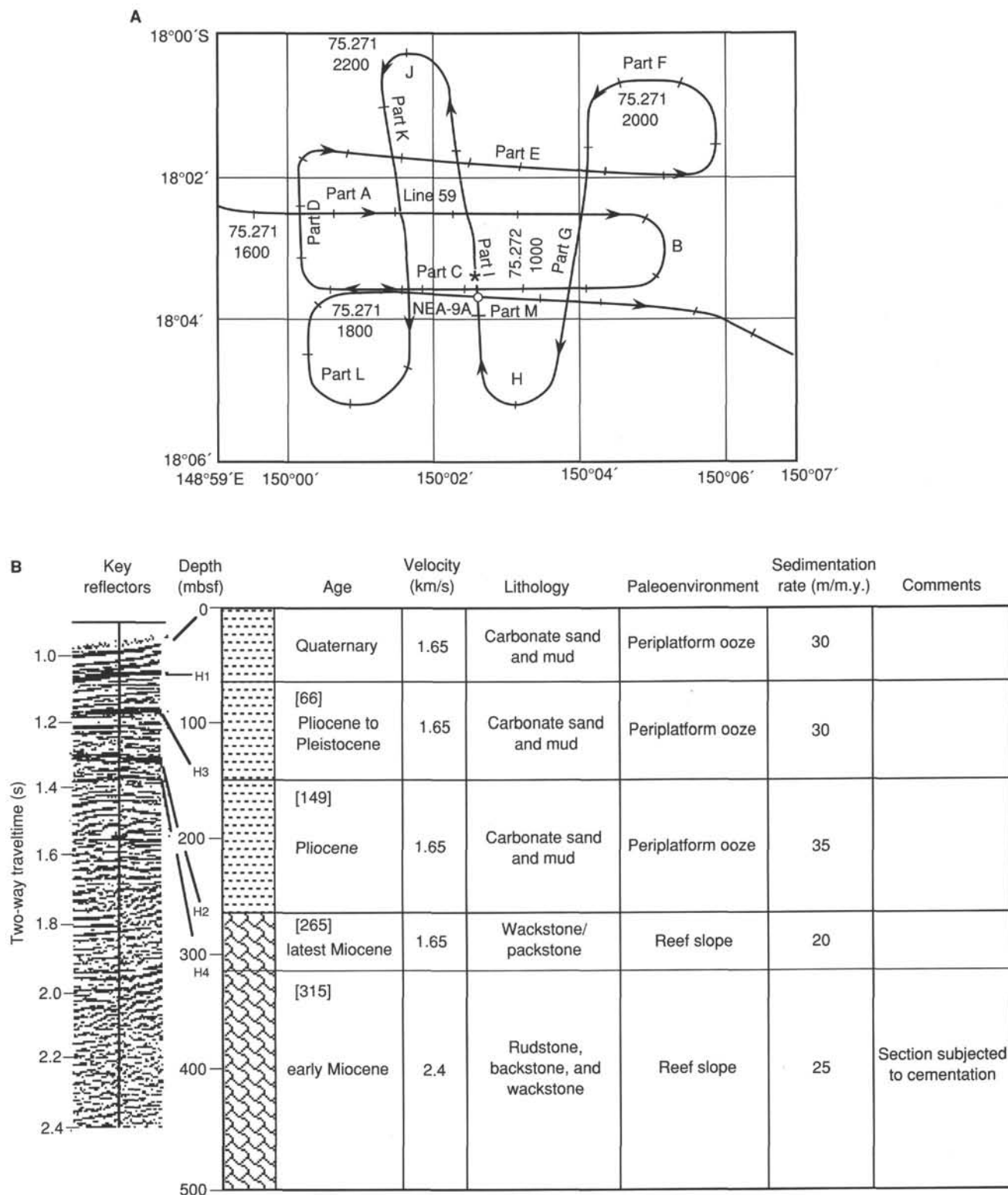


Figure 1. A. Distribution of site-survey data. B. Pre-drilling prognosis for Site 818.

Continuous APC cores (Cores 133-818B-1H through -32H) were taken from 0 to 302.9 mbsf, with 302.9 m cored and 314.6 m recovered (103.8% recovery). The BHA was pulled out of the hole and was back on deck at 0240L, 9 September. The beacons were recovered, and the ship made ready for transit to Site 819.

Table 1 contains the coring summary for Site 818.

SITE GEOPHYSICS

JOIDES Resolution separated from the beacon at Hole 817C at 0110L (JD 250/1510UTC) on 8 September 1990, and began the 2-hr transit to Site 818 (proposed Site NEA-9A) at 0318L (JD 250/1718UTC). A magnetometer was towed imme-

Table 1. Coring summary, Site 818.

Core no.	Date (Sept. 1990)	Time (UTC)	Depth (mbsf)	Length cored (m)	Length recovered (m)	Recovery (%)
<i>Hole 818A</i>						
1H	8	0050	0.1–9.6	9.5	9.60	101.0
Coring totals				9.5	9.60	101.0
<i>Hole 818B</i>						
1H	8	0120	0–8.4	8.4	8.39	99.9
2H	8	0135	8.4–17.9	9.5	9.90	104.0
3H	8	0155	17.9–27.4	9.5	9.49	99.9
4H	8	0220	27.4–36.9	9.5	10.00	105.2
5H	8	0240	36.9–46.4	9.5	9.88	104.0
6H	8	0305	46.4–55.9	9.5	9.92	104.0
7H	8	0330	55.9–65.4	9.5	9.87	104.0
8H	8	0350	65.4–74.9	9.5	9.92	104.0
9H	8	0415	74.9–84.4	9.5	9.97	105.0
10H	8	0435	84.4–93.9	9.5	9.93	104.0
11H	8	0435	93.9–103.4	9.5	9.75	102.0
12H	8	0520	103.4–112.9	9.5	9.45	99.5
13H	8	0545	112.9–122.4	9.5	9.96	105.0
14H	8	0605	122.4–131.9	9.5	9.84	103.0
15H	8	0630	131.9–141.4	9.5	9.56	100.0
16H	8	0650	141.4–150.9	9.5	9.98	105.0
17H	8	0720	150.9–160.4	9.5	9.77	103.0
18H	8	0745	160.4–169.9	9.5	9.85	103.0
19H	8	0805	169.9–179.4	9.5	9.78	103.0
20H	8	0825	179.4–188.9	9.5	9.88	104.0
21H	8	0850	188.9–198.4	9.5	9.98	105.0
22H	8	0915	198.4–207.9	9.5	9.91	104.0
23H	8	0935	207.9–217.4	9.5	9.99	105.0
24H	8	1005	217.4–226.9	9.5	9.92	104.0
25H	8	1025	226.9–236.4	9.5	9.95	105.0
26H	8	1055	236.4–245.9	9.5	9.95	105.0
27H	8	1120	245.9–255.4	9.5	9.85	103.0
28H	8	1145	255.4–264.9	9.5	9.99	105.0
29H	8	1210	264.9–274.4	9.5	9.98	105.0
30H	8	1235	274.4–283.9	9.5	9.94	104.0
31H	8	1255	283.9–293.4	9.5	9.95	105.0
32H	8	1305	293.4–302.9	9.5	10.07	106.0
Coring totals				302.9	314.57	103.9

Note that times are given in Universal Time Coordinated or UTC, which is 10 hr later than local time, L.

diately after our departure, and continuous bathymetric and magnetic data were recorded during the Line 5 transit while heading about 84° along the northern margin of the Townsville Trough. The ship arrived at a position of 18°07.010'S and 150°00.133'E, about 3.3 nmi south of Site 818, at 0448L (JD 250/1848UTC), ready to start the site location survey.

Site 818 lies in approximately 739 m of water on a small terrace on the upper slope of the southern Queensland Plateau adjacent to the Townsville Trough (Figs. 2 and 3) and about 26 km southwest of the edge of the modern Tregrosse Bank. The site is 52 km southwest of Site 812 and 34 km east-northeast of Site 817. It was selected with the aim of determining the composition and origin of slope facies immediately seaward of the Neogene carbonate platform of southern Queensland Plateau, thus permitting us to compare it with mixed carbonate/siliciclastic slope sites adjacent to the Great Barrier Reef (Sites 819 through 821). The area was first recognized as a potential ODP drilling target from a 1972 BMR sparker line (Line 13/079) and a 1973 Gulf Research and Development aquapulse line (Line QP-10; Fig. 3). In 1987, the BMR vessel *Rig Seismic* was used to conduct a site survey at this location (Symonds and Davies, 1988; Feary et al., 1990), and about 67 km of 24-channel, 80-in.³ water-gun seismic, magnetic, and bathymetric data were collected on a grid of north-south and east-west lines (BMR Line 75/59, Figs. 3 and 4). Pre-drilling interpretation of the seismic data was performed using a Landmark RT interactive seismic interpretation system, while

five structure-contour and four TWT-thickness maps were produced (Feary et al., 1990). This mapping showed that the site is located within a broad, buried channel that trends west-northwest toward the adjacent platform margin. Originally, we planned to drill Site 818 to 500 mbsf (Feary et al., 1990); however, owing to time constraints during Leg 133, we decided to focus on the higher-priority, shallower objectives, and the site was drilled to only 303 mbsf.

An important requirement of the Leg 133 site-location surveys was that seismic records obtained with the *JOIDES Resolution* be as close as possible in appearance to those collected during the 1987 site surveys by the *Rig Seismic*, thus reducing ambiguity when defining sites and when comparing the seismic stratigraphy between the two data sets. Accordingly, *JOIDES Resolution* seismic deployment systems were modified (see "Explanatory Notes" chapter, this volume).

The position of Site 818 within the site survey grid was based on two intersecting lines that were surveyed using only a Transit Satellite/dead-reckoning navigation system; coordinates thus were not as accurate as those for sites positioned using the global positioning system (GPS). With this in mind, we designed the site-location survey for this site to confirm the seismic character of the proposed site from *JOIDES Resolution* seismic data collected along a *Rig Seismic* line. Because "pin-point" accuracy was not required for drilling location in this instance, we decided to drop a beacon while collecting

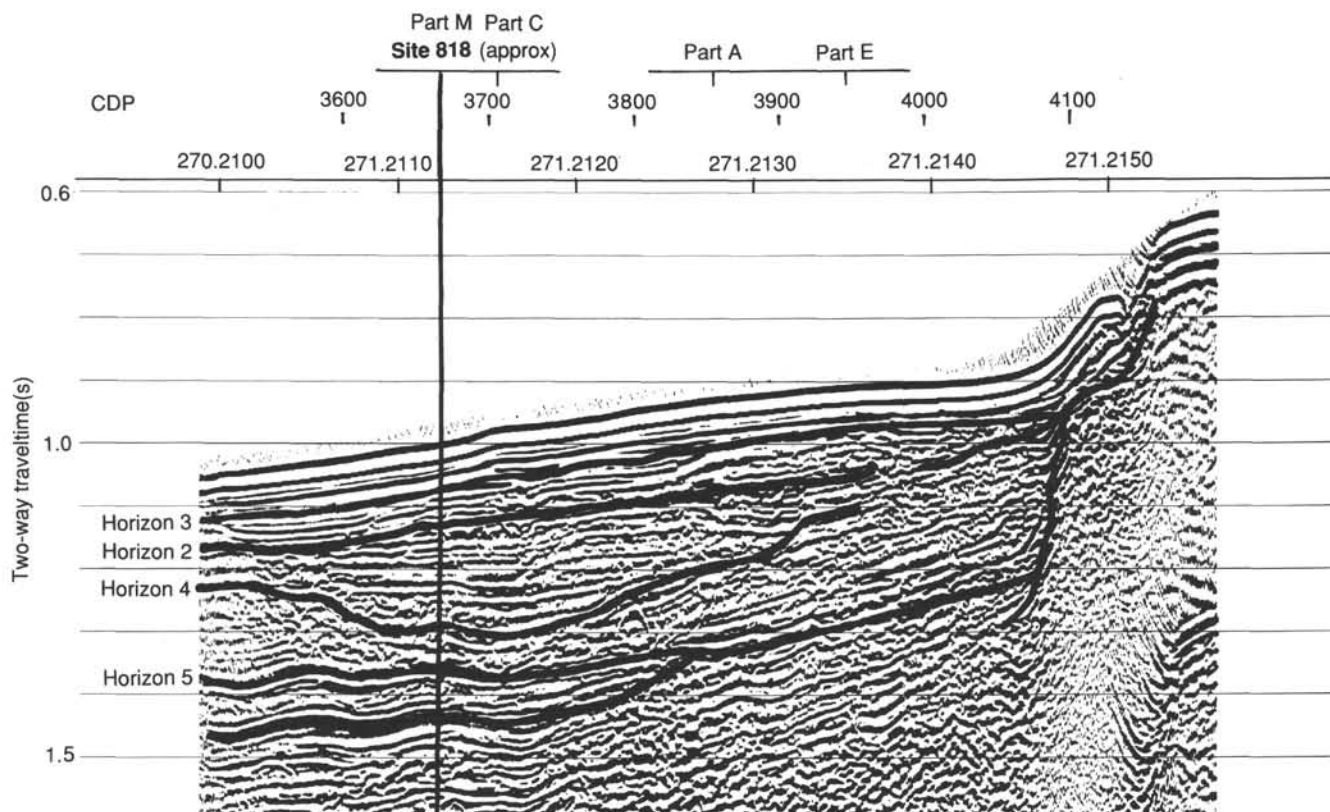


Figure 2. Multichannel SSI 80-in.³ water-gun, high-resolution seismic data, BMR Line 75/059, crossing proposed Site NEA-9A (Site 818).

seismic data by predicting the site location ahead of the displayed seismic record.

Distribution of regional seismic data in the area around the site is shown in Figure 3, and tracks of the original *Rig Seismic* site survey and the *JOIDES Resolution* site location survey are shown in Figure 4. Following a reduction in ship's speed to 5 kt, the *JOIDES Resolution*'s single-channel seismic profiling system was deployed, and seismic recording began at JD 250/1857UTC, 7 September 1990, in choppy seas (Beaufort Scale force 3–4), with 1- to 2-m swells. The *JOIDES Resolution* sailed north across Site 818, and a beacon was dropped at JD 250/1950UTC (Fig. 4). We stopped acquiring seismic data and retrieved our equipment at JD 250/2009UTC, while dynamic positioning of the ship over the beacon began at JD 250/2100UTC. Following the beacon drop, a mound about 10 m high appeared on our echo sounder and seismic profiles (Figs. 5 and 6). This feature had not been seen in the *Rig Seismic* site-survey data, which indicated that our beacon location was slightly different from that of the proposed site, although seismic characteristics at depth were similar in both the *Rig Seismic* and *JOIDES Resolution* data. During DP positioning over the beacon, the ship was offset as far as possible away from the mound, so that it would cause no problems while drilling the shallow part of the hole. The final coordinates of Hole 818A are 18°03.767'S and 150°02.533'E, at a water depth of 748.7 m (drill-pipe measurement from sea level).

About 9 km of seismic and magnetic data was collected during the site location survey; the ship's track was accurately positioned using GPS navigation. Our seismic equipment operated well, and fair quality monitor records were obtained (Fig. 5). Because of the compressed nature of these analog records, related mainly to the minimum available shot interval

of 9 s, we had difficulty discerning the detailed seismic characteristics of the site; however, correlation between seismic profiles of the *Rig Seismic* and *JOIDES Resolution* over the site generally was reasonable (Fig. 5). During both the transit to the site area and the site-location survey, we obtained a good quality 3.5-kHz echo sounder record with up to 40 m of sediment penetration in the vicinity of the site (Fig. 6). This profile illustrates the location of Site 818 adjacent to the carbonate platform and also shows that to the west of the site, the Queensland Plateau slope has been incised by a number of canyons up to 130 m deep.

Basement is not clearly defined in either the *JOIDES Resolution* or the *Rig Seismic* water-gun data across the site; however, it probably lies about 1.0 s two-way traveltime (TWT) below seafloor at the base of a band of strong subhorizontal reflectors that intersect the first water-bottom multiple just north of the site (Fig. 4). Site 818 is underlain by four main seismic units, although we only drilled in the upper three. The shallowest unit is about 0.23 s TWT (190 m) thick and consists of variable amplitude, generally discontinuous reflectors. Pre-drilling interpretation (Feary et al., 1990) suggested that this unit was composed of periplatform carbonate sand and mud, in the form of both channel and mounded facies. It is underlain by a 0.09-s-TWT (75-m)-thick channel-fill unit containing very low-amplitude, irregular reflectors that were interpreted as also representing periplatform sediments. The underlying unit is thin at the site (0.05 s TWT; 52 m), but thickens rapidly to the north and south, forming the walls of the channel. The unit is composed of subparallel, low-amplitude reflectors, which pre-drilling had been interpreted as platform (reef)-slope sediments. The top of the basal unit, which is at least 0.65 s TWT thick, may have just been intersected at the site. This unit consists of interbedded bands of high-amplitude subparallel

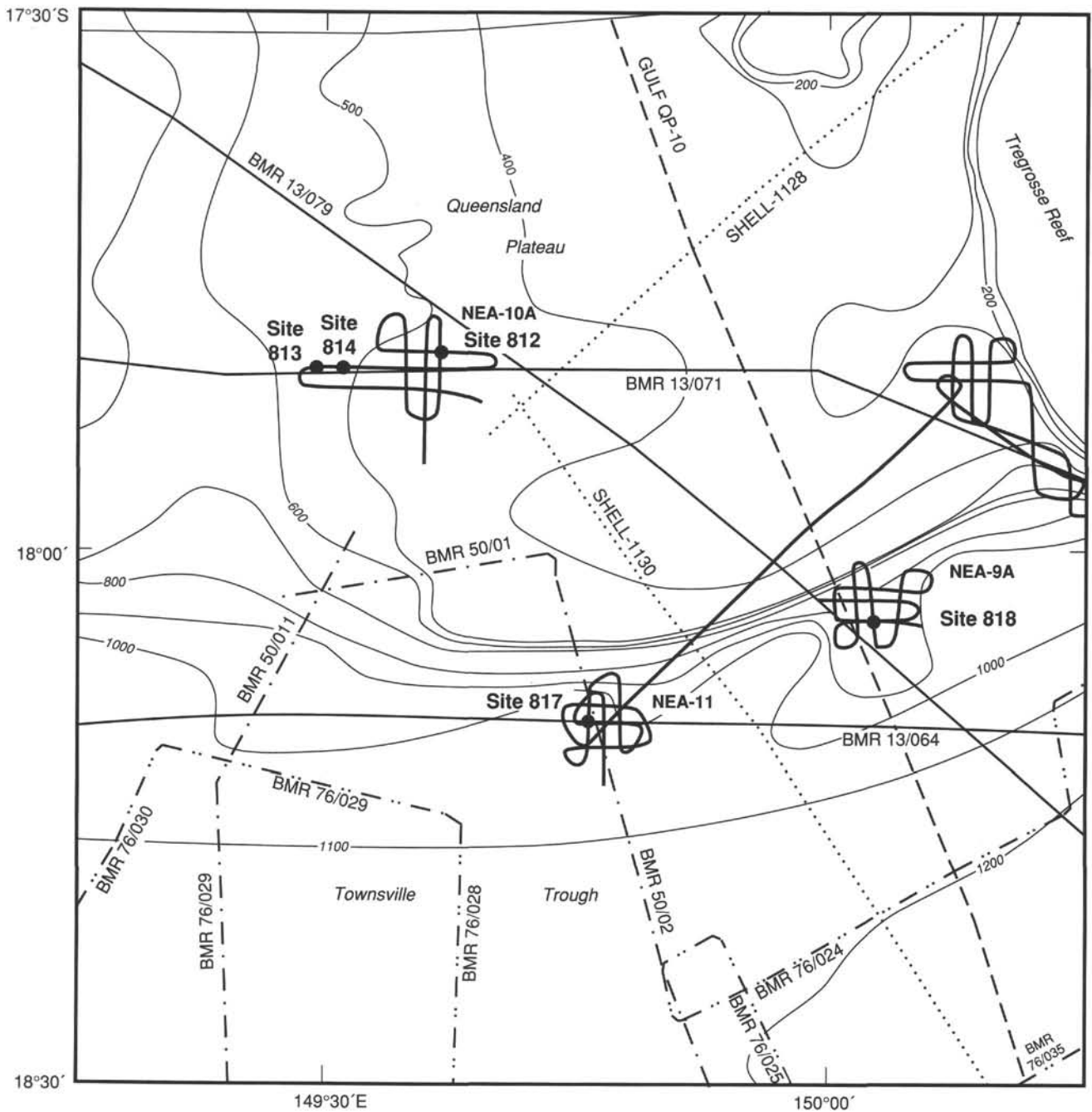


Figure 3. Track chart showing the distribution of regional seismic data in the area around Site 818. Also shows the locations of Sites 812, 813, 814, and 817, and the simplified bathymetry in meters.

and low-amplitude chaotic reflectors. To the north of the site, the unit contains thick zones of chaotic reflectors, which were thought to be platform-derived deposits before drilling. The complete unit was thought to represent platform-slope sediments.

To provide some predictive capability during drilling at Site 818, we estimated the reflection-time (TWT)/depth relationship below the seafloor using stacking-derived interval velocities from the BMR site-survey seismic lines across the site. In Figure 7, this relationship is compared with similarly derived TWT/depth relationships for other off-platform sites on the Queensland Plateau (Sites 811, 813, 814, and 817) and for DSDP Site 209 (Andrews, 1973).

LITHOSTRATIGRAPHY

Lithologic Units

Site 818 is located in 745 m of water on an isolated, gently inclined slope-terrace, 10 km south of the southern edge of Queensland Plateau, a partially drowned, Miocene tropical carbonate platform. The site is 30 km southwest of Tregrosse Reef, a modern 5100-km², atoll-type platform that is characterized by a 40- to 60-m-deep lagoon, which is rimmed by a barrier reef at sea level.

In Hole 818B, a 303-m-thick calcareous sedimentary sequence (having carbonate content values that range between

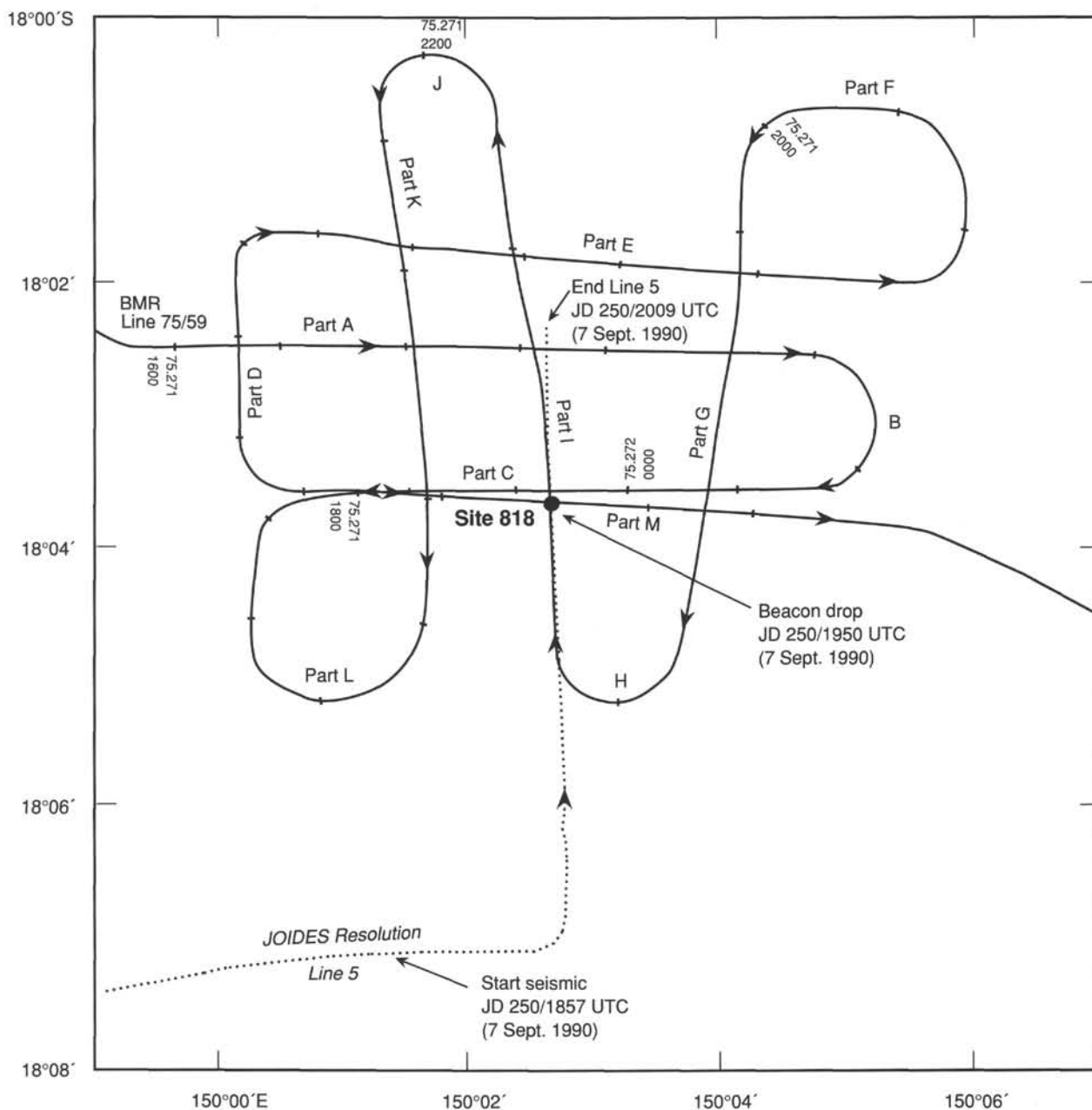


Figure 4. JOIDES Resolution Leg 133 site location tracks (dotted line) and Rig Seismic 1987 site survey tracks (solid line) around Site 818.

94% and 99%, see "Inorganic Geochemistry" section, this chapter; Fig. 8) was cored using the APC. This sequence mostly corresponds to a single 293-m-thick unit (Unit I) that consists of mixed pelagic and bank-derived carbonate sediments. Unit I was divided into four subunits on the basis of the proportions of bank-derived material in the sediments. The calcareous sediments of Subunits IB and ID generally contain more pelagic components than those of Subunits IA and IC and have been interpreted as representing time intervals during which productivity on Tregrosse Bank (and thus off-bank transport) was considerably reduced, either by drowning or by exposure of the shallow bank.

Core 133-818B-32H of Hole 818B terminated in the upper part of a second lithological unit (Unit II) that consists of well-indurated calcareous chalks with bioclasts and forami-

fers that is differentiated from the nannofossil ooze and chalks characteristic of the overlying Subunit ID. Stratigraphic distribution of the units and subunits is summarized in Figure 8; each is discussed in detail next.

Unit I (Cores 133-818B-1H to -31H-CC, 16 cm; depth, 0-293.4 mbsf; age, Pleistocene to early Pliocene)

Unit I consists of essentially homogeneous, almost pure carbonate (bulk carbonate values range between 94% and 98.5%; see "Inorganic Geochemistry" section, this chapter; Fig. 8), white to light gray ooze having nannofossils and micrite as its main components. On the basis of variations in the relative proportions of nannofossils and micrite, a series of oozes was differentiated between two extreme end-members of (1) nannofossil ooze and (2) micrite ooze. Intermediate

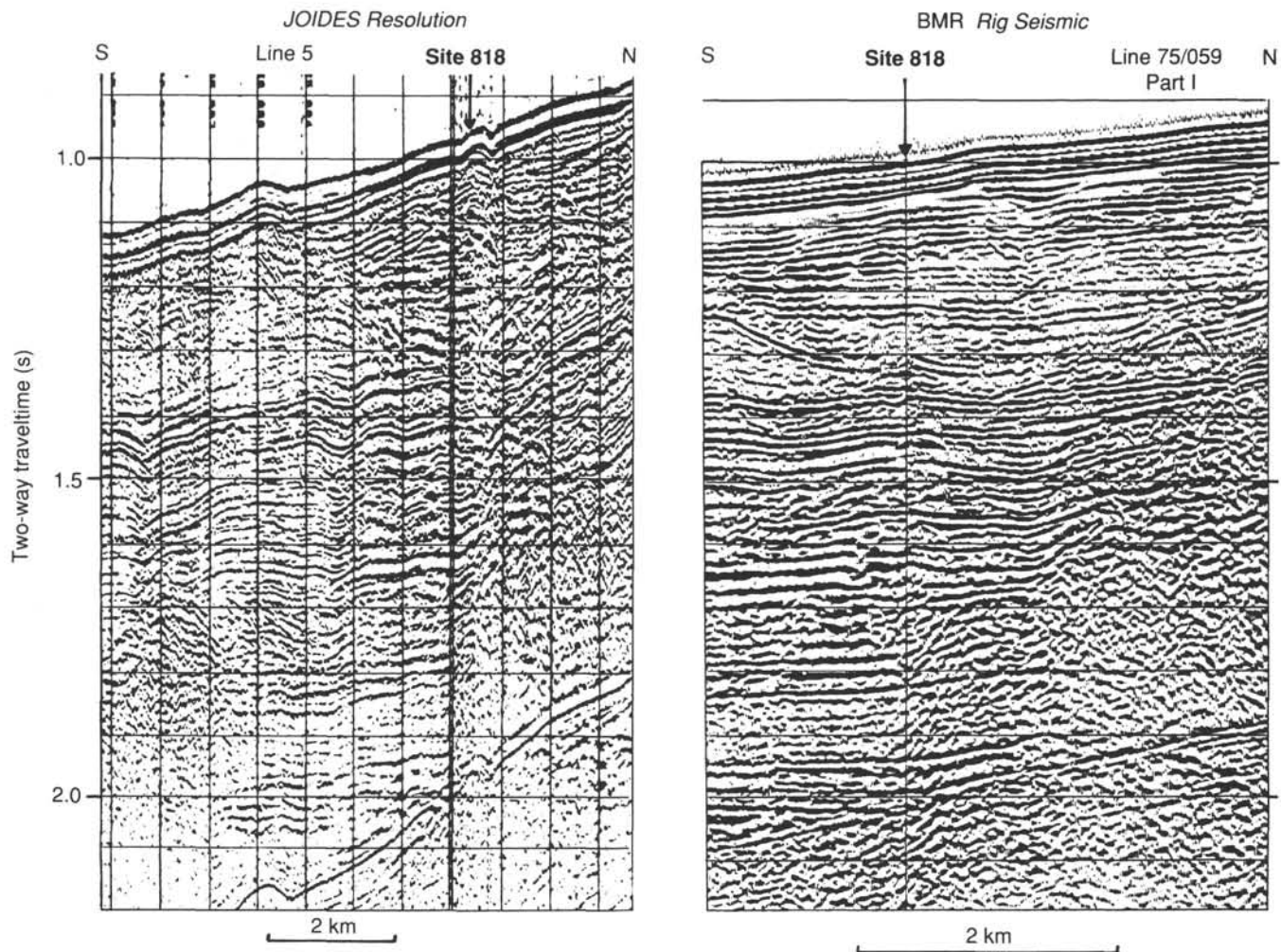


Figure 5. Comparison of JOIDES Resolution and Rig Seismic 80-in.³ water-gun seismic profiles across Site 818.

cases thus include nannofossil micrite ooze, micrite nannofossil ooze, nannofossil ooze with micrite, and micrite ooze with nannofossils. Proportions of bioclasts, foraminifers, and pteropods in these oozes usually reached values ranked only as secondary components. On rare occasions, however, their proportions were high enough to qualify as a major modifier, and thus some of these oozes can be designated micrite bioclastic ooze or foraminifer nannofossil ooze.

We based our differentiation of Unit I into four subunits essentially upon the two end-members of micrite ooze and nannofossil ooze. Micrite is predominant in Subunits IA and IC. These two subunits thus have been interpreted as true periplatform oozes, and the sediments consist of a mixture of significant proportions of bank-derived, fine materials (micrite *sensu lato*, mostly as aragonite and Mg-calcite) and, to a lesser extent, of pelagic fine-grained particles, mostly nannofossils and some planktonic foraminifers. Sediments in Subunits IB and ID are more pelagic (i.e., they contain more nannofossils) in character and have a smaller proportion of bank-derived micrite material, based on smear slide estimates, which, however, are qualitative. Our subdivision will need to be confirmed by more quantitative shore-based analyses. Because of their gradational transitions, subunit boundaries were selected *a priori* as core boundaries. The selection of four subunits in Unit I may be more meaningful when one considers that roughly the same subunits can be distinguished by (1)

bulk-density data (see "Physical Properties" section, this chapter), (2) variations of carbonate content (see "Inorganic Geochemistry" section, this chapter), and (3) variability of sedimentation rates (see "Sedimentation Rates" section, this chapter).

Subunit IA (Cores 133-818B-1H to -7H-CC, 15 cm; depth, 0 to 65.4 mbsf; age, Pleistocene)

In addition to abundance of nannofossils, sediments in Subunit IA can be characterized by a large proportion of fine calcareous particles (micrite), which were identified in smear slides. The coarser particles consist of planktonic and benthic foraminifers, pteropod tests, and bioclasts. Subunit IA also consists of variable white to very light gray micrite ooze that ranges from micrite ooze to foraminifer micrite ooze with bioclasts, pteropods, and nannofossils to nannofossil micrite ooze and rare micrite nannofossil ooze and nannofossil ooze with micrite, bioclasts, and foraminifers. The large proportions of micritic components in these oozes, which mostly correspond to high aragonite content values in these sediments (ranging between 50% and 70%) and, to a lesser extent, to some Mg-calcite, provide good evidence that sediments in Subunit IA are mostly bank-derived material that has been exported from Tregrosse Bank. Thus, these sediments can be called periplatform oozes after Schlager and James (1978).

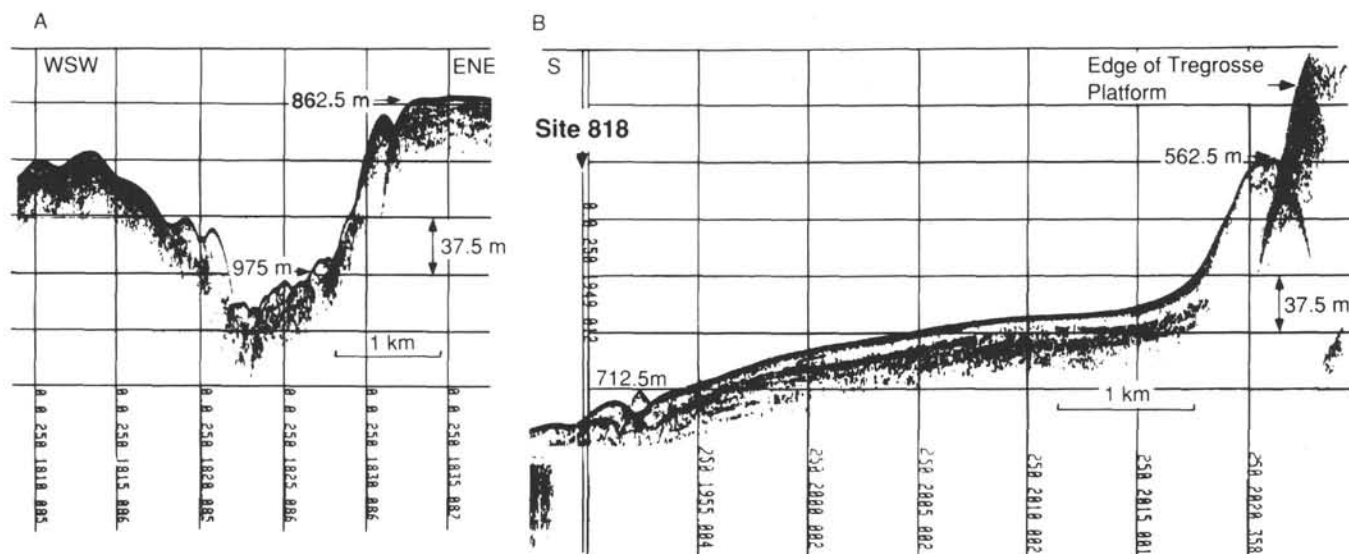


Figure 6. Portions of the *JOIDES Resolution* 3.5-kHz echo sounder profile collected during the transit to Site 818 (A) and the site-location survey (B).

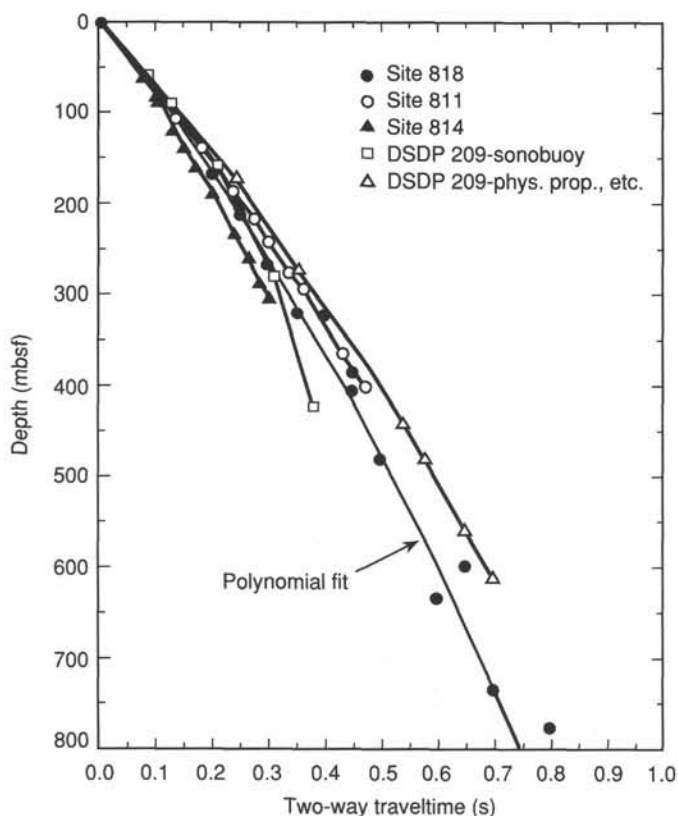


Figure 7. Comparison of TWT/depth curve estimated for Site 818 with those for Sites 811, 814, and 818, and DSDP Site 209 on the Queensland Plateau.

The monotonous periplatform ooze in Subunit IA is interrupted toward its base by the occurrence of two distinct layers that consist of floatstones with mud clasts and graded foraminiferal lithoclastic packstones. The upper layer is 45 cm thick and extends from Sections 133-818B-6H-2, 115 cm, to -6H-3, 10 cm. The lower one is 40 cm thick and extends from Sections 133-818B-6H-3, 125 cm, to -6H-4, 15 cm. We

interpreted these sandy foraminiferal ooze layers as calciturbidite layers. The upper turbidite layer was deposited on top of contorted ooze, which we interpreted as representing a slump. The lower layer seems to overlie dipping layers that we also interpreted as a slump. This 3-m-thick turbidite layer and slump package overlies micrite ooze (which we interpreted as periplatform ooze) down to the base of Subunit IA.

Subunit IB (Cores 133-818B-8H-CC to -11H-CC, 20 cm; depth, 65.4 to 103.4 mbsf; age, late late Pliocene to Pleistocene)

At first, sediments in Subunit IB resemble the overlying oozes of Subunit IA. However, they can be differentiated by their larger proportion of pelagic particles, mostly nannofossils and planktonic foraminifers. Subunit IB consists of variable white to very light gray and light gray micrite nannofossil ooze and micrite nannofossil ooze with foraminifers. Values of aragonite contents gradually decrease from 45% in the upper part of Subunit IB to 20% at its base, with an average value of 30%, half the average of the aragonite contents in Subunit IA (see "Inorganic Geochemistry" section, this chapter). The gradual decrease of aragonite contents with depth may reflect (besides diagenetic aragonite recrystallization) reduced bank-derived aragonite influx related to the partial or full exposure of shallow banks during the late late Pliocene, which has been globally recognized as an interval of lowstands in sea level (Droxler et al., 1988). Values of carbonate contents increase slightly from 94% in the upper part of Subunit IB to 97% at its base. As a general observation, the sediments of Subunit IB appear more pelagic than bank-derived in character. Sedimentation rates (2.4 cm/k.y.) in Subunit IB are lower than those in Subunit IA (5.7 cm/k.y.), roughly by a factor of two (see Fig. 10, "Sedimentation Rates" section, this chapter). Finally, no gravity-flow deposits have been described in Subunit IB, contrasting with the occurrence of a few turbidite layers in Subunit IA and in the underlying Subunit ID (see below).

Subunit IC (Cores 133-818B-12H to -21H-CC, 12 cm; depth, 103.4 to 198.4 mbsf; age, early late Pliocene)

Sediments in Subunit IC are mostly micritic and monotonous in character. The most common type of ooze in the 95-m-thick Subunit IC ranges from white to light gray micrite ooze to nannofossil micrite ooze, to intermediate micrite ooze

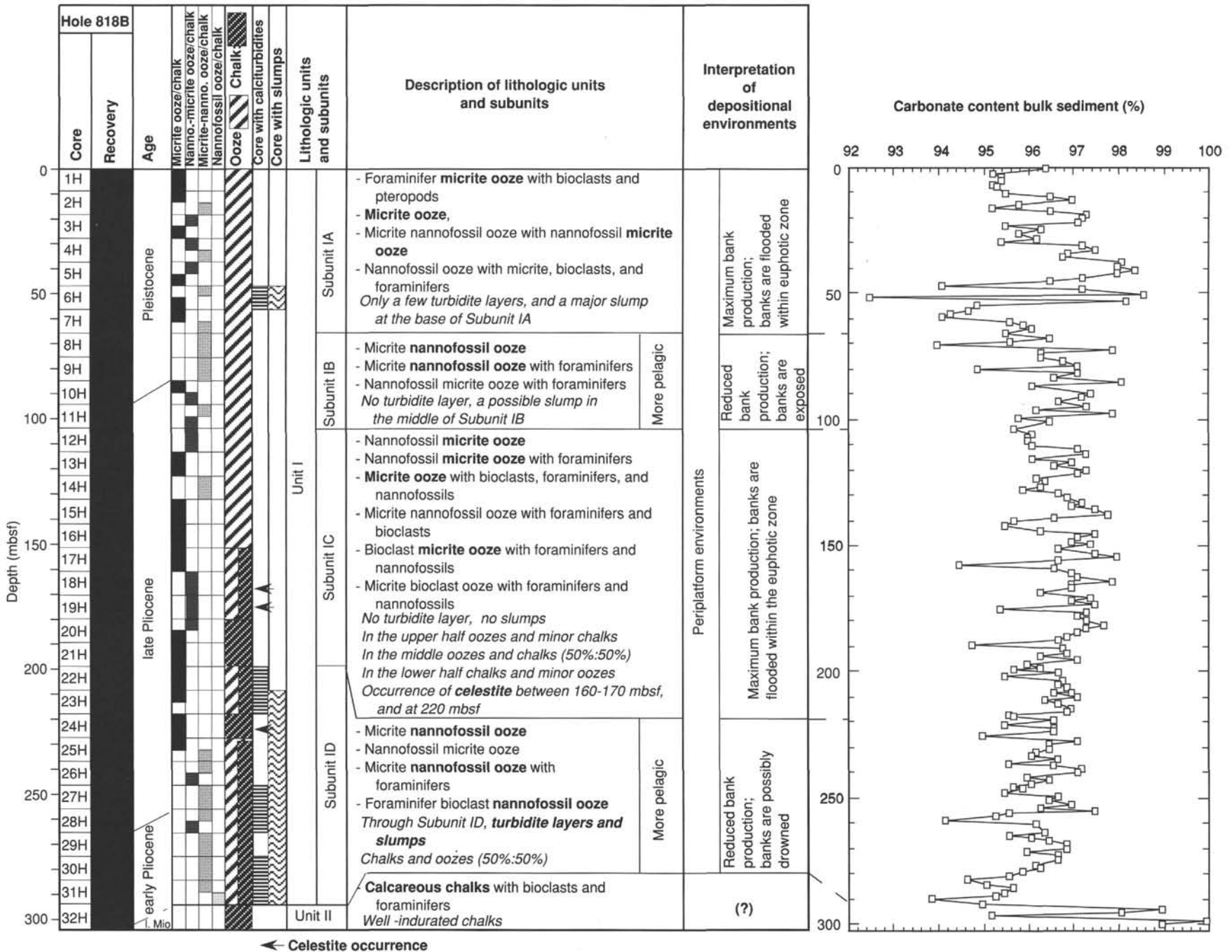


Figure 8. Description and interpretation of lithologic units and subunits for Site 818. Darkness of shading in components columns indicates relative abundance and variations of carbonate content in bulk sediments.

with bioclasts, foraminifers, and nannofossils to bioclastic micrite ooze and nannofossil micrite ooze with foraminifers. Aragonite contents decrease from 20% in the upper part of Subunit IC to only trace amounts at its bottom. Carbonate contents vary between 95% and 98%. No clear evidence exists in the entire subunit for redeposited material by gravity flows, although sedimentation rates average 19 cm/k.y., roughly an order of magnitude higher than average sedimentation rates in the overlying Subunit IB.

Transition from ooze to chalk was observed in Subunit IC in Cores 133-818B-17H, -18H and -19H, between 150 and 180 mbsf. At this ooze/chalk transition, in Cores 133-818B-18H and -19H, concretions and crystalline veins of celestite (usually associated with burrows) were observed. The lower part of Subunit IC, which corresponds to Cores 133-818B-20H and -21H, is totally chalky.

Subunit ID (Cores 133-818B-22H to -31H-CC, 16 cm; depth, 198.4 to 293.4 mbsf; age, early to late Pliocene)

Sediments in Subunit ID appear more pelagic than the overlying sediments of Subunit IC, although the boundary between the two subunits is gradual. Sediments deposited in the upper part of Subunit ID (Cores 133-818B-22H, -23H, and -24H) usually have a larger proportion of micrite than those in the lower part, where micrite nannofossil ooze/chalk and micrite nannofossil ooze/chalk with foraminifers and bioclasts are the most common sediments. Sediments in Subunit ID are a mixture of about 50% ooze and 50% chalk, in contrast to the lowermost part of Subunit IC (Cores 133-818B-20H and -21H), where sediments are exclusively chalk. Values of carbonate content (ranging between 94% and 97%) are similar to those observed in Subunit IC. Calcite with traces of dolomite is the only carbonate phase that was determined by X-ray diffraction (see "Inorganic Geochemistry" section, this chapter). Gravity-flow deposits and slumping are the main characteristics of Subunit ID.

Four distinct layers, which range from 20 to 130 cm thick, of coarse foraminiferal, lithoclastic, and bioclastic oozes having a characteristic sharp base and normal grading were observed in Cores 133-818B-22H, -27H, -30H, and -31H. These characteristics are typical features of calciturbidites. Phosphatized benthic and planktonic foraminifers, as well as glauconite grains, are scattered throughout these coarser layers. Gently to steeply inclined and contorted bedding is the most common sedimentological feature in Subunit ID. This bedding appears in each core of Subunit ID, with the exception of Core 133-818B-22H, and has been interpreted as slumps. This slump- and calciturbidite-rich subunit filled morphological depressions that were observed in the pseudo-three-dimensional interpretation of the site-survey seismic data (Feary et al., 1990, page 203), as described in the "Site Geophysics" section (this chapter).

Unit II (Cores 133-818B-32H to -32H-CC, 20 cm; depth, 293.4 to 302.9 mbsf; age, late Miocene)

Drilling in Core 133-818B-32H penetrated the top of lithological Unit II, where we recovered a well-indurated, light gray, calcareous chalk with bioclasts and foraminifers. The general appearance of this chalk and its brittle response to drilling are different from those of the overlying micrite nannofossil ooze/chalks of Unit I. An average carbonate content of 97% (which ranged between 96% and 98.5%) and an average bulk density (1.9 g/cm³) are higher than the overall average carbonate and bulk density values of the overlying Unit I (see "Inorganic Geochemistry" and "Physical Properties" sections, this chapter). Determinations of calcareous nannofossils and planktonic foraminifers indicate that sedi-

ments in Core 133-818B-32H are upper Miocene (see "Biostratigraphy" section, this chapter).

BIOSTRATIGRAPHY

Two holes were drilled at Site 818. Samples from Hole 818B were analyzed for calcareous nannofossils and planktonic and benthic foraminifers. The succession at this site is from Pleistocene to late Miocene age, with a relatively thick lower Pliocene section. A preliminary biostratigraphic subdivision is shown in Figure 9. Calcareous nannofossils indicate that the Pliocene/Pleistocene contact is within Core 133-818B-10H. The lower/upper Pliocene contact is in Core 133-818B-28H. The sample at the bottom of the hole contains only poorly preserved planktonic foraminifers, which indicates an age older than 5.2 and younger than 10.2 Ma.

Benthic foraminifers are well preserved. The assemblages indicate a middle bathyal paleodepth. Redeposition of shallower water materials in most of the samples is suggested by shallower faunal elements.

Calcareous Nannofossils

One sample per core (except for Core 133-818B-32H) from Hole 818B was examined for calcareous nannofossils. Upper Pleistocene through lower Pliocene nannofossils were recovered at Site 818. Nannofossils are generally abundant and well to moderately preserved in the Pleistocene interval. The Pliocene section contains common, poorly preserved nannofossils. The biostratigraphy for Site 818 is summarized in Figure 9.

Sample 133-818B-1H-CC contains few *Emiliania huxleyi*; it was assigned to Zone CN15 (0.275 Ma). The interval from Samples 133-818B-2H-6, 0 cm, through -5H-CC yielded common to abundant *Pseudoemiliania lacunosa* and *Gephyrocapsa caribbeanica* and thus can be placed in Subzone CN14a (0.465–0.93 Ma). Only rare specimens of *G. caribbeanica* are present in the interval from Samples 133-818B-6H-5, 150 cm, through -8H-5, 150 cm. *Calcidiscus macintyreii* is not present in this interval. This indicates Subzone CN13b (0.93–1.48 Ma). *Calcidiscus macintyreii* was found in Sample 133-818B-9H-6, 0 cm, although discoasters are absent. This sample was assigned to Subzone CN13a (1.48–1.88 Ma).

The highest occurrences of *Discoaster brouweri*, *D. pentaradiatus*, *D. surculus*, and *D. tamalis* are in Samples 133-818B-10H-5, 150 cm, -11H-5, 15 cm; -12H-5, 150 cm, and -20H-CC, respectively. These biohorizons delimit the tops of Subzones CN12d (1.88 Ma), CN12c (2.29 Ma), CN12b (2.42 Ma), and CN12a (2.6 Ma), respectively. The next lower marker species, *Reticulofenestra pseudoumbilica*, was found in Sample 133-818B-28H-CC, which represents the top of Subzone CN11b (3.51 Ma). Relatively common *Discoaster asymmetricus* occur down to Sample 133-818B-30H-CC, but not in the next lower sample at 133-818B-31H-CC; the bottom of Subzone 11b (3.88 Ma) thus has been placed between these samples. A fairly diverse lower Pliocene assemblage was found in Sample 133-818B-31H-CC, but it lacks *Amaurolithus*. This suggests an age of Subzone CN11a (3.88–4.24 Ma) for the sample. Two samples examined from Core 133-818B-32H (Samples 133-818B-32H-5, 150 cm, and -32H-CC) yielded poorly preserved assemblages without age-diagnostic species.

Planktonic Foraminifers

Generally, planktonic foraminifers are abundant and moderate to well preserved throughout Hole 818B, except for the bottom Sample 133-818B-31H-CC, which contains some poorly preserved specimens.

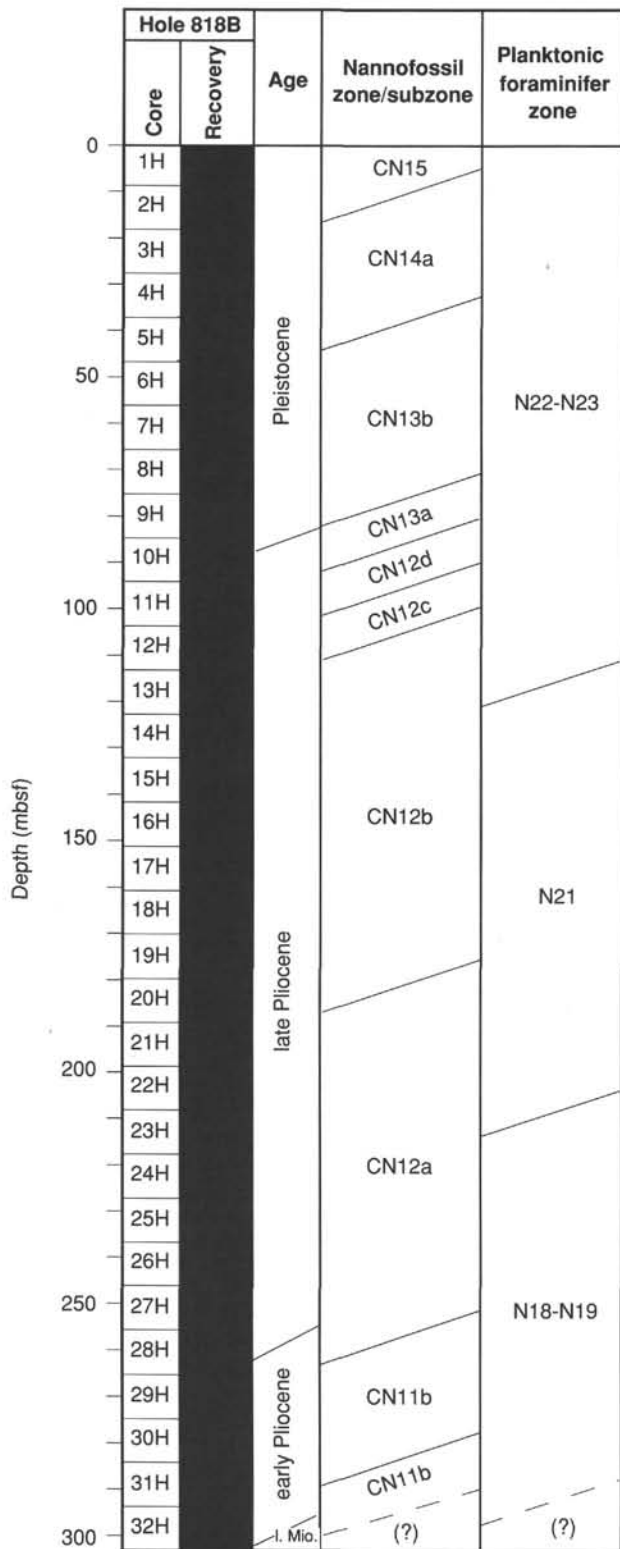


Figure 9. Biostratigraphy summary for Site 818.

The latest occurrences of *Globigerinoides fistulosus* (1.6 Ma) and *Globigerinoides obliquus* (1.8 Ma) can be found in Core 133-818B-9H, which delineates the lowest part of the Pleistocene. The lower limit of Zone N22-N23, as defined by the first occurrence of *Globorotalia truncatulinoides*, was placed in Core 133-818B-13H. Typical late Pliocene plank-

tonic foraminifers, such as *Globorotalia tosaensis*, *Globorotalia limabata*, and *Neogloboquadrina humerosa*, are present in Cores 133-818B-14H through -22H. This interval can be assigned to Zone N21. The latest occurrences of *Globoquadrina altispira* (2.9 Ma) and *Sphaeroidinellopsis seminulina* (3.0 Ma) are in Sample 133-818B-21H-CC. In the next lower core-catcher sample (133-818B-22H-CC), the first occurrence of *Globigerinoides fistulosus* (2.9 Ma) can be found.

The lower part of Hole 818B can be referred to Zone N18-N19. The dominance of *Globoquadrina altispira*, *Globigerinoides obliquus*, and *Globigerinoides trilobus* indicates that surface waters were tropical during that time. The highest occurrence of *Globigerinoides nepenthes* is in Sample 133-818B-31H-CC, which indicates either that the bottom of the hole is older than 3.9 Ma or that this interval has been slumped. The planktonic foraminifers in Sample 133-818B-32H-CC were badly preserved. The absence of *Globorotalia tumida tumida* and the presence of *Neogloboquadrina acostaensis* may indicate that this sample is older than 5.2 but younger than 10.2 Ma.

Benthic Foraminifers

Core-catcher samples examined from Hole 818B contain well-preserved benthic foraminifers. The benthic foraminiferal assemblages indicate a middle bathyal paleodepth (600–1000 m) for Hole 818B.

Most of the core-catcher samples examined contain middle bathyal species associations that include the depth-indicators *Bulimina mexicana*, *Cibicidoides bradyi*, *C. cicatricosus*, *C. mundulus*, *C. robertsonianus*, *Hanzawaia mantaensis*, *Hoeglundina elegans*, *Hyalinea balthica*, *Lenticulina peregrina*, *Nuttallides umbonifera*, *Planulina rugosa*, *Planulina wuellerstorfi*, *Plectofrondicularia vaughni*, *Pyrgo murrhina*, *Sigmoilopsis schlumbergeri*, *Sphaeroidina bulloides*, *Uvigerina pigmaea*, and *U. proboscidea* (van Morkhoven et al., 1986). In addition to these taxa, Sample 133-818B-10H-CC contains abundant *Bulimina aculeata*. This sample yields abundant *Globigerina bulloides*, which is an indicator of high productivity. *Bulimina aculeata* has been found to prefer nutrient abundance and to have great tolerance for high salinities and oxygen deficiency. It has also been correlated to high carbon values in certain areas (van Morkhoven et al., 1986).

Most of the samples that were examined included a small component of transported specimens, such as *Amphistegina* spp., *Asterigerina* spp., *Discorbis* spp., *Elphidium* spp., and *Planorbulina* spp. In addition, Sample 133-818B-1H-CC contains approximately 80% transported specimens, including *Amphistegina* spp., *Asterigerina* spp., *Cibicids lobatulus*, *Discorbis* spp., *Elphidium* spp., abundant miliolids, and *Planorbulina* spp. Similarly, Sample 133-818B-5H-CC contains about 20% transported specimens.

PALEOMAGNETISM

We were unable to define any reliable magnetic reversals in periplatform sediments at Hole 818B from shipboard paleomagnetic measurements. The absence of a resolvable shipboard magnetostratigraphy probably results from relatively weak magnetization in the pure carbonate sediments. Natural remanent magnetization (NRM) intensities for most of the core are near 10⁻¹ mA/m. After alternating field (AF) at 15 mT, these intensities generally were reduced by 50% to 80%. In the lower part of the core, values approach the lower measurement limit of the cryogenic magnetometer. Both the NRM and AF inclinations show considerable scatter, part of which may be attributed to the high water content (140% by volume, see "Physical Properties" section, this chapter), thus promoting intermittent resetting of the magnetization directions.

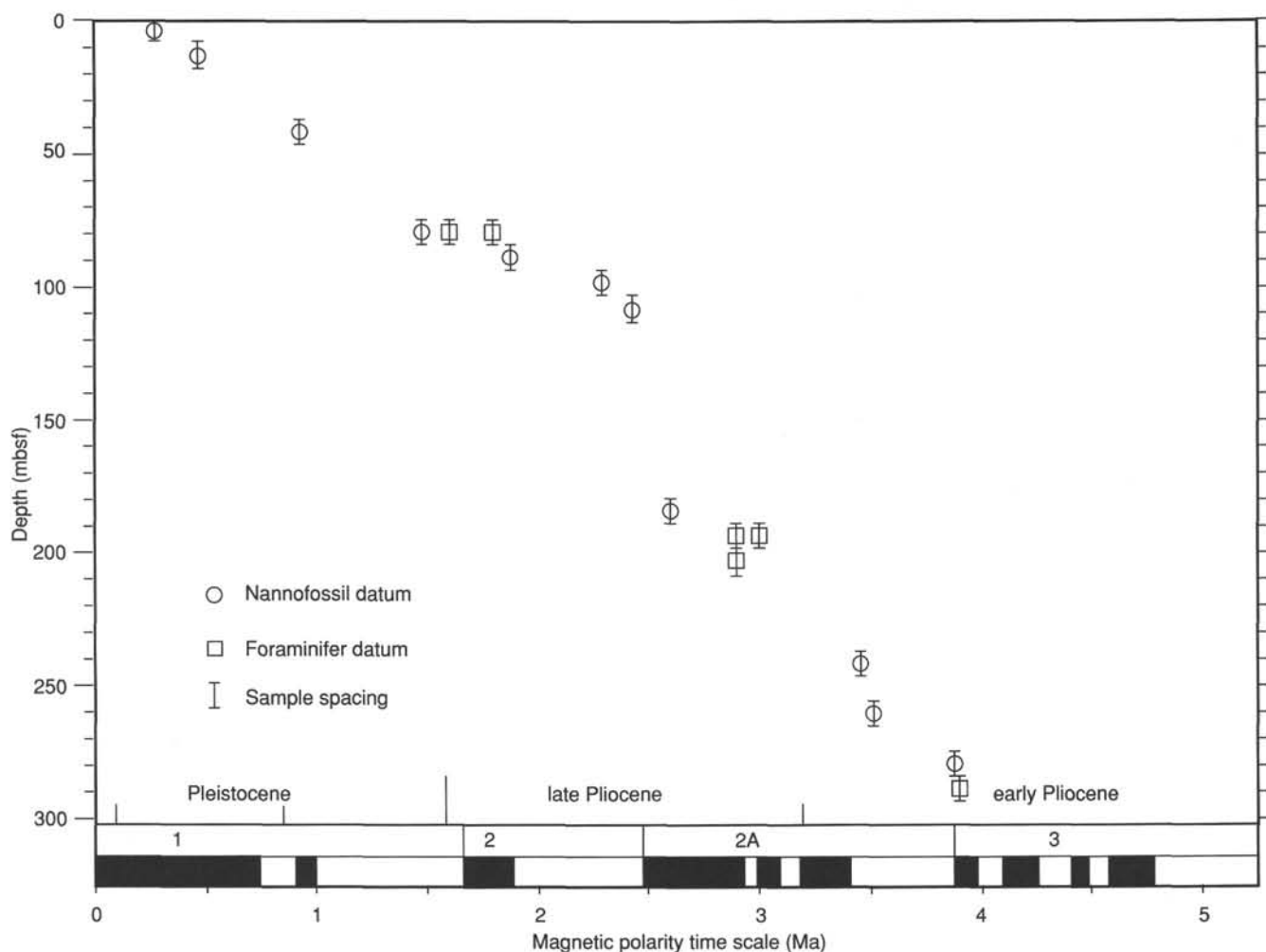


Figure 10. Plot of age vs. depth for Site 818.

A total of 351 oriented discrete samples were collected for analysis in a shore-based magnetically shielded laboratory to test whether a reliable polarity reversal stratigraphy can be ascertained at this site.

Whole-core volume magnetic susceptibility at Hole 818B shows weak values, except for two zones from 0 to about 10 mbsf and from 27 to 35 mbsf. These susceptibility peaks have no obvious correlation to lithologic changes or depositional features observed in the core. The upper peak may represent either a biogenic influx or a detrital pulse of ferrimagnetic material.

SEDIMENTATION RATES

The sediments at Site 818 provide an excellent biostratigraphic framework for calculating sedimentation rates. Even allowing for the relatively large sample spacing, the age-depth plot (Fig. 10) indicates significant fluctuations in sedimentation. Four distinct intervals can be recognized on the sedimentation rate curve: the first extends from 0 to about 85 mbsf and spans the last 1.5 m.y. of the Pleistocene. Sedimentation rate for this interval is 5.7 cm/k.y. This interval from 85 to 108 mbsf covers the time span from 1.5 to 2.42 Ma; that is, the earliest Pleistocene and the latest Pliocene, and the sedimentation rate for this segment is only about 2.4 cm/k.y. The time interval from 2.42 to 2.6 Ma is represented by sediments from about 108 to 184 mbsf, where the sedimentation rate jumps by

an order of magnitude to about 42 cm/k.y. for this segment. One should view this number with caution, however, because the very short time interval used to calculate the rate, even if incorrect by only a small amount, might introduce a large error. The mid-Pliocene and latest early Pliocene—2.6 to 3.88 Ma—is represented from about 184 to 279 mbsf, and the sedimentation rate for this interval is approximately 7.4 cm/k.y.

The nature of the sediment does not change radically, except in Core 133-818B-32H at the bottom of the hole. Consequently, the sedimentation rate does not seem to be controlled primarily by delivery of carbonate—or noncarbonate—detritus, although the former seems to vary in the section. Clearly, the order-of-magnitude increase in sedimentation rate during the late Pliocene was not accompanied by an order-of-magnitude decrease in abundance of pelagic component in these sediments.

INORGANIC GEOCHEMISTRY

Interstitial Waters

Interstitial water samples were taken from Cores 133-818B-1H to -10H and 133-818B-13H, -16H, -19H, -22H, -25H, -28H, and -31H. Samples were squeezed and analyzed according to the methods outlined in the "Explanatory Notes" chapter (this volume).

Table 2. Interstitial water data, Site 818.

Core, section, interval (cm)	Depth (mbsf)	pH	Alkalinity (mM)	Salinity (g/kg)	Calcium (mM)	Magnesium (mM)	Chloride (mM)	Silica (μM)	Strontium (μM)	Sulfate (mM)	Phosphate (μM)
Seawater	0.00	8.20	2.595	35.5	10.64	54.78	546.77	0	97	29.03	0.00
133-818B-											
1H-4, 145-150	4.49	7.46	3.488	34.8	10.03	52.94	535.21	131	196	27.33	1.95
2H-5, 145-150	12.99	7.59	3.323	35.0	9.99	53.61	537.14	661	211	27.98	0.81
3H-5, 145-150	22.46	7.30	4.699	36.2	8.79	54.82	540.03	137	449	27.72	1.30
4H-5, 145-150	31.99	7.28	6.179	36.0	8.32	54.97	550.62	172	603	27.19	1.62
5H-5, 145-150	41.49	7.30	6.373	36.0	8.61	54.30	555.43	185	662	26.57	1.62
6H-5, 145-150	50.99	7.31	6.289		9.12	53.77	555.43	172	685	26.42	1.30
7H-5, 145-150	60.49	7.26	6.519	36.0	9.97	53.70	562.17	156	704	26.76	1.13
8H-5, 145-150	69.99				11.04	51.97	562.17	148	716	26.93	1.62
9H-5, 145-150	79.49	7.72	6.679	36.2	11.24	52.45	564.09	141	685	26.66	0.97
10H-5, 145-150	88.99	7.38	6.497	36.2	11.42	52.61	571.79	135	746	26.56	1.13
13H-5, 145-150	120.53	7.27	6.471	38.0	12.73	52.39	587.20	141	716	26.60	1.95
16H-5, 145-150	148.91	7.24	6.269	38.2	13.44	52.50	606.45	139	704	27.59	1.62
19H-5, 145-150	177.50	7.28	5.787	38.5	14.77	53.34	615.11	143	638	28.25	1.78
22H-5, 145-150	206.00	7.30	5.057	40.2	15.75	53.53	620.89	137	601	28.54	1.30
25H-5, 145-150	234.51	7.24	4.412	40.2	18.32	53.46	634.36	148	599	29.83	1.30
28H-5, 145-150	262.00	7.29	3.413		21.29	51.68	619.92	152	470	32.21	0.65
31H-5, 145-150	291.00	7.30	2.862		20.94	50.25	606.45	185	217	31.21	0.65

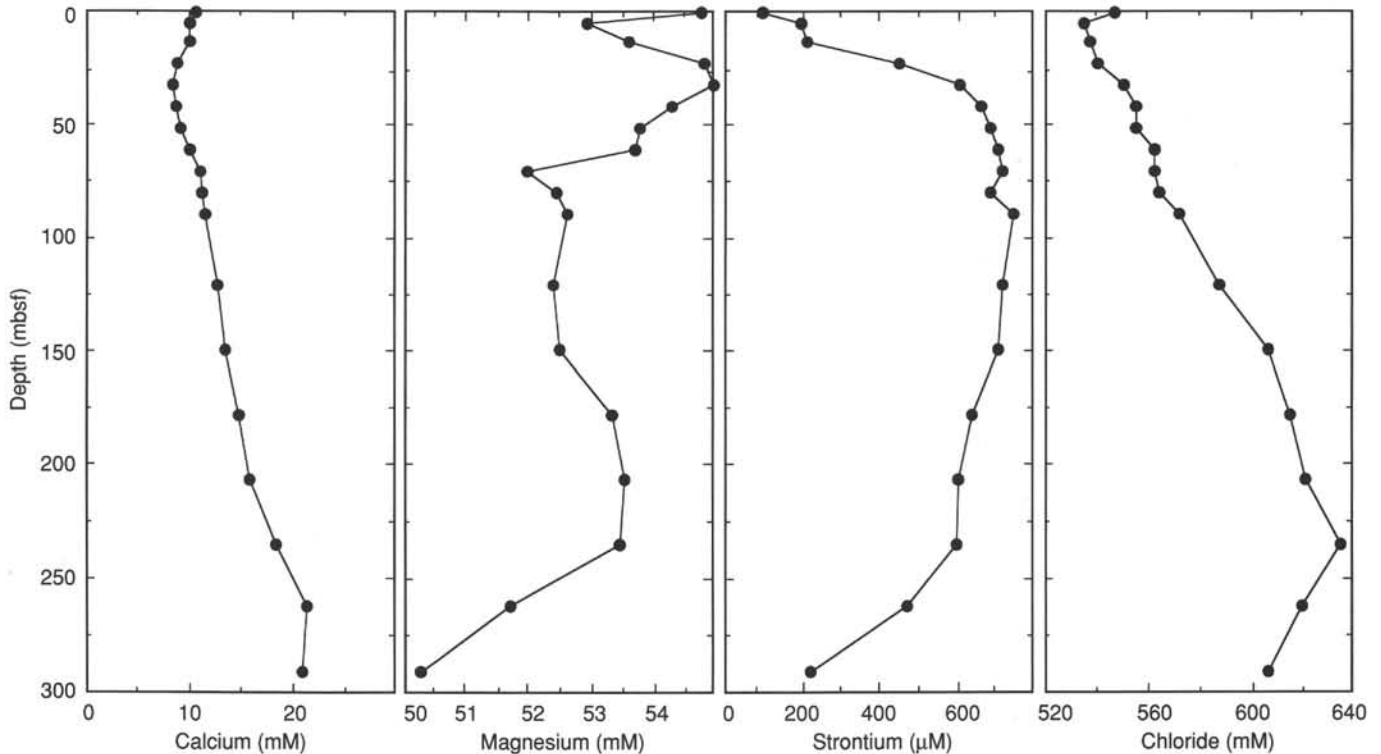


Figure 11. Calcium, magnesium, strontium, and chloride data as a function of depth, Site 818.

Calcium, Magnesium, and Strontium

Calcium concentrations increase steadily from a seawater value of 10.64 to 20.94 mM at 291 mbsf (Fig. 11, Table 2). The profile of interstitial water of Mg^{2+} decreases in the first sample from a seawater concentration of 54.8 to 52.9 mM. Below this depth, values increase to 55.0 mM, then decrease to 52.0 mM at 70 mbsf (Fig. 11, Table 2). With increasing depth, Mg^{2+} concentrations increase to approximately 53 mM. Below 262 mbsf, values decrease to 50.25 mM. Strontium concentrations increase rapidly from a seawater value of 97 to 685 μM at 79 mbsf. Below this depth, values slowly decline to a value of 217 μM at 291 mbsf (Fig. 11, Table 2).

When concentrations of Ca^{2+} and Mg^{2+} are normalized to surface-water salinity (Fig. 12), concentrations of Mg^{2+} decrease with increasing depth. This loss of Mg^{2+} is probably associated with the formation of minor amounts of dolomite in the sediments. Calcium is being consumed within the top 75 mbsf of the cored interval (Fig. 12), possibly as a result of the precipitation of authigenic calcite. Below 75 mbsf, concentrations of Ca^{2+} increase as a result of formation of dolomite and dissolution of aragonite. Re-mineralization of aragonite releases Sr^{2+} into the pore fluids.

At Site 818, celestite (SrSO_4) was found in Cores 133-818B-18H, -19H, and -29H. The ion molar product of SrSO_4 was calculated using interstitial water data taken at Site 818 (Fig. 13). Values greater than approximately 1.7×10^{-6} indicate that

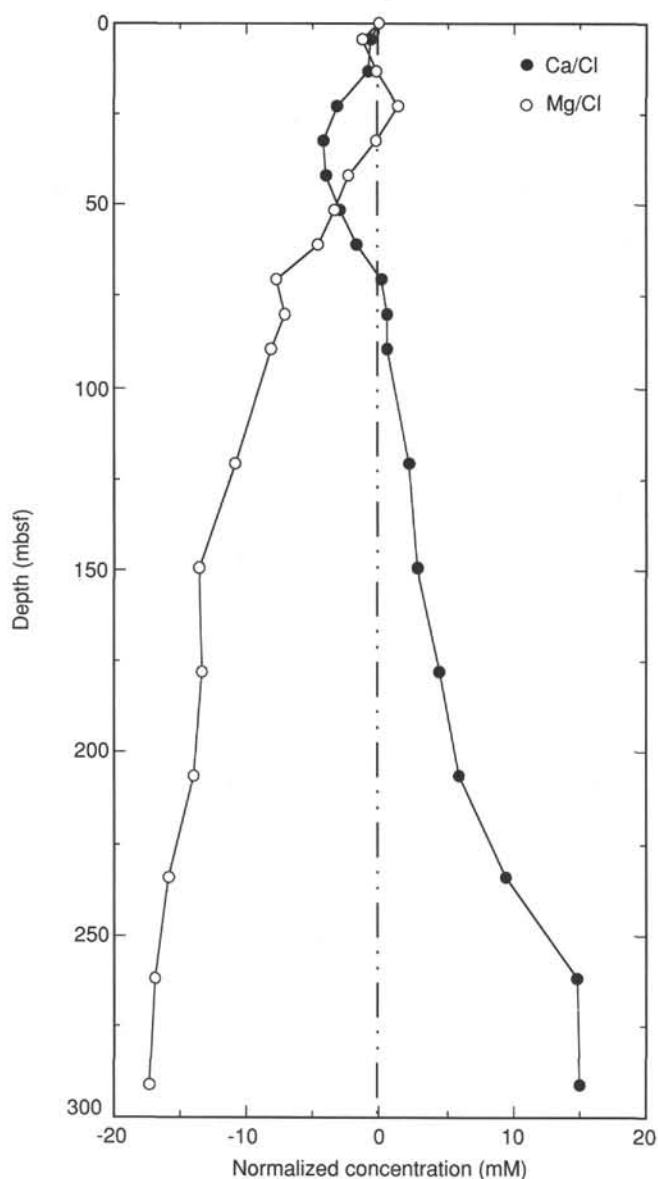


Figure 12. Calcium and magnesium concentrations normalized to surface-water salinity as a function of depth, Site 818.

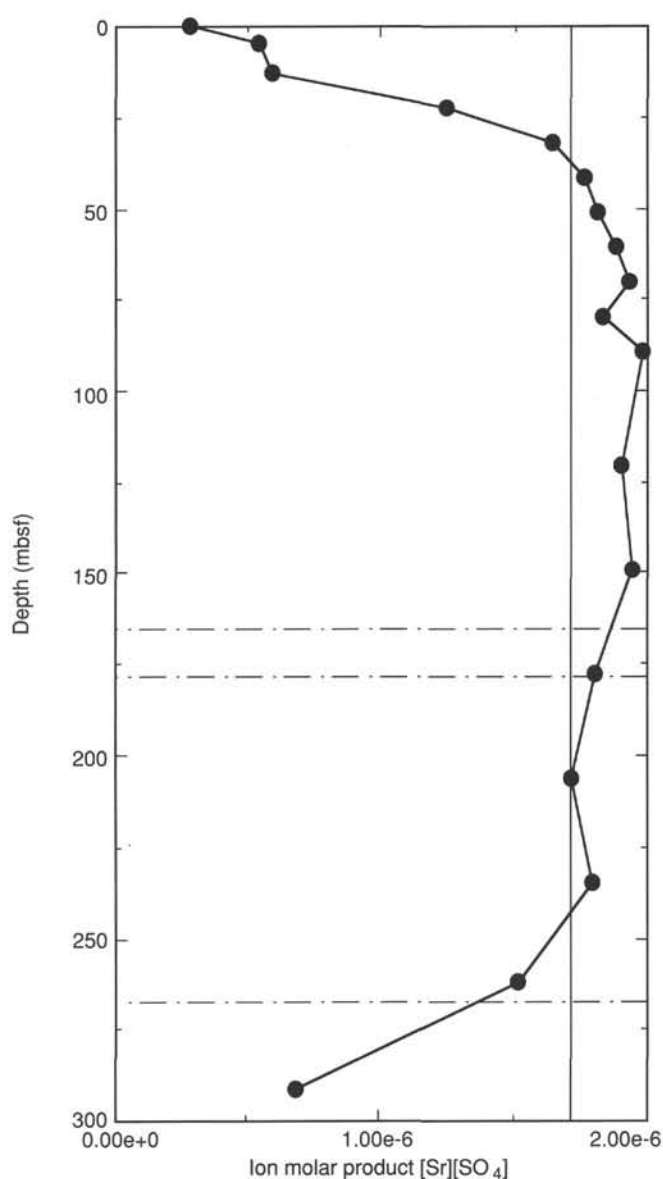


Figure 13. Ion molar product of strontium and sulfate, Site 818. Solid line is the approximate limit for celestite undersaturation in pore waters. To the right of this line celestite will precipitate. Dashed lines are the positions at which celestite was found in the sediments.

sedimentary precipitation of celestite should be occurring. Ion molar product values greater than this were found between 41.5 and 234.5 mbsf, yet celestite was found in only two cores in this interval. Should our predictions be correct, and celestite were present within this interval, only a small amount needs to be precipitated before pore-water Sr is significantly depleted (Swart and Guizikowski, 1988). Therefore, a portion of the precipitating SrSO_4 may be in quantities undetectable by XRD analysis as coatings and microcrystalline grains. In the case of Core 133-818B-29H, 140–150 cm, pore fluids are undersaturated with respect to SrSO_4 at the present time; thus, precipitation may have taken place at an earlier time, when concentrations of Sr^{2+} were sufficiently high.

Precipitation of celestite has been seen in DSDP cores from Lord Howe Rise (Baker, 1986; Kennett, von der Borch, et al., 1985), the central equatorial Pacific (Schlanger, Jackson, et al., 1976), in sediments from Leg 101 on the Bahamian Platform (Swart and Guizikowski, 1987), and in numerous other locations where active carbonate recrystallization occurs.

Chloride

Chloride values decrease slightly from a seawater value of 546.8 to 535.2 mM at 4.5 mbsf (Fig. 11, Table 2). Below this interval, values increase with increasing depth until 235 mbsf, where values decrease to 606.5 mM. This increase in Cl^- concentration is accompanied by an increase in salinity toward the bottom of the sampled interval, possibly as a result of the presence of evaporites at greater depth. An alternative explanation is that concentrations of Cl^- reflect a relict high salinity in sediments of Pliocene age.

Alkalinity, Sulfate, pH, and Phosphate

Concentrations of phosphate at Site 818 were low, with an average value of about $1.25 \mu\text{M}$. The profiles of alkalinity and sulfate mirror each other, which is supporting evidence for sulfate reduction and organic-matter diagenesis at this site

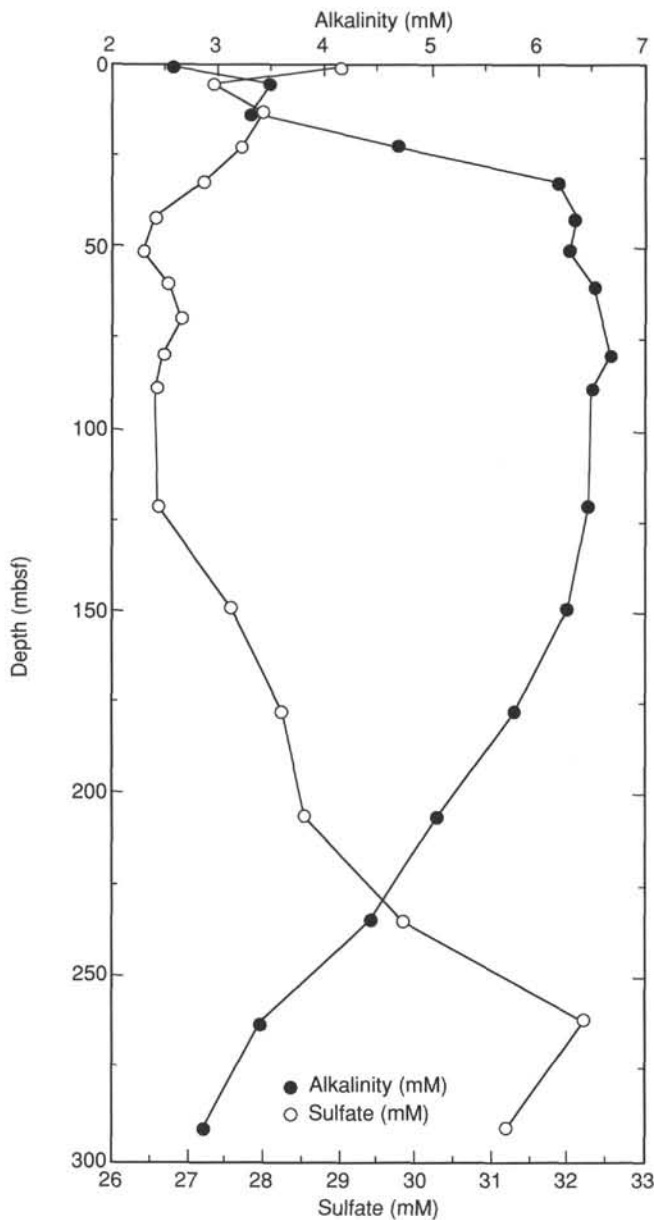


Figure 14. Alkalinity and sulfate data as a function of depth, Site 818.

(Fig. 14 and Table 2). Alkalinity values range from 2.595 mM in seawater to 6.679 mM at 79.5 mbsf. Sulfate values range from 26.20 (seawater) to 32.21 mM.

Silica

Concentrations of silica averaged approximately 150 μM throughout, except for a high value of 661 μM in Sample 133-818B-3H-5, 145–150 cm (Fig. 15 and Table 2). Concentrations of silica were low as a result of the small amount of biogenic silica and quartz in the sediments, as shown by X-ray diffraction (XRD) and micropaleontological analyses.

Carbonate Content and X-Ray Diffraction Data

Samples for XRD analyses were taken from interstitial-water squeeze cakes and physical properties samples. X-ray analyses at Site 818 indicate that sediments in the top 100 m are composed of equal amounts of aragonite and calcite (Fig.

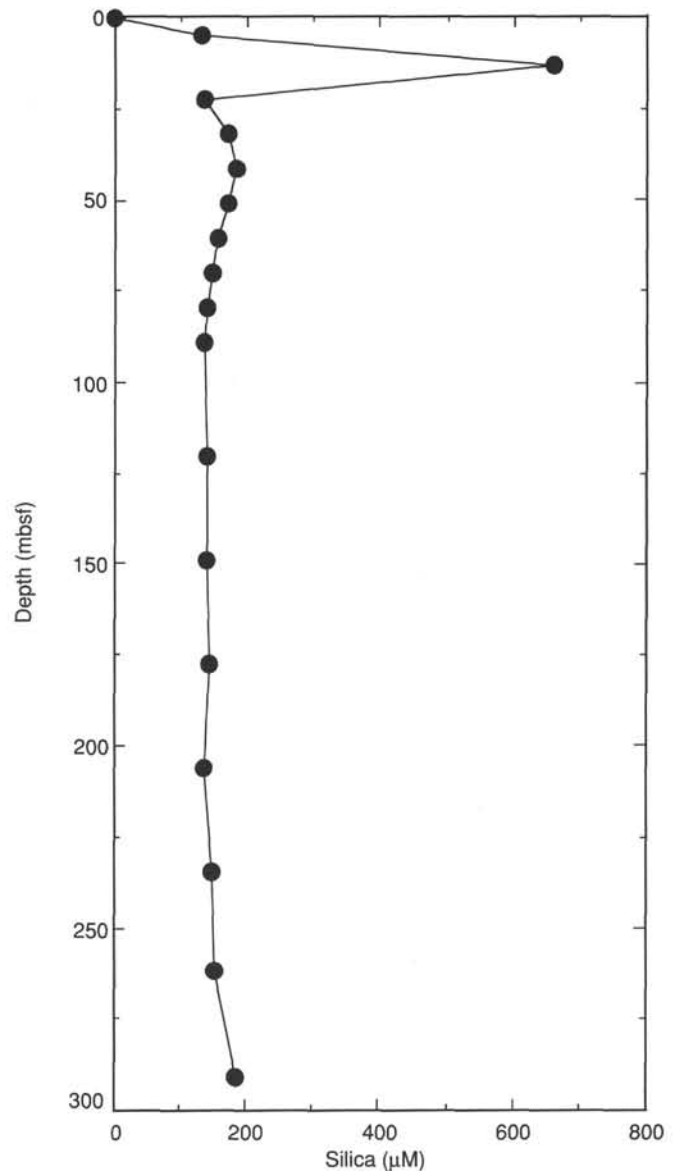


Figure 15. Silica contents of interstitial water as a function of depth at Site 818.

Table 3. X-ray diffraction data, Site 818.

Core, section, interval (cm)	Calcite (%)	Aragonite (%)	Quartz (%)	Dolomite (%)
133-818A-				
1H-4, 145-150	31.8	66.0	2.2	0.0
2H-5, 145-150	42.6	55.1	2.3	0.0
3H-5, 145-150	42.2	56.0	1.8	0.0
4H-5, 145-150	32.3	65.2	2.6	0.0
5H-5, 145-150	41.1	58.9	0.0	0.0
6H-5, 145-150	32.2	67.8	0.0	0.0
7H-5, 145-150	54.8	43.9	1.3	0.0
8H-5, 145-150	57.4	41.8	0.8	0.0
9H-5, 145-150	61.1	36.3	2.7	0.0
10H-5, 145-150	67.0	31.3	0.5	1.2
13H-5, 145-150	85.5	12.8	0.0	1.7
16H-5, 145-150	91.3	5.6	1.4	1.7
19H-5, 145-150	87.5	7.0	4.2	1.3
22H-5, 145-150	97.2	1.1	0.0	1.7
25H-5, 145-150	98.5	0.0	0.0	1.5
28H-5, 145-150	92.6	0.0	4.5	2.8
31H-5, 145-150	100.0	0.0	0.0	0.0

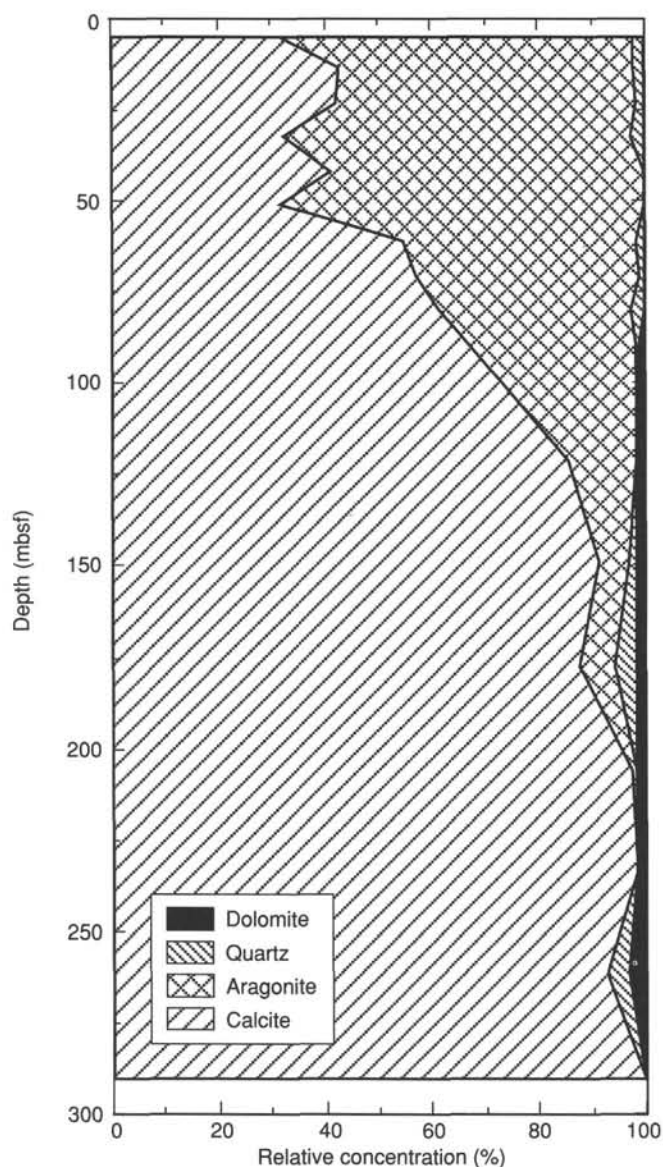


Figure 16. X-ray diffraction data, Site 818. All data are calculated as percentages relative to the concentration of calcite.

16, Table 3). High Mg-calcite was detected in one sample from 4.49 mbsf. Concentrations of aragonite are approximately 67% near the top of the section and decrease with depth. Below 210 m, aragonite is absent. As discussed previously, the disappearance of aragonite coincides with an increase in pore-water concentrations of Sr, which is indicative of carbonate dissolution and re-mineralization. Quartz concentrations are low at Site 818. Dolomite is absent in the top 80 m of Hole 818B. Below this depth, concentrations of dolomite never exceed 3%. Calcite is abundant over the entire sampled interval. Values range from 31.8% to 100%.

Carbonate values at Site 818 vary from 92.2% to 100% (Fig. 17A, Table 4). These data possess a high degree of variability, yet when smoothed by a running average for every five points, distinct trends of cyclic carbonate variations can be seen. These variations are either the result of dilution or dissolution of the carbonate fraction of the sediment. When the data are plotted vs. age (Fig. 17B), the low carbonate event between 0.9 and 1.0 Ma (observed in other sites of Leg 133) can be seen

clearly. The high density of points between 2.5 and 2.7 Ma results from the high sedimentation rates determined for this interval.

ORGANIC GEOCHEMISTRY

In addition to safety monitoring for hydrocarbons, the main purpose of shipboard organic geochemistry studies at Site 818 was to assess the amount and type of organic matter preserved in the Pleistocene to lower Pliocene sediments on the slope between Queensland Plateau and Townsville Trough.

We determined the total nitrogen, sulfur, carbon, and organic carbon contents of 11 samples using an NA 1500 Carlo Erba NCS analyzer.

Volatile Hydrocarbons

Light hydrocarbon gases (C_1 - C_3) in sediments were analyzed routinely as part of the ODP safety and pollution-prevention monitoring program, using the headspace technique and the Carle gas chromatograph. Results of 32 analyses from Hole 818B are presented in Table 5.

The sediments at Site 818 contained low concentrations of hydrocarbon gases and presented no safety problems. Concentrations of methane in headspace gas ranged between 2 and 10 ppm, while only trace amounts of ethane were detected.

Organic Carbon Contents

Total organic carbon (TOC) and total inorganic carbon contents recorded in Hole 818B are presented in Table 6. We observed low TOC values (Fig. 18) in these carbonate-rich sediments, while total sulfur and nitrogen concentrations were below detection limits of the NCS analyzer.

As a consequence of the low organic contents, we were unable to conduct detailed geochemical characterization of kerogen types using the Rock-Eval pyrolysis method, as originally planned. More detailed shore-based studies (elemental analysis and optical investigations of extracted kerogens) will permit characterization of the organic matter preserved in the sediments encountered at Site 818.

PHYSICAL PROPERTIES

Physical properties analyzed in cores from this site include bulk density, P -wave velocity, and magnetic susceptibility of unsplit cores and P -wave velocity, electrical-resistivity formation factor, shear strength, and index properties (including bulk density, grain density, water content, porosity, and void ratio) of split cores. Our methods are described in detail in the "Explanatory Notes" chapter (this volume).

Bulk Density

Bulk densities for Site 818 were determined from volume and mass measurements of discrete core samples and from absorption of gamma rays by whole-round cores (Figs. 19A and 19B; Table 7). In Figures 19A and 19B, an illustration of the similarity of bulk density determinations using different methods is presented. This figure also shows that bulk density is not obviously related to lithologic units on the basis of visual core descriptions. After an initial increase in bulk density was found in the uppermost 10 mbsf, some variation occurred around a mean of about 1.75 g/cm³ to about 50 mbsf, where there was a step increase to a mean of about 1.8 g/cm³. This was followed by a step decrease at about 90 mbsf (the three dashed lines above 100 mbsf in Fig. 19 outline this high-density layer that straddles the boundary between lithologic Subunits IA and IB). From about 90 mbsf, the density to a first approximation increases to the bottom of the hole, although some variations about this trend can be correlated between Hamilton Frame and

Table 4. Carbonate data, Site 818.

Core, section, interval (cm)	Depth (mbsf)	Sample type	Total carbon (%)	Inorganic carbon (%)	Organic carbon (%)	CaCO ₃ (%)
133-818B-						
1H-1, 80-82	0.80	PP		11.57		96.4
1H-2, 80-82	2.30	PP		11.43		95.2
1H-3, 80-82	3.80	PP	11.71	11.45	0.26	95.4
1H-4, 80-82	5.30	PP		11.45		95.4
1H-5, 80-82	6.80	PP		11.43		95.2
1H-6, 40-43	7.90	PP		11.44		95.3
2H-2, 80-82	10.09	PP		11.47		95.5
2H-3, 80-82	11.59	PP		11.58		96.5
2H-4, 80-82	13.09	PP		11.65		97.0
2H-5, 80-82	14.59	PP		11.50		95.8
2H-6, 80-82	16.09	PP		11.43		95.2
2H-7, 80-82	17.59	PP		11.59		96.5
3H-1, 79-81	18.69	PP		11.68		97.3
3H-2, 79-81	20.19	PP		11.67		97.2
3H-3, 79-81	21.69	PP		11.66		97.1
3H-4, 79-81	23.19	PP		11.47		95.5
3H-5, 79-81	24.69	PP		11.56		96.3
3H-6, 79-81	26.19	PP		11.50		95.8
4H-1, 80-83	28.20	PP		11.55		96.2
4H-2, 80-83	29.70	PP		11.45		95.4
4H-3, 80-83	31.20	PP	11.76	11.67	0.09	97.2
4H-4, 80-83	32.70	PP		11.71		97.5
4H-5, 80-83	34.20	PP		11.63		96.9
4H-6, 87-90	35.77	PP		11.62		96.8
5H-1, 87-90	37.77	PP		11.78		98.1
5H-2, 87-90	39.27	PP		11.77		98.0
5H-3, 87-90	40.77	PP		11.81		98.4
5H-4, 87-90	42.27	PP		11.77		98.0
5H-5, 87-90	43.77	PP		11.67		97.2
5H-6, 87-90	45.27	PP		11.59		96.5
6H-1, 80-83	47.20	PP		11.30		94.1
6H-2, 80-83	48.70	PP		11.67		97.2
6H-3, 80-83	50.20	PP		11.84		98.6
6H-4, 80-83	51.70	PP		11.10		92.5
6H-5, 80-83	53.20	PP		11.79		98.2
6H-6, 80-83	54.70	PP		11.39		94.9
7H-1, 87-89	56.77	PP		11.37		94.7
7H-2, 87-89	58.27	PP		11.32		94.3
7H-3, 87-89	59.77	PP	11.60	11.30	0.30	94.1
7H-4, 87-89	61.27	PP		11.48		95.6
7H-5, 83-85	62.73	PP		11.51		95.9
7H-6, 87-90	64.27	PP		11.54		96.1
8H-1, 85-88	66.25	PP		11.46		95.5
8H-2, 85-88	67.75	PP		11.59		96.5
8H-3, 85-88	69.25	PP		11.48		95.6
8H-4, 85-88	70.75	PP		11.29		94.0
8H-5, 85-88	72.25	PP		11.75		97.9
8H-6, 85-88	73.75	PP		11.56		96.3
9H-1, 83-85	75.73	PP		11.56		96.3
9H-2, 83-85	77.23	PP		11.62		96.8
9H-3, 83-85	78.73	PP		11.66		97.1
9H-4, 83-85	80.23	PP		11.39		94.9
9H-5, 83-85	81.73	PP		11.66		97.1
9H-6, 83-85	83.23	PP		11.60		96.6
10H-1, 100-103	85.40	PP		11.78		98.1
10H-2, 100-103	86.90	PP		11.54		96.1
10H-3, 100-103	88.40	PP	11.69	11.63	0.06	96.9
10H-4, 100-103	89.90	PP		11.69		97.4
10H-5, 100-103	91.40	PP		11.67		97.2
10H-6, 100-103	92.90	PP		11.61		96.7
11H-1, 98-100	94.88	PP		11.68		97.3
11H-2, 101-103	96.41	PP		11.55		96.2
11H-3, 101-103	97.91	PP		11.75		97.9
11H-4, 99-101	99.39	PP		11.50		95.8
11H-5, 99-101	100.89	PP		11.59		96.5
12H-1, 100-103	104.40	PP		11.49		95.7
12H-2, 100-103	105.90	PP		11.54		96.1
12H-3, 100-103	107.40	PP		11.52		96.0
12H-4, 100-103	108.90	PP		11.52		96.0
12H-5, 105-109	110.45	PP		11.54		96.1
12H-6, 100-103	111.90	PP		11.66		97.1
13H-1, 101-103	113.91	PP		11.68		97.3
13H-2, 100-103	115.45	PP		11.54		96.1
13H-3, 100-103	117.00	PP	11.69	11.64	0.05	97.0
13H-4, 100-103	118.53	PP		11.60		96.6
13H-5, 100-103	120.03	PP		11.68		97.3
13H-6, 100-103	121.53	PP		11.66		97.1

Table 4 (continued).

Core, section, interval (cm)	Depth (mbsf)	Sample type	Total carbon (%)	Inorganic carbon (%)	Organic carbon (%)	CaCO ₃ (%)
14H-1, 103-105	123.43	PP		11.55		96.2
14H-2, 103-105	124.93	PP		11.57		96.4
14H-3, 111-114	126.51	PP		11.56		96.3
14H-4, 110-114	128.00	PP		11.51		95.9
14H-5, 104-106	129.44	PP		11.61		96.7
14H-6, 110-112	131.00	PP		11.63		96.9
15H-1, 110-112	133.00	PP		11.67		97.2
15H-2, 100-103	134.40	PP		11.65		97.0
15H-3, 106-108	135.96	PP		11.71		97.5
15H-4, 111-112	137.51	PP		11.74		97.8
15H-5, 111-112	139.01	PP		11.60		96.6
15H-6, 111-112	140.51	PP		11.49		95.7
16H-1, 107-110	142.47	PP		11.46		95.5
16H-2, 115-118	144.05	PP	11.82	11.56	0.11	96.3
16H-3, 111-114	145.51	PP		11.71		97.5
16H-4, 100-103	146.90	PP		11.66		97.1
16H-5, 101-104	148.41	PP		11.65		97.0
16H-6, 75-78	149.65	PP		11.69		97.4
17H-1, 60-63	151.50	PP		11.61		96.7
17H-2, 60-63	153.00	PP		11.71		97.5
17H-3, 60-63	154.50	PP		11.77		98.0
17H-4, 60-63	156.00	PP		11.61		96.7
17H-5, 60-63	157.50	PP		11.34		94.5
17H-6, 60-63	159.00	PP		11.60		96.6
18H-1, 70-73	161.10	PP		11.64		97.0
18H-2, 70-73	162.60	PP		11.66		97.1
18H-3, 70-73	164.10	PP		11.75		97.9
18H-4, 70-73	165.60	PP		11.64		97.0
18H-5, 70-73	167.10	PP		11.64		97.0
18H-6, 70-73	168.60	PP		11.56		96.3
19H-1, 60-63	170.50	PP		11.69		97.4
19H-2, 60-63	172.00	PP		11.65		97.0
19H-3, 60-63	173.50	PP	11.75	11.71	0.04	97.5
19H-4, 60-63	175.00	PP		11.45		95.4
19H-5, 60-63	176.50	PP		11.68		97.3
19H-6, 60-63	178.00	PP		11.66		97.1
20H-1, 60-63	180.00	PP		11.68		97.3
20H-2, 60-63	181.50	PP		11.73		97.7
20H-3, 60-63	183.00	PP		11.68		97.3
20H-4, 60-63	184.50	PP		11.66		97.1
20H-5, 60-63	186.00	PP		11.63		96.9
20H-6, 60-63	187.50	PP		11.61		96.7
21H-1, 60-63	189.50	PP		11.38		94.8
21H-2, 61-64	191.01	PP		11.62		96.8
21H-3, 61-64	192.51	PP		11.63		96.9
21H-4, 61-64	194.01	PP		11.56		96.3
21H-5, 61-64	195.51	PP		11.66		97.1
21H-6, 61-64	197.01	PP		11.53		96.0
21H-7, 61-64	198.51	PP		11.56		96.3
22H-1, 60-63	199.00	PP		11.49		95.7
22H-2, 60-63	200.50	PP		11.61		96.7
22H-3, 60-63	202.00	PP	11.53	11.46	0.07	95.5
22H-4, 60-63	203.50	PP		11.62		96.8
22H-5, 60-63	205.00	PP		11.61		96.7
22H-6, 60-63	206.50	PP		11.63		96.9
22H-7, 60-63	208.00	PP		11.65		97.0
23H-1, 60-62	208.50	PP		11.60		96.6
23H-2, 60-62	210.00	PP		11.66		97.1
23H-3, 60-62	211.50	PP		11.57		96.4
23H-4, 60-62	213.00	PP		11.61		96.7
23H-5, 60-62	214.50	PP		11.64		97.0
23H-6, 60-62	216.00	PP		11.63		96.9
23H-7, 60-62	217.50	PP		11.48		95.6
24H-1, 60-63	218.00	PP		11.49		95.7
24H-2, 60-63	219.50	PP		11.60		96.6
24H-3, 60-63	221.00	PP		11.46		95.5
24H-4, 60-63	222.50	PP		11.60		96.6
24H-5, 60-63	224.00	PP		11.60		96.6
24H-6, 60-63	225.50	PP		11.40		95.0
25H-1, 61-63	227.51	PP		11.66		97.1
25H-2, 61-63	229.01	PP		11.59		96.5
25H-3, 61-63	230.51	PP	11.66	11.58	0.08	96.5
25H-4, 61-63	232.01	PP		11.55		96.2
25H-5, 61-63	233.51	PP		11.54		96.1
25H-6, 61-63	235.01	PP		11.61		96.7
25H-7, 60-63	236.50	PP		11.48		95.6
26H-1, 60-63	237.00	PP		11.60		96.6
26H-2, 60-63	238.50	PP		11.67		97.2

Table 4 (continued).

Core, section, interval (cm)	Depth (mbsf)	Sample type	Total carbon (%)	Inorganic carbon (%)	Organic carbon (%)	CaCO ₃ (%)
26H-3, 60-63	240.00	PP		11.66		97.1
26H-4, 60-63	241.50	PP		11.52		96.0
26H-5, 60-63	243.00	PP		11.58		96.5
26H-6, 60-63	244.50	PP		11.54		96.1
26H-7, 60-63	246.00	PP		11.49		95.7
27H-1, 60-63	246.50	PP		11.51		95.9
27H-2, 60-63	248.00	PP		11.47		95.5
27H-3, 60-63	249.50	PP		11.61		96.7
27H-4, 60-63	251.00	PP		11.59		96.5
27H-5, 60-63	252.50	PP		11.64		97.0
27H-6, 60-63	254.00	PP		11.56		96.3
27H-7, 60-63	255.50	PP		11.70		97.5
28H-1, 60-63	256.00	PP		11.48		95.6
28H-2, 60-63	257.50	PP		11.44		95.3
28H-3, 60-63	259.00	PP	11.75	11.31	0.44	94.2
28H-4, 60-63	260.50	PP		11.55		96.2
28H-6, 60-63	263.50	PP		11.57		96.4
28H-7, 60-63	265.00	PP		11.48		95.6
29H-1, 60-63	265.50	PP		11.54		96.1
29H-2, 60-63	267.00	PP		11.59		96.5
29H-3, 60-63	268.50	PP		11.63		96.9

Table 4 (continued).

Core, section, interval (cm)	Depth (mbsf)	Sample type	Total carbon (%)	Inorganic carbon (%)	Organic carbon (%)	CaCO ₃ (%)
29H-4, 60-63	270.00	PP		11.63		96.9
29H-5, 60-63	271.50	PP		11.53		96.0
29H-6, 60-63	273.00	PP		11.61		96.7
30H-1, 60-63	275.00	PP		11.61		96.7
30H-2, 60-63	276.60	PP		11.55		96.2
30H-3, 60-63	278.00	PP		11.56		96.3
30H-4, 60-63	279.50	PP		11.51		95.9
30H-5, 60-63	281.00	PP		11.48		95.6
30H-6, 60-63	282.50	PP		11.37		94.7
31H-1, 60-63	284.50	PP		11.42		95.1
31H-2, 60-63	286.00	PP		11.49		95.7
31H-3, 60-63	287.50	PP		11.46		95.5
31H-4, 60-63	289.00	PP	11.54	11.44	0.10	95.3
31H-5, 60-63	290.50	PP		11.27		93.9
31H-6, 60-63	292.00	PP		11.40		95.0
32H-1, 60-63	294.00	PP		11.89		99.0
32H-2, 60-63	295.50	PP		11.78		98.1
32H-3, 60-63	297.00	PP		11.43		95.2
32H-4, 60-63	298.50	PP		12.00		100.0
32H-5, 60-63	300.00	PP		11.88		99.0

PP = physical properties sample.

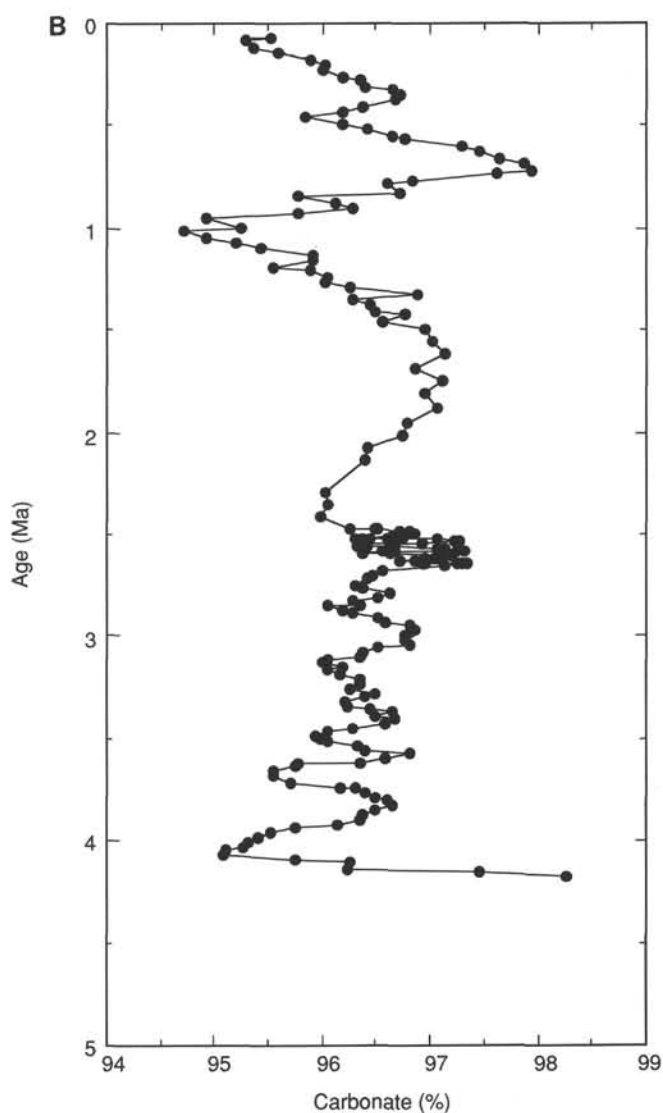
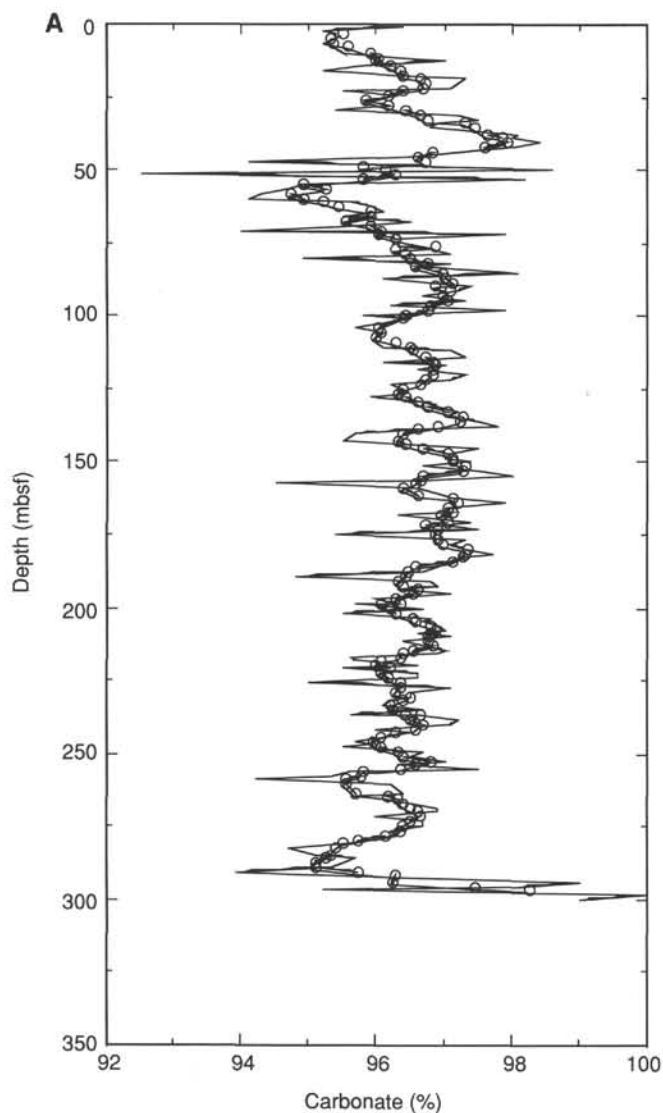


Figure 17. A. Raw (solid line) and smoothed (open circles) carbonate data, Site 818 as a function of depth. B. Smoothed carbonate data plotted vs. age, Site 818.

Table 5. Volatile hydrocarbon data from headspace analysis at Site 818.

Core, section, interval (cm)	Depth (mbsf)	Sample type	Volume (mL)	Gas chromat.	C ₁ (ppm)	C ₂ (ppm)	C ₃ (ppm)
133-818B-							
1H-4, 145-146	5.95	HS	5	CAR132	2	0	0
2H-5, 145-146	15.24	HS	5	CAR132	3	0	0
3H-5, 149-150	25.39	HS	5	CAR132	4	0	0
4H-5, 145-146	34.85	HS	5	CAR132	4	0	0
5H-5, 145-146	44.35	HS	5	CAR132	5	0	0
6H-5, 145-146	53.85	HS	5	CAR132	7	0	0
7H-5, 140-141	63.3	HS	5	CAR132	7	0	0
8H-5, 145-146	72.85	HS	5	CAR132	7	0	0
9H-5, 140-141	82.3	HS	5	CAR132	10	1	0
10H-5, 145-146	91.85	HS	5	CAR132	8	1	0
11H-5, 149-150	101.39	HS	5	CAR132	7	1	0
12H-5, 149-150	110.89	HS	5	CAR132	10	1	0
13H-5, 140-141	120.43	HS	5	CAR132	7	1	0
14H-5, 149-150	129.89	HS	5	CAR132	7	1	0
15H-5, 149-150	139.39	HS	5	CAR132	7	1	0
16H-5, 140-141	148.8	HS	5	CAR132	8	1	0
17H-5, 149-150	158.39	HS	5	CAR132	6	0	0
18H-5, 149-150	167.89	HS	5	CAR132	8	1	0
19H-5, 149-150	177.39	HS	5	CAR132	4	0	0
20H-5, 149-150	186.89	HS	5	CAR132	6	0	0
21H-5, 149-150	196.39	HS	5	CAR132	8	0	0
22H-5, 149-150	205.89	HS	5	CAR132	8	0	0
23H-5, 149-150	215.39	HS	5	CAR132	6	0	0
24H-5, 149-150	224.89	HS	5	CAR132	4	0	0
25H-5, 149-150	234.39	HS	5	CAR132	5	0	0
26H-5, 149-150	243.89	HS	5	CAR132	4	0	0
27H-5, 149-150	253.39	HS	5	CAR132	4	0	0
28H-5, 149-150	262.89	HS	5	CAR132	3	0	0
29H-5, 149-150	272.39	HS	5	CAR132	4	0	0
30H-5, 149-150	281.89	HS	5	CAR132	3	0	0
31H-5, 149-150	291.39	HS	5	CAR132	5	0	0
32H-5, 149-150	300.89	HS	5	CAR132	3	0	0

HS = headspace sample.

Table 6. Concentrations of total organic carbon, inorganic carbon, total carbon, total nitrogen, and sulfur in sediments from Site 818.

Core, section, interval (cm)	Depth (mbsf)	Sample type	Total organic carbon (%)	Total inorganic carbon (%)	Total carbon (%)	Total nitrogen (%)	Total sulfur (%)
133-818B-							
1H-3, 80-82	3.8	PP	0.25	11.45	11.7	0	0
4H-3, 80-83	31.2	PP	0.1	11.65	11.75	0	0
7H-3, 87-89	59.77	PP	0.3	11.3	11.6	0	0
10H-3, 100-103	88.4	PP	0.05	11.65	11.7	0	0
13H-3, 100-103	117	PP	0.05	11.65	11.7	0	0
16H-3, 111-114	145.51	PP	0.1	11.7	11.8	0	0
19H-3, 60-63	173.5	PP	0.04	11.7	11.75	0	0
22H-3, 60-63	202	PP	0.05	11.45	11.5	0	0
25H-3, 61-63	230.51	PP	0.1	11.55	11.65	0	0
28H-3, 60-63	259	PP	0.45	11.3	11.75	0	0
31H-4, 60-63	289	PP	0.1	11.45	11.55	0	0

PP = physical properties sample.

GRAPE density measurements and also can be correlated with variations in velocity.

P-Wave Velocity

P-wave velocities were measured in whole-round cores using the multisensor track (MST) and in discrete core samples using the Hamilton frame (Table 8 and Figs. 19C and 19D). As with densities, some features of velocity structures at this site can be seen in velocity vs. depth plots generated from different sets of measurements and distinguish portions of velocity structures at different depths, i.e., features that do not correlate with lithologic unit boundaries.

As with density, a step increase in velocity occurs at about 50 mbsf from values fluctuating at about 1.75 km/s to values averaging around 1.8 km/s. At 90 mbsf, velocity decreases before beginning an approximately linear increase to the bottom of the hole. As was often observed, features of velocity structures also were seen in density structures, where variations in one quantity were proportional to variations in another quantity, contrary to the inverse relationship suggested by the physics of sound in an isotropic medium, in which velocity is inversely proportional to the square root of density. The explanation of this apparent paradox must lie in the overwhelming influence of increases

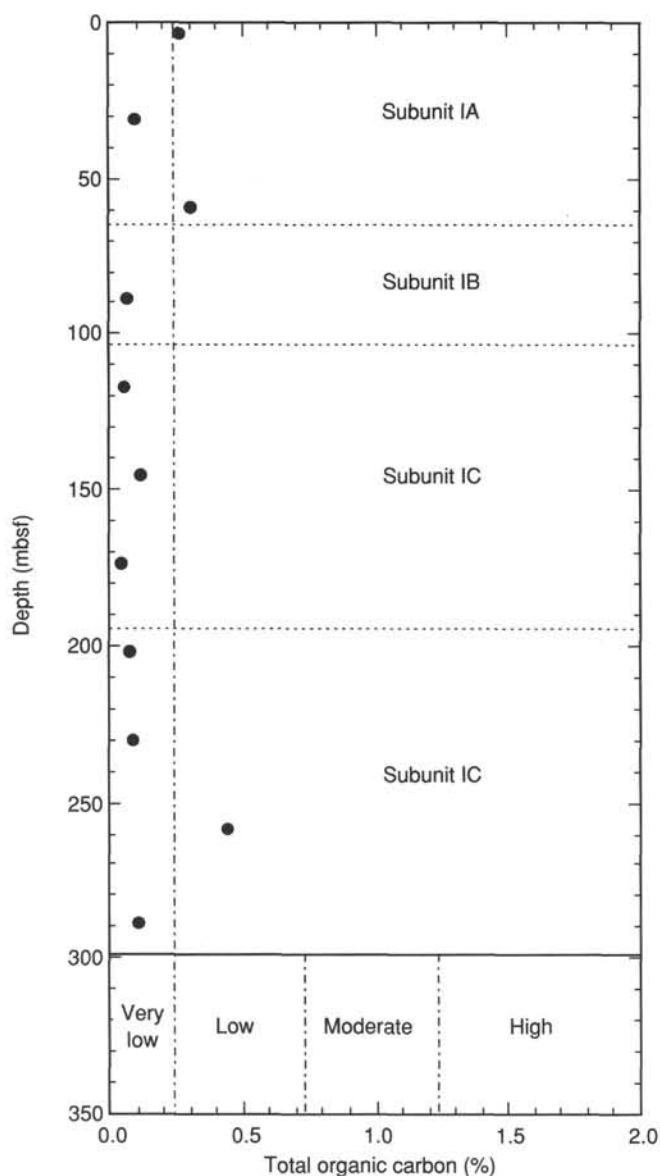


Figure 18. Distribution with depth of total organic carbon contents in sediments at Site 818.

in bulk and shear moduli that must accompany increases in bulk density.

Porosity

Porosity was one of the index properties determined from discrete core samples, using mass balance and the pycnometer (Table 7). A graph of porosity vs. depth is shown in Figure 19E. Similarly, the water content, derived from the same set of index property measurements, also is plotted vs. depth in this figure. A plot of water content vs. porosity is depicted in Figure 20. Here, we also have the expected close correlation of porosity to dry-water content.

Porosity and water content show a first-order linear decrease with depth, with a negative excursion between 45 and 90 mbsf that coincides roughly with the region of high velocity and bulk density. The boundaries of this low-porosity zone do not coincide with lithologic unit boundaries nor with major changes in rates of deposition.

Table 7. Index properties, Site 818.

Core, section, interval (cm)	Depth (mbsf)	Bulk density (g/cm ³)	Grain density (g/cm ³)	Porosity (%)	Water content (%)	Void ratio
133-818B-						
1H-1, 79-82	0.79	1.79	2.79	61.7	54.7	1.61
1H-2, 79-82	2.29	1.72	2.93	66.3	65.2	1.97
1H-3, 79-82	3.79	1.73	2.72	63.2	59.7	1.71
1H-4, 79-82	5.29	1.75	2.75	63.5	59.3	1.74
1H-5, 79-82	6.79	1.73	2.72	62.8	59.2	1.69
1H-6, 40-43	7.90	1.73	2.77	64.1	61.4	1.79
2H-1, 79-82	9.19	1.82	2.73	60.7	52.0	1.55
2H-2, 79-82	10.08	1.71	2.75	62.1	59.0	1.64
2H-3, 79-82	11.58	1.82	2.65	59.7	50.6	1.48
2H-4, 79-82	13.08	1.80	2.74	60.0	52.0	1.50
2H-5, 79-82	14.58	1.77	2.75	61.5	55.3	1.60
2H-6, 79-82	16.08	1.77	2.80	61.1	54.8	1.57
3H-1, 79-82	18.69	1.81	2.78	60.3	51.8	1.52
3H-2, 79-82	20.19	1.74	2.75	63.3	59.2	1.72
3H-3, 79-82	21.69	1.79	2.75	59.0	50.8	1.44
3H-4, 79-82	23.19	1.76	2.79	61.7	56.0	1.61
3H-5, 79-82	24.69	1.83	2.77	58.5	48.8	1.41
3H-6, 79-82	26.19	1.78	2.73	59.7	52.3	1.48
4H-1, 80-83	28.20	1.73	2.77	63.3	59.9	1.72
4H-2, 80-83	29.70	1.74	2.81	61.8	57.3	1.62
4H-3, 80-83	31.20	1.78	2.76	61.1	54.2	1.57
4H-4, 80-83	32.70	1.80	2.77	64.6	58.2	1.83
4H-5, 80-83	34.20	1.69	2.70	60.3	57.9	1.52
4H-6, 87-90	35.77	1.86	2.77	63.1	53.5	1.71
5H-1, 87-90	37.77	1.79	2.71	59.9	52.2	1.49
5H-2, 79-82	39.19	1.83	2.73	63.1	54.8	1.71
5H-3, 87-90	40.77	1.81	2.75	57.6	48.2	1.36
5H-4, 87-90	42.27	1.80	2.80	59.0	50.4	1.44
5H-5, 87-90	43.77	1.80	2.16	60.8	53.0	1.55
5H-6, 87-90	45.27	1.77	2.66	61.4	55.0	1.59
6H-1, 80-83	47.20	1.77	2.76	63.3	57.8	1.73
6H-2, 80-83	48.70	1.72	2.83	59.8	55.6	1.49
6H-3, 80-83	50.20	1.88	2.75	52.8	40.4	1.12
6H-4, 80-83	51.70	1.78	2.72	61.7	55.0	1.61
6H-5, 80-83	53.20	1.89	2.80	55.8	43.5	1.26
6H-6, 80-83	54.70	1.81	2.78	57.7	48.3	1.37
7H-1, 87-90	56.77	1.77	2.72	56.6	48.8	1.31
7H-2, 87-90	58.27	1.99	2.80	58.0	42.6	1.38
7H-3, 87-90	59.77	1.81	2.75	56.9	47.4	1.32
7H-4, 87-90	61.27	1.79	2.87	58.7	50.5	1.42
7H-5, 83-86	62.73	1.81	2.76	58.0	48.7	1.38
7H-6, 87-90	64.27	1.82	2.74	58.9	49.4	1.43
8H-1, 85-88	66.25	1.80	2.64	57.5	48.5	1.35
8H-2, 85-88	67.75	1.84	2.80	56.7	46.0	1.31
8H-3, 85-88	69.25	1.75	2.73	57.1	50.0	1.33
8H-4, 85-88	70.75	1.86	2.73	55.7	44.4	1.26
8H-5, 85-88	72.25	1.92	2.76	50.1	36.4	1.00
8H-6, 85-88	73.75	1.94	2.78	56.7	42.8	1.31
9H-1, 83-86	75.73	1.80	2.64	58.2	49.4	1.39
9H-2, 85-88	77.25	1.80	2.56	58.3	49.8	1.40
9H-3, 85-88	78.75	1.82	2.56	56.8	46.9	1.32
9H-4, 85-88	80.25	1.77	2.70	59.8	53.0	1.49
9H-5, 85-88	81.75	1.80	2.72	59.0	50.8	1.44
9H-6, 85-88	83.25	1.78	2.84	58.1	50.1	1.39
10H-1, 101-104	85.41	1.86	2.70	52.6	40.9	1.11
10H-2, 101-104	86.91	1.86	2.69	54.2	42.5	1.19
10H-3, 101-104	88.41	1.76	2.70	60.5	54.3	1.53
10H-4, 101-104	89.91	1.76	2.71	59.1	52.7	1.45
10H-5, 101-104	91.41	1.76	2.78	59.4	52.8	1.46
10H-6, 101-104	92.91	1.80	2.69	58.0	49.2	1.38
11H-1, 98-101	94.88	1.74	2.71	60.7	55.5	1.54
11H-2, 101-104	96.41	1.73	2.75	60.3	55.4	1.52
11H-3, 101-104	97.91	1.77	2.68	59.1	52.1	1.45
11H-4, 101-104	99.41	1.76	2.71	60.8	54.8	1.55
11H-5, 101-104	100.91	1.76	2.71	59.7	53.5	1.48
11H-6, 101-104	102.41	1.77	2.56	60.6	53.9	1.54
12H-1, 101-104	104.41	1.76	2.67	60.0	53.6	1.50
12H-2, 101-104	105.91	1.78	2.73	58.2	50.3	1.39
12H-3, 101-104	107.41	1.77	2.66	59.7	52.8	1.48
12H-4, 101-104	108.91	1.80	2.70	59.8	51.7	1.49
12H-5, 105-108	110.45	1.75	2.65	60.3	54.6	1.52
12H-6, 101-104	111.91	1.71	2.84	59.8	55.7	1.49
13H-1, 101-104	113.91	1.80	2.76	58.7	50.4	1.42
13H-2, 101-104	115.46	1.84	2.84	58.4	48.3	1.40
13H-3, 101-104	117.01	1.74	2.63	60.1	54.5	1.50

Table 7 (continued).

Core, section, interval (cm)	Depth (mbsf)	Bulk density (g/cm ³)	Grain density (g/cm ³)	Porosity (%)	Water content (%)	Void ratio
13H-4, 101-104	118.54	1.73	2.76	60.9	56.6	1.56
13H-5, 101-104	120.04	1.85	2.61	54.2	42.8	1.18
13H-6, 101-104	121.54	1.78	2.62	58.5	50.7	1.41
14H-1, 101-104	123.41	1.77	2.64	58.5	51.1	1.41
14H-2, 101-104	124.91	1.74	2.55	60.4	55.5	1.53
14H-3, 111-114	126.51	1.76	2.73	59.3	52.7	1.46
14H-4, 111-114	128.01	1.77	2.77	61.5	55.3	1.60
14H-5, 101-104	129.41	1.77	2.75	59.2	52.0	1.45
14H-6, 106-109	130.96	1.77	2.73	59.2	52.3	1.45
15H-1, 110-113	133.00	1.77	2.75	58.5	51.0	1.41
15H-2, 101-104	134.41	1.81	2.71	59.5	51.0	1.47
15H-3, 105-108	135.95	1.79	2.73	57.5	49.1	1.35
15H-4, 111-114	137.51	1.79	2.73	58.2	50.1	1.39
15H-5, 111-114	139.01	1.76	2.77	59.2	52.4	1.45
15H-6, 111-114	140.51	1.77	2.70	59.4	52.3	1.46
16H-1, 107-110	142.47	1.79	2.70	57.6	49.1	1.36
16H-2, 115-118	144.05	1.78	2.71	58.4	50.7	1.40
16H-3, 111-114	145.51	1.80	2.78	59.6	51.3	1.48
16H-4, 100-103	146.90	1.82	2.73	57.3	47.8	1.34
16H-5, 101-104	148.41	1.77	2.77	57.1	49.2	1.33
16H-6, 75-78	149.65	1.82	2.74	59.5	50.3	1.47
17H-1, 60-63	151.50	1.76	2.70	59.1	52.3	1.44
17H-2, 60-63	153.00	1.80	2.78	59.2	50.9	1.45
17H-3, 60-63	154.50	1.81	2.77	57.2	48.0	1.34
17H-4, 60-63	156.00	1.82	2.71	58.6	49.3	1.41
17H-5, 60-63	157.50	1.81	2.71	58.3	49.2	1.40
17H-6, 60-63	159.00	1.79	2.72	58.4	50.2	1.40
18H-1, 70-73	161.10	1.79	2.76	56.6	47.8	1.31
18H-2, 70-73	162.60	1.79	2.71	59.8	52.2	1.49
18H-3, 70-73	164.10	1.74	2.72	57.5	51.1	1.36
18H-4, 70-73	165.60	1.78	2.67	60.1	52.7	1.51
18H-5, 70-73	167.10	1.74	2.74	58.6	52.4	1.41
18H-6, 70-73	168.60	1.77	2.71	58.6	51.1	1.41
19H-1, 60-63	170.50	1.80	2.78	58.3	49.8	1.40
19H-2, 60-63	172.00	1.83	2.62	57.1	46.8	1.33
19H-3, 60-63	173.50	1.79	2.77	57.6	49.4	1.36
19H-4, 60-63	175.00	1.80	2.74	56.9	47.8	1.32
19H-5, 60-63	176.50	1.83	2.74	56.5	46.4	1.30
19H-6, 60-63	178.00	1.84	2.72	57.1	46.6	1.33
20H-1, 60-63	180.00	1.82	2.75	56.6	46.8	1.31
20H-2, 60-63	181.50	1.85	2.86	58.3	47.7	1.40
20H-3, 60-63	183.00	1.82	2.77	57.8	48.1	1.37
20H-4, 60-63	184.50	1.80	2.70	57.6	48.7	1.36
20H-5, 60-63	186.00	1.79	2.74	58.5	50.5	1.41
20H-6, 60-63	187.50	1.79	2.74	60.2	52.8	1.51
21H-1, 60-63	189.50	1.82	2.75	54.1	43.8	1.18
21H-2, 60-63	191.00	1.81	2.73	55.1	45.3	1.23
21H-3, 60-63	192.50	1.84	2.76	53.7	42.7	1.16
21H-4, 60-63	194.00	1.74	2.52	53.8	46.3	1.17
21H-5, 60-63	195.50	1.85	2.77	53.6	42.2	1.16
21H-6, 60-63	197.00	1.85	2.71	53.9	42.7	1.17
22H-1, 60-63	199.00	1.81	2.89	56.3	46.8	1.29
22H-2, 60-63	200.50	1.79	2.77	56.9	48.2	1.32
22H-3, 60-63	202.00	1.78	2.78	59.2	51.5	1.45
22H-4, 60-63	203.50	1.81	2.74	57.1	47.6	1.33
22H-5, 60-63	205.00	1.79	2.73	56.7	47.9	1.31
22H-6, 60-63	206.50	1.80	2.79	57.8	49.1	1.37
22H-7, 60-63	208.00	1.86	2.71	54.4	42.9	1.19
23H-1, 60-63	208.50	1.79	2.73	56.2	47.5	1.28
23H-2, 60-63	210.00	1.85	2.72	53.2	41.7	1.14
23H-3, 60-63	211.50	1.81	2.78	56.1	46.5	1.28
23H-4, 60-63	213.00	1.86	2.70	53.9	42.3	1.17
23H-5, 60-63	214.50	1.93	2.71	48.5	34.8	0.94
23H-6, 60-63	216.00	1.84	2.70	54.6	43.6	1.20
23H-7, 60-63	217.50	1.84	2.78	55.2	44.5	1.23
24H-1, 60-63	218.00	1.79	2.69	57.1	48.4	1.33
24H-2, 60-63	219.50	1.73	2.70	56.1	49.9	1.28
24H-3, 60-63	221.00	1.79	2.65	59.1	50.9	1.44
24H-4, 60-63	222.50	1.79	2.76	57.8	49.4	1.37
24H-5, 60-63	224.00	1.80	2.66	57.1	48.3	1.33
24H-6, 60-63	225.50	1.80	2.64	56.9	48.0	1.32
25H-1, 60-63	227.50	1.84	2.71	56.0	45.2	1.27
25H-2, 60-63	229.00	1.85	2.67	54.6	43.3	1.20
25H-3, 60-63	230.50	1.81	2.77	55.1	45.3	1.23
25H-4, 60-63	232.00	1.82	2.76	55.6	45.6	1.25
25H-5, 60-63	233.50	1.82	2.79	56.8	47.1	1.31
25H-6, 60-63	235.00	1.82	2.76	57.3	47.5	1.34

Table 7 (continued).

Core, section, interval (cm)	Depth (mbsf)	Bulk density (g/cm ³)	Grain density (g/cm ³)	Porosity (%)	Water content (%)	Void ratio
25H-7, 60-63	236.50	1.82	2.75	56.2	46.4	1.28
26H-1, 60-63	237.00	1.76	2.73	57.8	50.5	1.37
26H-2, 60-63	238.50	1.81	2.76	55.2	45.6	1.23
26H-3, 60-63	240.00	1.79	2.70	56.8	48.1	1.32
26H-4, 60-63	241.50	1.78	2.73	58.8	51.2	1.43
26H-5, 60-63	243.00	1.81	2.72	57.1	47.8	1.33
26H-6, 60-63	244.50	1.82	2.73	55.8	45.9	1.26
27H-2, 60-63	248.00	1.79	2.68	56.1	47.4	1.28
27H-3, 60-63	249.50	1.81	2.95	49.0	38.4	0.96
27H-4, 60-63	251.00	1.81	2.72	56.5	47.2	1.30
27H-5, 60-63	252.50	1.81	2.74	56.4	46.9	1.30
27H-6, 60-63	254.00	1.80	3.17	39.2	28.7	0.65
27H-7, 60-63	255.50	1.85	2.74	54.0	42.6	1.17
28H-1, 60-63	256.00	1.85	2.74	55.7	44.8	1.26
28H-2, 60-63	257.50	1.85	2.73	54.9	43.7	1.22
28H-3, 60-63	259.00	1.85	2.73	55.1	44.1	1.23
28H-4, 60-63	260.50	1.86	2.71	54.9	43.2	1.22
28H-6, 60-63	263.50	1.83	2.72	55.5	45.1	1.25
28H-7, 60-63	265.00	1.87	2.70	51.9	39.8	1.08
29H-1, 60-63	265.50	1.87	2.77	56.9	45.1	1.32
29H-2, 60-63	267.00	1.86	2.72	55.5	44.0	1.25
29H-3, 60-63	268.50	1.81	2.68	56.1	46.5	1.28
29H-4, 60-63	270.00	1.81	2.74	54.7	45.0	1.21
29H-5, 60-63	271.50	1.89	2.69	51.8	38.9	1.08
29H-6, 60-63	273.00	1.90	2.69	52.8	39.9	1.12
30H-1, 60-63	275.00	1.85	2.73	55.2	43.9	1.23
30H-2, 60-63	276.50	1.88	2.75	52.6	40.1	1.11
30H-3, 60-63	278.00	1.88	2.70	54.5	42.4	1.20
30H-4, 60-63	279.50	1.85	2.67	55.7	44.5	1.26
30H-5, 60-63	281.00	1.82	2.70	53.5	42.9	1.15
30H-6, 60-63	282.50	1.83	2.75	53.9	43.2	1.17
31H-1, 60-63	284.50	1.85	2.73	54.4	43.2	1.19
31H-2, 60-63	286.00	1.89	2.71	52.6	40.0	1.11
31H-3, 60-63	287.50	1.85	2.78	53.2	41.8	1.14
31H-4, 60-63	289.00	1.87	2.68	54.5	42.6	1.20
31H-5, 60-63	290.50	1.88	2.74	53.3	41.0	1.14
31H-6, 60-63	292.00	1.86	2.74	54.5	42.7	1.20
32H-1, 60-63	294.00	1.97	2.78	47.7	33.0	0.91
32H-2, 60-63	295.50	1.92	2.74	50.9	37.4	1.04
32H-3, 60-63	297.00	1.85	2.70	53.1	41.8	1.13
32H-4, 60-63	298.50	1.95	2.71	49.9	35.5	1.00
32H-5, 60-63	300.00	1.95	2.91	48.0	33.8	0.92

Electrical-Resistivity Formation Factor

We measured the electrical-resistivity formation factor at three intervals in sections from Hole 818A (see Table 9 and Figs. 19F and 20). Formation factor data from the upper 100 m of Hole 818B show an unexpected proportional relationship to porosity and water content in its general decrease with depth, but the fine structure of the formation-factor/depth relationship shows the expected inverse relationship to water content (see dashed lines of correlation in Fig. 19). From 50 mbsf, formation factor increases downward to a peak at about 160 mbsf, before decreasing again until 250 mbsf. This long-wavelength variation does not parallel changes in porosity, which indicate steady decline over the same interval.

Shear Strength

We measured shear strength in the upper section of Hole 818B (Table 10 and Fig. 19H). Shear strengths increase downward to a depth at which the formation becomes too brittle for measuring vane shear—approximately coinciding with a major change in sediment accumulation rates at 190 mbsf. Some of the fine structure in the shear strength vs. depth function correlates with fine structure in the formation factor and water content functions.

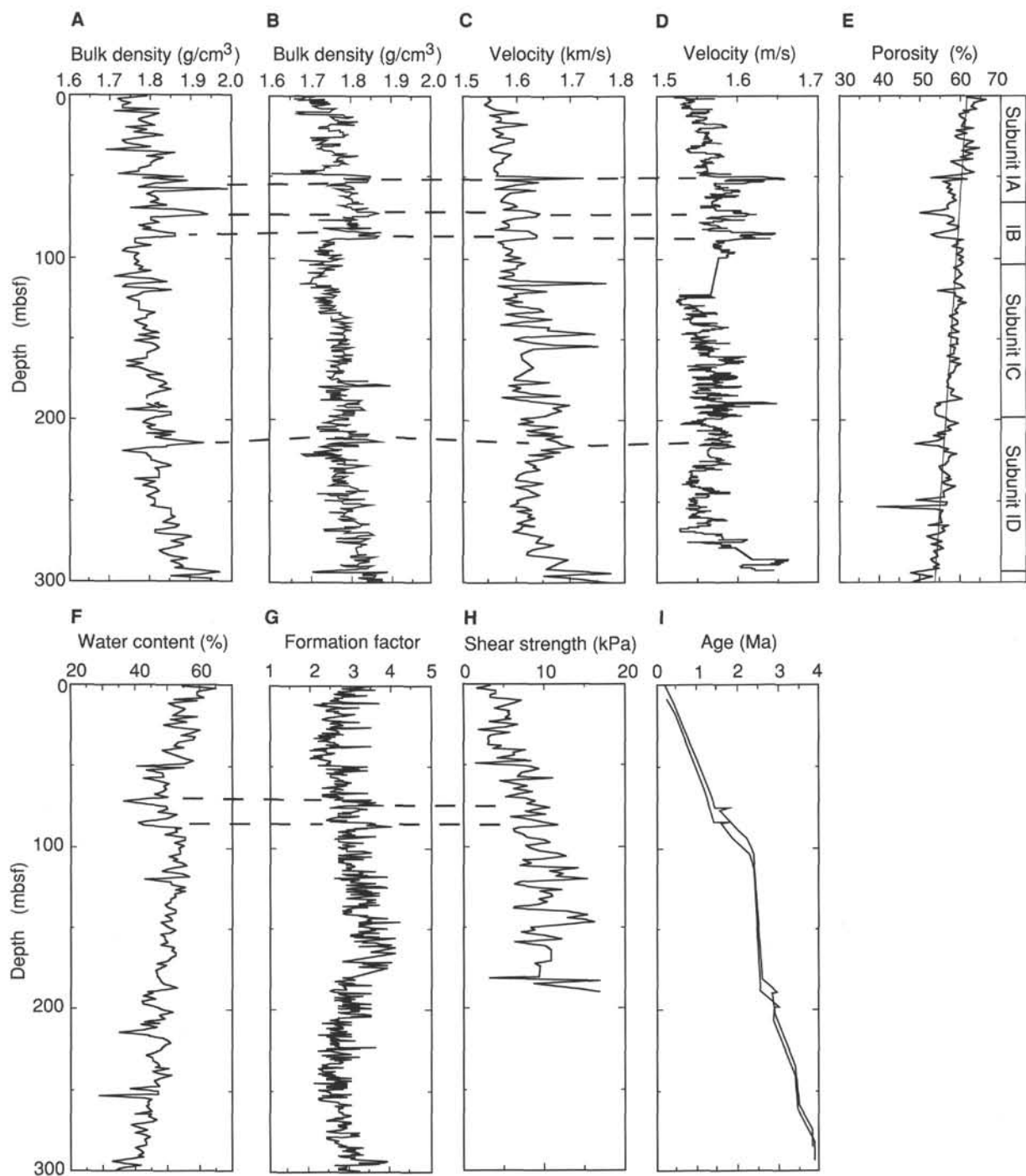


Figure 19. Comparison of velocity with bulk density derived from different sets of measurements, Site 818. **A.** Bulk density calculated from pycnometer and mass observations of discrete samples from split cores. **B.** Bulk-density determined from GRAPE measurements of whole-round cores. **C.** Velocity is determined from traveltime and distance measurements of discrete samples from split cores. **D.** Velocity determined from MST observations of whole-round cores. **E.** Porosity; least-squares linear regression is of the form $Y = 61 - 2.7 \times 10^{-2}X$, where Y is porosity, X is depth, and the regression coefficient $R = 0.70$. Dashed lines highlight details that appear consistently in all sets of observations. **F.** Water content. **G.** Electrical resistivity formation factor. **H.** Shear strength. **I.** Age-depth curves are derived from paleontological dating of core-catcher samples. The two curves indicate possible depth range of dates. Depth ranges are approximately 10 m, the length of a core, which is the sample spacing. Dashed horizontal lines emphasize detailed features that show up consistently in the various sets of measurements. Subunit designations are after “Lithostratigraphy” chapter (this volume).

Table 8. Compressional wave velocity, Site 818.

Core, section, interval (cm)	Depth (mbsf)	Distance (mm)	Traveltime (μ s)	Velocity (m/s)
133-818B-				
1H-1, 79-82	0.79	29.50	21.50	1547
1H-2, 79-82	2.29	27.24	19.98	1552
1H-3, 79-82	3.79	29.51	21.53	1545
1H-4, 79-82	5.29	28.30	20.81	1539
1H-5, 79-82	6.79	28.97	21.12	1550
1H-6, 40-43	7.90	27.80	20.26	1560
2H-2, 79-82	10.08	29.07	20.61	1602
2H-3, 79-82	11.58	30.46	22.10	1549
2H-4, 79-82	13.08	29.70	21.37	1570
2H-5, 79-82	14.58	30.22	21.70	1570
2H-6, 79-82	16.08	28.91	20.94	1563
2H-7, 79-82	17.58	29.40	20.63	1619
3H-1, 79-82	18.69	28.59	20.66	1569
3H-2, 79-82	20.19	28.67	20.87	1555
3H-3, 79-82	21.69	28.85	20.91	1562
3H-4, 79-82	23.19	28.98	20.84	1576
3H-5, 79-82	24.69	28.23	20.51	1562
3H-6, 79-82	26.19	28.41	20.27	1595
4H-1, 80-83	28.20	27.93	19.97	1595
4H-2, 80-83	29.70	27.75	20.10	1571
4H-3, 80-83	31.20	28.02	20.42	1558
4H-4, 80-83	32.70	28.08	20.54	1550
4H-5, 80-83	34.20	30.64	22.16	1554
4H-6, 87-90	35.77	29.33	20.89	1591
5H-1, 87-90	37.77	29.60	21.22	1577
5H-2, 79-82	39.19	28.86	20.81	1572
5H-3, 87-90	40.77	28.76	20.70	1576
5H-4, 87-90	42.27	28.86	20.90	1563
5H-5, 87-90	43.77	28.68	20.85	1558
5H-6, 87-90	45.27	29.65	21.48	1557
6H-1, 80-83	47.20	29.78	21.48	1564
6H-2, 80-83	48.70	29.11	21.08	1562
6H-3, 80-83	50.20	29.20	19.47	1723
6H-4, 80-83	51.70	29.07	21.09	1559
6H-5, 80-83	53.20	29.59	20.52	1641
6H-6, 80-83	54.70	28.99	20.60	1598
7H-1, 87-90	56.77	29.59	21.41	1560
7H-2, 87-90	58.27	30.02	20.86	1634
7H-3, 87-90	59.77	30.13	21.44	1588
7H-4, 87-90	61.27	29.11	20.88	1580
7H-5, 83-86	62.73	29.74	21.35	1574
7H-6, 87-90	64.27	28.15	20.37	1570
8H-1, 85-88	66.25	29.19	20.78	1593
8H-2, 85-88	67.75	28.95	20.55	1601
8H-3, 85-88	69.25	28.02	20.23	1575
8H-4, 85-88	70.75	28.98	20.40	1617
8H-5, 85-88	72.25	28.58	19.89	1642
8H-6, 85-88	73.75	28.98	20.21	1635
9H-1, 83-86	75.73	28.02	20.04	1593
9H-2, 85-88	77.25	27.80	20.13	1572
9H-3, 85-88	78.75	28.89	20.69	1584
9H-4, 85-88	80.25	28.98	20.73	1586
9H-5, 85-88	81.75	28.34	20.61	1559
9H-6, 85-88	83.25	25.57	18.23	1621
10H-1, 101-104	85.41	27.23	19.10	1638
10H-2, 101-104	86.91	27.41	19.23	1636
10H-3, 101-104	88.41	26.62	19.29	1580
10H-4, 101-104	89.91	25.75	18.87	1566
10H-5, 101-104	91.41	27.03	19.59	1576
10H-6, 101-104	92.91	27.19	19.69	1576
11H-1, 98-101	94.88	27.58	19.77	1593
11H-2, 101-104	96.41	27.45	19.71	1590
11H-3, 101-104	97.91	27.80	20.05	1579
11H-4, 101-104	99.41	28.54	20.23	1607
11H-5, 101-104	100.91	29.28	21.03	1576
11H-6, 101-104	102.41	29.54	20.78	1614
12H-1, 101-104	104.41	27.14	19.41	1601
12H-2, 101-104	105.91	28.85	20.48	1601
12H-3, 101-104	107.41	28.50	20.58	1571
12H-4, 101-104	108.91	27.54	19.74	1593
12H-5, 105-108	110.45	28.45	20.28	1596
12H-6, 101-104	111.91	28.29	20.48	1568
13H-1, 101-104	113.91	27.71	19.75	1603
13H-2, 101-104	115.46	28.86	18.89	1765
13H-3, 101-104	117.01	27.62	20.08	1565
13H-4, 101-104	118.54	28.68	20.47	1592

Table 8 (continued).

Core, section, interval (cm)	Depth (mbsf)	Distance (mm)	Traveltime (μ s)	Velocity (m/s)
13H-5, 101-104	120.04	28.40	19.65	1655
13H-6, 101-104	121.54	28.28	20.18	1596
14H-1, 101-104	123.41	29.06	20.64	1599
14H-2, 101-104	124.91	27.80	20.10	1574
14H-3, 111-114	126.51	28.24	20.00	1611
14H-4, 111-114	128.01	28.15	20.27	1579
14H-5, 101-104	129.41	25.94	18.69	1597
14H-6, 106-109	130.96	28.77	20.01	1642
15H-1, 110-113	133.00	28.98	20.04	1651
15H-2, 101-104	134.41	28.95	20.76	1581
15H-3, 105-108	135.95	27.54	19.59	1608
15H-4, 111-114	137.51	27.19	18.83	1664
15H-5, 111-114	139.01	27.40	19.50	1608
15H-6, 111-114	140.51	28.41	20.53	1571
16H-1, 107-110	142.47	29.51	20.27	1661
16H-2, 115-118	144.05	29.11	20.06	1657
16H-3, 111-114	145.51	29.55	19.77	1713
16H-4, 100-103	146.90	29.12	19.22	1745
16H-5, 101-104	148.41	27.64	19.59	1614
16H-6, 75-78	149.65	27.98	20.01	1594
17H-1, 60-63	151.50	28.76	20.20	1623
17H-2, 60-63	153.00	28.08	19.31	1670
17H-3, 60-63	154.50	28.42	18.76	1751
17H-4, 60-63	156.00	28.16	19.74	1631
17H-6, 60-63	159.00	28.58	20.25	1607
18H-2, 70-73	162.60	27.71	19.68	1609
18H-5, 70-73	167.10	28.81	20.14	1631
19H-2, 60-63	172.00	30.82	21.69	1604
19H-3, 60-63	173.50	29.49	20.93	1597
19H-4, 60-63	175.00	30.50	21.60	1594
19H-5, 60-63	176.50	30.07	20.63	1659
19H-6, 60-63	178.00	30.46	21.67	1586
20H-1, 60-63	180.00	30.12	21.20	1608
20H-2, 60-63	181.50	30.46	21.59	1593
20H-3, 60-63	183.00	30.42	21.20	1625
20H-4, 60-63	184.50	29.29	19.94	1680
20H-5, 60-63	186.00	27.50	19.92	1573
20H-6, 60-63	187.50	28.38	20.13	1606
21H-2, 60-63	191.00	28.98	19.59	1697
21H-3, 60-63	192.50	28.24	19.43	1668
21H-4, 60-63	194.00	27.45	18.81	1683
21H-5, 60-63	195.50	28.85	19.83	1664
21H-6, 60-63	197.00	28.98	20.03	1652
21H-7, 60-63	198.50	29.42	20.77	1608
22H-2, 60-63	200.50	28.68	20.08	1629
22H-3, 60-63	202.00	28.98	20.54	1603
22H-4, 60-63	203.50	28.38	19.43	1676
22H-5, 60-63	205.00	29.69	20.47	1652
22H-6, 60-63	206.50	28.50	20.11	1618
22H-7, 60-63	208.00	28.81	19.74	1671
23H-1, 60-63	208.50	29.33	20.59	1619
23H-2, 60-63	210.00	27.54	18.83	1686
23H-3, 60-63	211.50	28.81	19.91	1654
23H-4, 60-63	213.00	28.54	19.55	1674
23H-5, 60-63	214.50	28.98	19.73	1683
23H-6, 60-63	216.00	27.54	18.66	1705
23H-7, 60-63	217.50	28.63	19.52	1683
24H-1, 60-63	218.00	28.62	19.87	1646
24H-2, 60-63	219.50	28.97	19.75	1680
24H-3, 60-63	221.00	28.15	19.83	1622
24H-4, 60-63	222.50	28.75	19.74	1667
24H-5, 60-63	224.00	29.20	20.21	1648
24H-6, 60-63	225.50	29.59	20.79	1616
25H-1, 60-63	227.50	31.03	21.46	1636
25H-2, 60-63	229.00	30.03	20.91	1630
25H-3, 60-63	230.50	31.21	21.51	1642
25H-4, 60-63	232.00	29.98	21.03	1616
25H-5, 60-63	233.50	28.59	20.31	1602
25H-6, 60-63	235.00	27.67	19.74	1601
25H-7, 60-63	236.50	29.41	20.88	1597
26H-1, 60-63	237.00	29.08	20.65	1599
26H-2, 60-63	238.50	29.98	20.69	1648
26H-3, 60-63	240.00	29.38	20.59	1622
26H-4, 60-63	241.50	29.12	20.70	1597
26H-5, 60-63	243.00	30.22	21.12	1621
26H-6, 60-63	244.50	29.59	20.65	1629
26H-7, 60-63	246.00	28.15	19.63	1642
27H-2, 60-63	248.00	28.99	20.43	1614

Table 8 (continued).

Core, section, interval (cm)	Depth (mbsf)	Distance (mm)	Traveltime (μ s)	Velocity (m/s)
27H-3, 60-63	249.50	28.76	20.43	1601
27H-4, 60-63	251.00	29.50	20.87	1603
27H-5, 60-63	252.50	29.37	20.96	1587
27H-6, 60-63	254.00	29.50	20.75	1614
27H-7, 60-63	255.50	30.04	20.94	1628
28H-1, 60-63	256.00	29.98	21.20	1600
28H-2, 60-63	257.50	29.85	20.82	1628
28H-3, 60-63	259.00	30.46	21.29	1619
28H-4, 60-63	260.50	31.36	21.70	1633
28H-6, 60-63	263.50	29.55	20.94	1599
28H-7, 60-63	265.00	30.55	21.20	1633
29H-1, 60-63	265.50	30.38	21.36	1609
29H-2, 60-63	267.00	30.69	21.56	1608
29H-3, 60-63	268.50	31.12	22.00	1593
29H-4, 60-63	270.00	29.98	20.96	1622
29H-5, 60-63	271.50	29.81	20.58	1648
29H-6, 60-63	273.00	30.13	20.83	1643
30H-1, 60-63	275.00	29.68	20.65	1634
30H-2, 60-63	276.50	32.04	21.74	1667
30H-3, 60-63	278.00	30.25	20.75	1658
30H-4, 60-63	279.50	29.24	20.43	1629
30H-5, 60-63	281.00	29.29	20.56	1620
30H-6, 60-63	282.50	29.90	20.97	1617
31H-1, 60-63	284.50	30.07	20.60	1662
31H-2, 60-63	286.00	29.42	19.86	1696
31H-3, 60-63	287.50	28.16	19.27	1679
31H-6, 60-63	292.00	29.77	20.50	1654
32H-1, 60-63	294.00	29.81	19.35	1774
32H-2, 60-63	295.50	29.91	20.63	1649
32H-3, 60-63	297.00	29.59	20.09	1683
32H-5, 60-63	300.00	30.42	19.72	1772

SEISMIC STRATIGRAPHY

The stratigraphic section at Site 818 was divided into five seismic sequences, of which four were drilled (Fig. 21). Each of the sequences is briefly described next and is correlated with lithostratigraphy encountered at the site.

Sequence 1 extends from the seafloor down approximately 0.08 to 1.072 s at Site 818. Much of the character of this sequence is obscured by a strong source pulse at the seafloor. Generally, this sequence is characterized by wavy discontinuous reflectors of various amplitude and frequency. It overlaps sequence 2.

Sequence 2 occurs between 1.072 and 1.175 s at Site 818 (Fig. 22) and is characterized by wavy reflectors of moderate amplitude and frequency.

Sequence 3 occurs between 1.175 and 1.312 s at Site 818 (Fig. 22). The lower boundary is characterized by onlap both to the north and south (Fig. 21). Reflectors tend to be subparallel, with low to high amplitude and moderate frequency.

Sequence 4 occurs between 1.312 and 1.370 s at Site 818 (Fig. 22), but thickens both to the north and south (Fig. 21) to form the walls of a channel in which sequence 3 was deposited. The sequence is characterized by subparallel, low-amplitude reflectors.

Sequence 5 occurs between 1.370 and 1.420 s at Site 818 (Fig. 22). The upper surface is characterized by erosional truncation and moderate to low amplitude discontinuous reflectors.

Site 818 was not logged; thus, correlation between seismic sequences and lithostratigraphy encountered at the site is based on an approximate velocity/depth curve (Fig. 7) constructed from interval velocities that were derived from the stacking velocities used to process these seismic data. None-

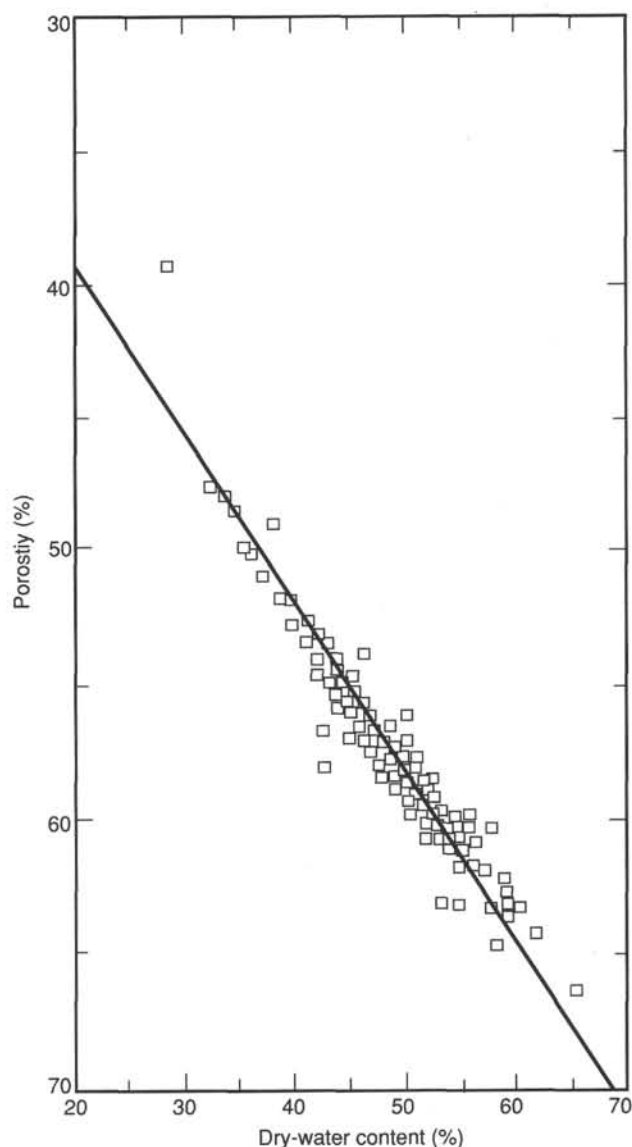


Figure 20. Dry-water content vs. porosity for Site 818. Data are derived from mass and pycnometer volume measurements of discrete samples from cores. Least-squares linear regression is of the form $Y = -43 + 1.6X$, where Y is porosity, X is depth, and the regression coefficient $R = 0.96$.

theless, the sequences correlated well with units identified in the lithostratigraphy.

Sequences 1 through 3 form a total thickness of approximately 300 m that corresponds to the Pliocene-Pleistocene periplatform ooze with minor turbidite beds and slumped horizons of lithologic Unit I (Fig. 22). These three sequences form a broad, mounded, overlapping channel fill. Sequence 4 forms the walls of the channel (Fig. 21), which has been cut on the slope in front of a carbonate platform. The top of sequence 4 consists of calcareous chalk.

SUMMARY AND CONCLUSIONS

For a discussion of this site, the reader is directed to the "Summary and Conclusions" section of the "Site 817" chapter (this volume).

REFERENCES

- Andrews, J. E., 1973. Correlation of seismic reflectors. In Burns, R. E., Andrews, J. E., et al., *Init. Repts. DSDP, 21*: Washington (U.S. Govt. Printing Office), 459–479.
- Baker, P. A., 1986. Pore-water chemistry of carbonate-rich sediments, Lord Howe Rise, southwest Pacific Ocean. In Kennett, J. P., von der Borch, C. C., et al., *Init. Repts. DSDP, 90*: Washington (U.S. Government Printing Office), 1249–1256.
- Droxler, A. W., Bruce, C. H., Sager, W. W., and Watkins, D. H., 1988. Pliocene-Pleistocene variations in aragonite content and planktonic oxygen-isotope record in Bahamian periplatform ooze, Hole 633A. In Austin, J. A., Jr., Schlager, W., et al., *Proc. ODP, Sci. Results, 101*: College Station, TX (Ocean Drilling Program), 221–244.
- Feary, D. A., Pigram, C. J., Davies, P. J., Symonds, P. A., Droxler, A. W., and Peerdeman, F., 1990. Ocean Drilling Program—Leg 133 safety package. *Bur. Miner. Res. Aust. Rec.*, 1990/6.
- Kennett, J. P., von der Borch, C. C., et al., 1986. *Init. Repts. DSDP, 90*: Washington (U.S. Govt. Printing Office).
- Schlager, W., and James, N. P., 1978. Low-magnesian calcite limestones forming at the deep-sea floor, Tongue of the Ocean, Bahamas. *Sedimentology*, 15:675–702.
- Schlanger, S. O., Jackson, E. D., et al., 1976. *Init. Repts. DSDP, 33*: Washington (U.S. Govt. Printing Office).
- Swart, P. K., and Guzikowski, M., 1988. Interstitial-water chemistry and diagenesis of periplatform sediments from the Bahamas, ODP Leg 101. In Austin, J. A., Jr., Schlager, W., et al., *Proc. ODP, Sci. Results, 101*: College Station, TX (Ocean Drilling Program), 363–380.
- Symonds, P. A., and Davies, P. J., 1988. Structure, stratigraphy, evolution and regional framework of the Townsville Trough and Marion Plateau region—research cruise proposal, project 9131.11. *Bur. Miner. Res. Aust. Rec.*, 1988/48.
- van Morkhoven, F.P.C.M., Berggren, W. A., Edwards, A. S., et al., 1986. Cenozoic cosmopolitan deep-water benthic foraminifera. *Bull. Cent. Rech. Explor.-Prod. Elf-Aquitaine*, Mem. 11.

Ms 133-111

NOTE: All core description forms (“barrel sheets”) and core photographs have been printed on coated paper and bound separately as Part 2 of this volume, beginning on page 813.

Table 9. Electrical-resistivity formation factor data, Site 818.

Core, section, interval (cm)	Depth (mbsf)	Seawater (ohms)	Sample (ohms)	Formation factor
133-818B-				
1H-1, 20-20	0.20	2.9	10.0	3.45
1H-1, 70-70	0.70	2.9	9.2	3.17
1H-1, 120-120	1.20	2.9	9.7	3.34
1H-2, 20-20	1.70	2.9	8.2	2.83
1H-2, 70-70	2.20	2.9	10.3	3.55
1H-2, 120-120	2.70	2.9	9.3	3.21
1H-3, 20-20	3.20	3.0	8.5	2.83
1H-3, 70-70	3.70	2.9	7.7	2.66
1H-3, 120-120	4.20	2.8	7.5	2.68
1H-4, 20-20	4.70	2.8	8.6	3.07
1H-4, 70-70	5.20	2.9	7.4	2.55
1H-4, 120-120	5.70	2.9	8.2	2.83
1H-5, 20-20	6.20	2.9	9.9	3.41
1H-5, 70-70	6.70	2.9	8.1	2.79
1H-5, 120-120	7.20	2.9	8.1	2.79
1H-6, 20-20	7.70	2.8	7.3	2.61
1H-6, 70-70	8.20	2.8	7.6	2.71
2H-2, 20-20	9.49	2.8	7.0	2.50
2H-2, 70-70	9.99	2.8	8.2	2.93
2H-2, 120-120	10.49	2.8	10.3	3.68
2H-3, 20-20	10.99	2.8	6.4	2.29
2H-3, 70-70	11.49	2.9	6.9	2.38
2H-3, 120-120	11.99	3.0	6.2	2.07
2H-4, 20-20	12.49	2.9	6.6	2.28
2H-4, 70-70	12.99	2.9	8.1	2.79
2H-4, 120-120	13.49	2.9	9.3	3.21
2H-5, 20-20	13.99	2.9	7.1	2.45
2H-5, 70-70	14.49	2.8	7.4	2.64
2H-5, 120-120	14.99	2.8	6.7	2.39
2H-6, 20-20	15.49	2.8	6.8	2.43
2H-6, 70-70	15.99	2.8	7.5	2.68
2H-6, 120-120	16.49	2.8	7.3	2.61
2H-7, 20-20	16.99	2.8	7.9	2.82
2H-7, 70-70	17.49	2.8	8.8	3.14
2H-7, 120-120	17.99	2.8	7.9	2.82
3H-1, 20-20	18.10	2.9	8.3	2.86
3H-1, 70-70	18.60	2.9	8.3	2.86
3H-1, 120-120	19.10	2.9	7.6	2.62
3H-2, 20-20	19.60	2.8	6.7	2.39
3H-2, 70-70	20.10	2.8	6.7	2.39
3H-2, 120-120	20.60	2.8	6.4	2.29
3H-3, 20-20	21.10	2.9	6.6	2.28
3H-3, 70-70	21.60	2.9	7.3	2.52
3H-3, 120-120	22.10	2.9	9.4	3.24
3H-4, 20-20	22.60	2.9	7.6	2.62
3H-4, 70-70	23.10	2.9	7.1	2.45
3H-4, 120-120	23.60	2.9	7.9	2.72
3H-5, 20-20	24.10	2.9	8.0	2.76
3H-5, 70-70	24.60	2.9	7.6	2.62
3H-5, 120-120	25.10	2.9	7.5	2.59
3H-6, 20-20	25.60	2.9	7.3	2.52
3H-6, 70-70	26.10	2.9	10.2	3.52
3H-6, 120-120	26.60	2.9	7.0	2.41
4H-1, 20-20	27.60	2.9	7.5	2.59
4H-1, 70-70	28.10	2.9	7.7	2.66
4H-1, 120-120	28.60	2.9	7.9	2.72
4H-2, 20-20	29.10	2.9	6.8	2.34
4H-2, 70-70	29.60	2.9	7.8	2.69
4H-2, 120-120	30.10	2.9	8.0	2.76
4H-3, 20-20	30.60	2.9	6.4	2.21
4H-3, 70-70	31.10	2.9	6.8	2.34
4H-3, 120-120	31.60	2.9	7.5	2.59
4H-4, 20-20	32.10	2.9	6.2	2.14
4H-4, 70-70	32.60	2.9	7.3	2.52
4H-4, 120-120	33.10	2.9	6.9	2.38
4H-5, 20-20	33.60	2.9	6.3	2.17
4H-5, 70-70	34.10	2.9	6.9	2.38
4H-5, 120-120	34.60	2.9	7.3	2.52
4H-6, 20-20	35.10	2.9	7.6	2.62
4H-6, 70-70	35.60	2.9	7.5	2.59
4H-6, 120-120	36.10	2.9	7.9	2.72
4H-7, 20-20	36.60	3.0	7.3	2.43
4H-7, 70-70	37.10	3.0	8.1	2.70
5H-1, 20-20	37.10	2.9	7.3	2.52
5H-1, 70-70	37.60	2.9	10.2	3.52
5H-1, 120-120	38.10	2.9	7.1	2.45

Table 9 (continued).

Core, section, interval (cm)	Depth (mbsf)	Seawater (ohms)	Sample (ohms)	Formation factor
5H-2, 20-20	38.60	3.0	6.2	2.07
5H-2, 70-70	39.10	3.0	7.3	2.43
5H-2, 120-120	39.60	3.0	6.1	2.03
5H-3, 20-20	40.10	3.0	6.9	2.30
5H-3, 70-70	40.60	3.0	7.2	2.40
5H-3, 120-120	41.10	3.0	7.3	2.43
5H-4, 20-20	41.60	3.0	7.8	2.60
5H-4, 70-70	42.10	3.0	7.4	2.47
5H-4, 120-120	42.60	3.0	7.5	2.50
5H-5, 20-20	43.10	3.2	6.7	2.09
5H-5, 70-70	43.60	3.2	7.3	2.28
5H-5, 120-120	44.10	3.2	6.7	2.09
5H-6, 20-20	44.60	3.2	6.5	2.03
5H-6, 70-70	45.10	3.2	7.0	2.19
5H-6, 120-120	45.60	3.2	7.4	2.31
6H-1, 20-20	46.60	3.0	7.4	2.47
6H-1, 70-70	47.10	3.0	7.4	2.47
6H-1, 120-120	47.60	3.0	7.5	2.50
6H-2, 20-20	48.10	3.0	7.1	2.37
6H-2, 70-70	48.60	3.0	7.5	2.50
6H-2, 120-120	49.10	2.9	6.3	2.17
6H-3, 20-20	49.60	2.9	9.0	3.10
6H-3, 70-70	50.10	2.9	9.8	3.38
6H-3, 120-120	50.60	2.9	8.2	2.83
6H-4, 20-20	51.10	2.9	9.2	3.17
6H-4, 70-70	51.60	2.9	7.0	2.41
6H-4, 120-120	52.10	2.9	8.3	2.86
6H-5, 20-20	52.60	2.9	9.8	3.38
6H-5, 70-70	53.10	3.0	7.7	2.57
6H-5, 120-120	53.60	3.0	8.4	2.80
6H-6, 20-20	54.10	3.0	7.2	2.40
6H-6, 70-70	54.60	3.0	8.7	2.90
6H-6, 120-120	55.10	3.0	7.4	2.47
7H-1, 20-20	56.10	3.0	7.4	2.47
7H-1, 70-70	56.60	2.8	7.0	2.50
7H-1, 120-120	57.10	2.8	7.5	2.68
7H-2, 20-20	57.60	2.9	7.9	2.72
7H-2, 70-70	58.10	2.9	8.2	2.83
7H-2, 120-120	58.60	2.9	7.5	2.59
7H-3, 20-20	59.10	2.9	8.0	2.76
7H-3, 70-70	59.60	2.9	8.8	3.03
7H-3, 120-120	60.10	2.9	8.0	2.76
7H-4, 20-20	60.60	2.9	7.5	2.59
7H-4, 70-70	61.10	2.9	7.7	2.66
7H-4, 120-120	61.60	2.9	8.5	2.93
7H-5, 20-20	62.10	3.0	8.1	2.70
7H-5, 70-70	62.60	3.0	6.9	2.30
7H-5, 120-120	63.10	2.8	7.4	2.64
7H-6, 20-20	63.60	2.8	7.7	2.75
7H-6, 70-70	64.10	2.8	7.2	2.57
7H-6, 120-120	64.60	2.8	7.3	2.61
8H-1, 20-20	65.60	2.8	7.1	2.54
8H-1, 70-70	66.10	2.8	9.5	3.39
8H-1, 120-120	66.60	2.8	8.9	3.18
8H-2, 20-20	67.10	2.9	6.7	2.31
8H-2, 70-70	67.60	2.9	7.8	2.69
8H-2, 120-120	68.10	2.9	6.8	2.34
8H-3, 20-20	68.60	2.9	7.1	2.45
8H-3, 70-70	69.10	2.9	8.1	2.79
8H-3, 120-120	69.60	2.8	7.5	2.68
8H-4, 20-20	70.10	2.9	7.4	2.55
8H-4, 70-70	70.60	2.8	9.9	3.54
8H-4, 120-120	71.10	2.8	9.2	3.29
8H-5, 20-20	71.60	2.8	7.9	2.82
8H-5, 70-70	72.10	2.8	10.1	3.61
8H-5, 120-120	72.60	2.8	9.1	3.25
8H-6, 20-20	73.10	2.7	8.7	3.22
8H-6, 70-70	73.60	2.7	10.2	3.78
8H-6, 120-120	74.10	2.7	7.9	2.93
9H-1, 20-20	75.10	2.7	6.7	2.48
9H-1, 70-70	75.60	2.7	8.4	3.11
9H-1, 120-120	76.10	2.7	9.3	3.44
9H-2, 20-20	76.60	2.7	8.5	3.15
9H-2, 70-70	77.10	2.7	8.7	3.22
9H-2, 120-120	77.60	2.7	8.0	2.96
9H-3, 20-20	78.10	2.7	7.5	2.78
9H-3, 70-70	78.60	2.7	8.0	2.96
9H-3, 120-120	79.10	2.7	7.4	2.74

Table 9 (continued).

Core, section, interval (cm)	Depth (mbsf)	Seawater (ohms)	Sample (ohms)	Formation factor
9H-4, 20-20	79.60	2.7	7.3	2.70
9H-4, 70-70	80.10	2.7	7.4	2.74
9H-4, 120-120	80.60	2.7	8.5	3.15
9H-5, 20-20	81.10	2.7	7.8	2.89
9H-5, 70-70	81.60	2.7	7.3	2.70
9H-5, 120-120	82.10	2.7	6.7	2.48
9H-6, 20-20	82.60	2.7	6.6	2.44
9H-6, 70-70	83.10	2.7	7.8	2.89
9H-6, 120-120	83.60	2.7	6.8	2.52
10H-1, 20-20	84.60	2.8	9.7	3.46
10H-1, 70-70	85.10	2.8	10.1	3.61
10H-1, 120-120	85.60	2.8	9.8	3.50
10H-2, 20-20	86.10	2.8	9.6	3.43
10H-2, 70-70	86.60	2.8	10.0	3.57
10H-2, 120-120	87.10	2.8	11.1	3.96
10H-3, 20-20	87.60	2.8	8.6	3.07
10H-3, 70-70	88.10	2.8	9.5	3.39
10H-3, 120-120	88.60	2.8	8.2	2.93
10H-4, 20-20	89.10	2.8	8.6	3.07
10H-4, 70-70	89.60	2.8	7.7	2.75
10H-4, 120-120	90.10	2.8	7.6	2.71
10H-5, 20-20	90.60	2.7	7.7	2.85
10H-5, 70-70	91.10	2.7	8.1	3.00
10H-5, 120-120	91.60	2.7	7.5	2.78
10H-6, 20-20	92.10	2.7	8.3	3.07
10H-6, 70-70	92.60	2.7	7.2	2.67
10H-6, 120-120	93.10	2.7	9.7	3.59
11H-1, 20-20	94.10	2.7	7.0	2.59
11H-1, 70-70	94.60	2.7	7.4	2.74
11H-1, 120-120	95.10	2.7	7.4	2.74
11H-2, 20-20	95.60	2.7	7.4	2.74
11H-2, 70-70	96.10	2.7	7.3	2.70
11H-2, 120-120	96.60	2.7	8.9	3.30
11H-3, 20-20	97.10	2.7	7.7	2.85
11H-3, 70-70	97.60	2.7	7.7	2.85
11H-3, 120-120	98.10	2.7	7.6	2.81
11H-4, 20-20	98.60	2.7	8.4	3.11
11H-4, 70-70	99.10	2.7	7.6	2.81
11H-4, 120-120	99.60	2.7	7.3	2.70
11H-5, 20-20	100.10	2.7	7.6	2.81
11H-5, 70-70	100.60	2.7	7.9	2.93
11H-5, 120-120	101.10	2.7	7.8	2.89
11H-6, 20-20	101.60	2.7	7.7	2.85
11H-6, 70-70	102.10	2.7	8.9	3.30
11H-6, 120-120	102.60	2.7	9.5	3.52
12H-1, 20-20	103.60	2.7	8.2	3.04
12H-1, 70-70	104.10	2.7	7.4	2.74
12H-1, 120-120	104.60	2.7	7.5	2.78
12H-2, 20-20	105.10	2.7	8.8	3.26
12H-2, 70-70	105.60	2.7	9.4	3.48
12H-2, 120-120	106.10	2.7	7.4	2.74
12H-3, 20-20	106.60	2.7	8.9	3.30
12H-3, 70-70	107.10	2.7	7.3	2.70
12H-3, 120-120	107.60	2.7	7.4	2.74
12H-4, 20-20	108.10	2.6	7.2	2.77
12H-4, 70-70	108.60	2.6	7.1	2.73
12H-4, 120-120	109.10	2.6	7.7	2.96
12H-5, 20-20	109.60	2.6	7.5	2.88
12H-5, 70-70	110.10	2.6	7.6	2.92
12H-5, 120-120	110.60	2.6	7.8	3.00
12H-6, 20-20	111.10	2.6	8.0	3.08
12H-6, 70-70	111.60	2.6	7.9	3.04
12H-6, 120-120	112.10	2.6	7.5	2.88
13H-1, 20-20	113.10	2.6	7.9	3.04
13H-1, 70-70	113.60	2.6	7.3	2.81
13H-1, 120-120	114.10	2.6	9.4	3.62
13H-2, 20-20	114.65	2.6	8.4	3.23
13H-2, 70-70	115.15	2.6	8.5	3.27
13H-2, 120-120	115.65	2.6	8.2	3.15
13H-3, 20-20	116.20	2.6	7.3	2.81
13H-3, 70-70	116.70	2.6	8.8	3.38
13H-3, 120-120	117.20	2.6	7.5	2.88
13H-4, 20-20	117.73	2.6	10.0	3.85
13H-4, 70-70	118.23	2.6	6.8	2.62
13H-4, 120-120	118.73	2.6	6.9	2.65
13H-5, 20-20	119.23	2.6	7.2	2.77
13H-5, 70-70	119.73	2.6	8.3	3.19
13H-5, 120-120	120.23	2.6	7.8	3.00

Table 9 (continued).

Core, section, interval (cm)	Depth (mbsf)	Seawater (ohms)	Sample (ohms)	Formation factor
13H-6, 20-20	120.73	2.6	7.9	3.04
13H-6, 70-70	121.23	2.6	7.9	3.04
13H-6, 120-120	121.73	2.6	9.3	3.58
14H-1, 20-20	122.60	2.6	7.5	2.88
14H-1, 70-70	123.10	2.6	9.0	3.46
14H-1, 120-120	123.60	2.6	9.6	3.69
14H-2, 20-20	124.10	2.6	10.1	3.88
14H-2, 70-70	124.60	2.6	8.0	3.08
14H-2, 120-120	125.10	2.6	7.6	2.92
14H-3, 20-20	125.60	2.6	8.7	3.35
14H-3, 70-70	126.10	2.6	8.0	3.08
14H-3, 120-120	126.60	2.6	9.1	3.50
14H-4, 20-20	127.10	2.6	7.5	2.88
14H-4, 70-70	127.60	2.6	9.6	3.69
14H-4, 120-120	128.10	2.6	7.9	3.04
14H-5, 20-20	128.60	2.6	8.2	3.15
14H-5, 70-70	129.10	2.6	9.7	3.73
14H-5, 120-120	129.60	2.6	9.3	3.58
14H-6, 20-20	130.10	2.6	8.4	3.23
14H-6, 70-70	130.60	2.6	7.5	2.88
14H-6, 120-120	131.10	2.6	7.5	2.88
15H-1, 20-20	132.10	2.6	9.4	3.62
15H-1, 70-70	132.60	2.6	8.7	3.35
15H-1, 120-120	133.10	2.6	8.8	3.38
15H-2, 20-20	133.60	2.6	9.4	3.62
15H-2, 70-70	134.10	2.6	8.3	3.19
15H-2, 120-120	134.67	2.6	8.6	3.31
15H-3, 20-20	135.10	2.6	9.5	3.65
15H-3, 70-70	135.60	2.6	7.3	2.81
15H-3, 120-120	136.10	2.6	8.5	3.27
15H-4, 20-20	136.60	2.6	8.8	3.38
15H-4, 70-70	137.10	2.6	8.1	3.12
15H-4, 120-120	137.60	2.6	7.6	2.92
15H-5, 20-20	138.10	2.6	7.9	3.04
15H-5, 70-70	138.60	2.6	7.3	2.81
15H-5, 120-120	139.10	2.6	7.4	2.85
15H-6, 20-20	139.60	2.6	7.9	3.04
15H-6, 70-70	140.10	2.6	7.3	2.81
15H-6, 120-120	140.60	2.6	7.5	2.88
16H-1, 20-20	141.60	2.6	8.8	3.38
16H-1, 70-70	142.10	2.6	8.3	3.19
16H-1, 120-120	142.60	2.6	8.9	3.42
16H-2, 20-20	143.10	2.6	10.2	3.92
16H-2, 70-70	143.60	2.6	9.2	3.54
16H-2, 120-120	144.10	2.6	8.8	3.38
16H-3, 20-20	144.60	2.6	8.7	3.35
16H-3, 70-70	145.10	2.6	9.2	3.54
16H-3, 120-120	145.60	2.6	8.2	3.15
16H-4, 20-20	146.10	2.6	11.0	4.23
16H-4, 70-70	146.60	2.6	8.3	3.19
16H-4, 120-120	147.00	2.6	9.2	3.54
16H-5, 20-20	147.60	2.6	8.3	3.19
16H-5, 70-70	148.10	2.6	8.3	3.19
16H-5, 120-120	148.60	2.6	8.6	3.31
16H-6, 20-20	149.10	2.6	9.2	3.54
16H-6, 70-70	149.60	2.6	10.2	3.92
16H-6, 120-120	150.10	2.6	9.0	3.46
17H-1, 20-20	151.10	2.6	9.4	3.62
17H-1, 70-70	151.60	2.6	8.2	3.15
17H-1, 120-120	152.10	2.6	9.5	3.65
17H-2, 20-20	152.60	2.6	8.7	3.35
17H-2, 70-70	153.10	2.6	7.9	3.04
17H-2, 120-120	153.60	2.6	8.6	3.31
17H-3, 20-20	154.10	2.6	7.7	2.96
17H-3, 70-70	154.60	2.6	9.5	3.65
17H-3, 120-120	155.10	2.6	8.1	3.12
17H-4, 20-20	155.60	2.6	9.5	3.65
17H-4, 70-70	156.10	2.6	10.7	4.12
17H-4, 120-120	146.60	2.6	9.7	3.73
17H-5, 20-20	157.10	2.6	8.1	3.12
17H-5, 70-70	157.60	2.6	8.7	3.35
17H-5, 120-120	158.10	2.6	8.5	3.27
17H-6, 20-20	158.60	2.6	9.4	3.62
17H-6, 70-70	159.10	2.6	9.7	3.73
17H-6, 120-120	159.60	2.6	10.3	3.96
18H-1, 20-20	160.60	2.6	8.4	3.23
18H-1, 70-70	161.10	2.6	9.6	3.69
18H-1, 120-120	161.60	2.6	10.6	4.08

Table 9 (continued).

Core, section, interval (cm)	Depth (mbsf)	Seawater (ohms)	Sample (ohms)	Formation factor
18H-3, 20-20	163.60	2.6	9.6	3.69
18H-3, 70-70	164.10	2.6	9.0	3.46
18H-3, 120-120	164.60	2.6	10.6	4.08
19H-1, 20-20	170.10	2.6	7.3	2.81
19H-1, 70-70	170.60	2.6	8.9	3.42
19H-1, 120-120	171.10	2.6	10.4	4.00
19H-2, 20-20	171.60	2.6	8.6	3.31
19H-2, 70-70	172.10	2.6	10.2	3.92
19H-2, 120-120	172.60	2.6	9.5	3.65
19H-3, 20-20	173.10	2.6	8.2	3.15
19H-3, 70-70	173.60	2.6	8.4	3.23
19H-3, 120-120	174.10	2.6	10.2	3.92
20H-1, 20-20	179.60	2.6	7.8	3.00
20H-1, 70-70	180.10	2.6	7.3	2.81
20H-1, 120-120	180.60	2.6	7.7	2.96
20H-2, 20-20	181.10	2.6	8.1	3.12
20H-2, 70-70	181.60	2.6	7.4	2.85
20H-2, 120-120	182.10	2.7	7.1	2.63
20H-3, 20-20	182.60	2.8	7.4	2.64
20H-3, 70-70	183.10	2.8	8.5	3.04
20H-3, 120-120	183.60	2.8	8.8	3.14
20H-4, 20-20	184.10	2.8	7.6	2.71
20H-4, 70-70	184.60	2.8	9.9	3.54
20H-4, 120-120	185.10	2.8	7.8	2.79
20H-6, 20-20	187.10	2.8	8.0	2.86
20H-6, 70-70	187.60	2.8	7.2	2.57
20H-6, 120-120	188.10	2.8	7.0	2.50
21H-1, 20-20	189.10	2.8	7.4	2.64
21H-1, 70-70	189.60	2.8	9.8	3.50
21H-1, 120-120	190.10	2.8	7.5	2.68
21H-2, 20-20	190.60	2.8	7.8	2.79
21H-2, 70-70	191.10	2.8	8.4	3.00
21H-2, 120-120	191.60	2.8	9.3	3.32
21H-3, 20-20	192.10	2.8	7.3	2.61
21H-3, 70-70	192.60	2.8	7.5	2.68
21H-3, 120-120	193.10	2.8	8.7	3.11
21H-4, 20-20	193.60	2.8	7.2	2.57
21H-4, 70-70	194.10	2.8	8.3	2.96
21H-4, 120-120	194.60	2.8	7.7	2.75
21H-5, 20-20	195.10	2.8	7.7	2.75
21H-5, 70-70	195.60	2.8	8.8	3.14
21H-5, 120-120	196.10	2.8	9.9	3.54
21H-6, 20-20	196.60	2.8	7.8	2.79
21H-6, 70-70	197.10	2.8	8.9	3.18
21H-6, 120-120	197.60	2.8	7.5	2.68
21H-7, 20-20	198.10	2.8	8.6	3.07
21H-7, 70-70	198.60	2.8	9.8	3.50
22H-1, 20-20	198.60	2.8	7.5	2.68
22H-1, 70-70	199.10	2.8	8.7	3.11
22H-1, 120-120	199.60	2.6	8.2	3.15
22H-2, 20-20	200.10	2.6	7.7	2.96
22H-2, 70-70	200.60	2.6	8.3	3.19
22H-2, 120-120	201.10	2.6	7.3	2.81
22H-3, 20-20	201.60	2.6	7.1	2.73
22H-3, 70-70	202.10	2.6	7.7	2.96
22H-3, 120-120	202.60	2.6	8.5	3.27
22H-4, 20-20	203.10	2.6	9.0	3.46
22H-4, 70-70	203.60	2.6	7.8	3.00
22H-4, 120-120	204.10	2.6	9.2	3.54
22H-5, 20-20	204.60	2.9	7.7	2.66
22H-5, 70-70	205.10	2.9	7.7	2.66
22H-5, 120-120	205.60	2.9	7.8	2.69
22H-6, 20-20	206.10	2.9	7.3	2.52
22H-6, 70-70	206.60	2.9	7.1	2.45
22H-6, 120-120	207.10	2.8	8.4	3.00
23H-1, 20-20	208.10	3.0	6.8	2.27
23H-1, 70-70	208.60	3.0	8.9	2.97
23H-1, 120-120	209.10	3.0	7.9	2.63
23H-2, 20-20	209.60	3.0	8.1	2.70
23H-2, 70-70	210.10	3.0	8.5	2.83
23H-2, 120-120	210.60	3.0	8.3	2.77
23H-3, 20-20	211.10	3.0	7.3	2.43
23H-3, 70-70	211.60	3.0	8.3	2.77
23H-3, 120-120	212.10	3.0	7.6	2.53
23H-4, 20-20	212.60	3.0	8.3	2.77
23H-4, 70-70	213.10	3.0	8.8	2.93
23H-4, 120-120	213.60	3.0	8.2	2.73
23H-5, 20-20	214.10	3.1	7.7	2.48

Table 9 (continued).

Core, section, interval (cm)	Depth (mbsf)	Seawater (ohms)	Sample (ohms)	Formation factor
23H-5, 70-70	214.70	3.1	9.3	3.00
23H-5, 120-120	215.10	3.1	6.9	2.23
23H-6, 20-20	215.60	3.1	8.0	2.58
23H-6, 70-70	216.10	3.1	9.4	3.03
23H-6, 120-120	216.60	3.1	7.5	2.42
24H-1, 20-20	217.60	3.1	8.4	2.71
24H-1, 70-70	218.10	3.1	7.7	2.48
24H-1, 120-120	218.60	3.1	9.6	3.10
24H-2, 20-20	219.10	3.1	7.6	2.45
24H-2, 70-70	219.60	3.1	8.1	2.61
24H-2, 120-120	220.10	3.1	8.2	2.65
24H-3, 20-20	220.60	3.1	7.7	2.48
24H-3, 70-70	221.10	3.1	7.8	2.52
24H-3, 120-120	221.60	3.1	8.3	2.68
24H-4, 20-20	222.10	3.1	7.9	2.55
24H-4, 70-70	222.60	3.1	8.6	2.77
24H-4, 120-120	223.10	3.1	11.2	3.61
24H-5, 20-20	223.60	3.1	7.5	2.42
24H-5, 70-70	224.10	3.1	9.8	3.16
24H-5, 120-120	224.50	3.1	7.7	2.48
24H-6, 20-20	225.10	3.1	6.9	2.23
24H-6, 70-70	225.60	3.1	7.8	2.52
24H-6, 120-120	226.10	3.0	8.1	2.70
25H-1, 20-20	227.10	3.1	9.3	3.00
25H-1, 70-70	227.60	3.1	7.1	2.29
25H-1, 120-120	228.10	3.1	7.3	2.35
25H-2, 20-20	228.60	3.1	7.5	2.42
25H-2, 70-70	229.10	3.1	9.8	3.16
25H-2, 120-120	229.60	3.1	8.1	2.61
25H-3, 20-20	230.10	3.1	7.7	2.48
25H-3, 70-70	230.60	3.1	9.2	2.97
25H-3, 120-120	231.10	3.1	7.9	2.55
25H-4, 20-20	231.60	3.1	8.4	2.71
25H-4, 70-70	232.10	3.1	8.7	2.81
25H-4, 120-120	232.60	3.1	8.2	2.65
25H-5, 20-20	233.10	3.0	7.4	2.47
25H-5, 70-70	233.60	3.0	7.2	2.40
25H-5, 120-120	234.10	3.0	7.0	2.33
25H-6, 20-20	234.60	3.0	7.3	2.43
25H-6, 70-70	235.10	3.0	6.9	2.30
25H-6, 120-120	235.60	3.0	8.5	2.83
25H-7, 20-20	236.10	3.0	7.2	2.40
25H-7, 70-70	236.60	3.1	7.1	2.29
26H-1, 20-20	236.60	3.1	6.9	2.23
26H-1, 70-70	237.10	3.1	7.0	2.26
26H-1, 120-120	237.60	3.1	7.1	2.29
26H-2, 20-20	238.10	3.1	8.0	2.58
26H-2, 70-70	238.60	3.1	7.8	2.52
26H-2, 120-120	239.10	3.1	6.9	2.23
26H-3, 20-20	239.60	3.1	7.8	2.52
26H-3, 70-70	240.10	3.1	7.9	2.55
26H-3, 120-120	240.60	3.1	7.2	2.32
26H-4, 20-20	241.10	3.1	7.8	2.52
26H-4, 70-70	241.60	3.1	9.2	2.97
26H-4, 110-110	242.00	3.1	7.3	2.35
26H-5, 20-20	242.60	3.1	8.2	2.65
26H-5, 70-70	243.10	3.1	7.3	2.35
26H-5, 120-120	243.60	3.1	9.3	3.00
26H-6, 20-20	244.10	3.1	8.0	2.58
26H-6, 70-70	244.60	3.1	8.6	2.77
26H-6, 120-120	245.10	3.1	9.0	2.90
26H-7, 20-20	245.60	3.1	6.5	2.10
26H-7, 70-70	246.10	3.1	8.9	2.87
27H-1, 20-20	246.10	3.0	8.5	2.83
27H-1, 70-70	246.60	3.0	7.3	2.43
27H-1, 120-120	247.10	3.0	8.7	2.90
27H-2, 20-20	247.60	3.0	8.6	2.87
27H-2, 70-70	248.10	3.0	7.2	2.40
27H-2, 120-120	248.60	3.0	8.4	2.80
27H-3, 20-20	249.10	3.3	8.0	2.42
27H-3, 70-70	249.60	3.0	6.7	2.23
27H-3, 120-120	250.10	3.0	7.2	2.40
27H-4, 20-20	250.60	3.0	7.3	2.43
27H-4, 70-70	251.10	3.0	7.4	2.47
27H-4, 120-120	251.60	3.1	7.6	2.45
27H-5, 20-20	252.10	3.1	9.4	3.03
27H-5, 70-70	252.60	3.1	7.5	2.42
27H-5, 120-120	253.10	3.1	7.2	2.32

Table 9 (continued).

Core, section, interval (cm)	Depth (mbsf)	Seawater (ohms)	Sample (ohms)	Formation factor
27H-6, 20-20	253.60	3.1	8.9	2.87
27H-6, 70-70	254.10	3.1	6.7	2.16
27H-6, 120-120	254.60	3.1	7.1	2.29
28H-1, 20-20	255.60	3.1	6.9	2.23
28H-1, 70-70	256.10	3.1	7.0	2.26
28H-1, 120-120	256.60	3.1	8.2	2.65
28H-2, 20-20	257.10	3.1	8.2	2.65
28H-2, 70-70	257.60	3.1	8.5	2.74
28H-2, 120-120	258.10	3.1	8.2	2.65
28H-3, 20-20	258.60	3.1	9.2	2.97
28H-3, 70-70	259.10	3.1	8.3	2.68
28H-3, 120-120	259.60	3.1	8.1	2.61
28H-4, 20-20	260.10	3.1	8.6	2.77
28H-4, 70-70	260.60	3.1	8.8	2.84
28H-4, 120-120	261.10	3.1	8.3	2.68
28H-6, 20-20	263.10	3.1	8.2	2.65
28H-6, 70-70	263.60	3.1	8.8	2.84
28H-6, 120-120	264.10	3.1	8.8	2.84
29H-1, 20-20	265.10	3.0	9.0	3.00
29H-1, 70-70	265.60	3.0	9.1	3.03
29H-1, 120-120	266.10	3.0	8.6	2.87
29H-2, 20-20	266.60	3.0	7.9	2.63
29H-2, 70-70	267.10	3.0	8.3	2.77
29H-2, 120-120	267.60	3.0	7.4	2.47
29H-3, 20-20	268.10	3.0	7.3	2.43
29H-3, 70-70	268.60	3.0	8.0	2.67
29H-3, 120-120	269.10	3.0	9.0	3.00
29H-4, 20-20	269.60	3.0	8.4	2.80
29H-4, 70-70	270.10	3.0	8.9	2.97
29H-4, 120-120	270.60	3.0	8.1	2.70
29H-5, 20-20	271.10	3.0	8.4	2.80
29H-5, 70-70	271.60	3.0	8.6	2.87
29H-5, 120-120	272.10	3.0	8.2	2.73
29H-6, 20-20	272.60	3.1	9.1	2.94
29H-6, 70-70	273.10	3.1	8.8	2.84
29H-6, 120-120	273.60	3.1	8.6	2.77
30H-1, 20-20	274.60	3.1	8.3	2.68
30H-1, 70-70	275.10	3.1	7.4	2.39
30H-1, 120-120	275.60	3.1	8.3	2.68
30H-2, 20-20	276.10	3.1	9.8	3.16
30H-2, 70-70	276.60	3.1	9.6	3.10
30H-2, 120-120	277.10	3.1	9.4	3.03
30H-3, 20-20	277.60	3.1	10.0	3.23
30H-3, 70-70	278.10	3.1	8.8	2.84

Table 9 (continued).

Core, section, interval (cm)	Depth (mbsf)	Seawater (ohms)	Sample (ohms)	Formation factor
30H-3, 120-120	278.60	3.1	7.5	2.42
30H-4, 20-20	279.10	3.1	7.6	2.45
30H-4, 70-70	279.60	3.1	7.4	2.89
30H-4, 120-120	280.10	3.1	7.7	2.48
30H-5, 20-20	280.60	3.1	8.2	2.65
30H-5, 70-70	281.10	3.1	7.9	2.55
30H-5, 120-120	281.60	3.1	7.9	2.55
31H-1, 20-20	284.10	3.1	9.1	2.94
31H-1, 70-70	284.60	3.1	8.4	2.71
31H-1, 120-120	285.10	3.1	10.3	3.32
31H-2, 20-20	285.60	3.1	9.1	2.94
31H-2, 70-70	286.10	3.1	9.6	3.10
31H-2, 120-120	286.60	3.1	9.5	3.06
31H-3, 20-20	287.10	3.1	8.8	2.84
31H-3, 70-70	287.60	3.1	9.7	3.13
31H-3, 120-120	288.10	3.0	9.5	3.17
31H-4, 20-20	288.60	3.0	9.6	3.20
31H-4, 70-70	289.10	3.0	8.9	2.97
31H-4, 120-120	289.60	3.0	9.8	3.27
31H-5, 20-20	290.10	3.0	8.1	2.70
31H-5, 70-70	290.60	3.0	8.8	2.93
31H-5, 120-120	291.10	3.0	9.4	3.13
31H-6, 20-20	291.60	3.0	9.0	3.00
31H-6, 70-70	292.10	3.0	9.1	3.03
31H-6, 120-120	292.60	3.0	10.0	3.33
32H-1, 20-20	293.60	3.0	11.6	3.87
32H-1, 70-70	294.10	3.0	11.5	3.83
32H-1, 120-120	294.60	3.0	9.7	3.23
32H-2, 20-20	295.10	3.0	11.1	3.70
32H-2, 70-70	295.60	3.0	7.7	2.57
32H-2, 120-120	296.10	3.0	8.7	2.90
32H-3, 20-20	296.60	3.0	8.6	2.87
32H-3, 70-70	297.10	3.0	8.2	2.73
32H-3, 120-120	297.60	3.0	8.5	2.83
32H-4, 20-20	298.10	3.0	8.6	2.87
32H-4, 70-70	298.60	3.0	8.1	2.70
32H-4, 120-120	299.10	3.0	9.5	3.17
32H-5, 20-20	299.60	3.0	9.4	3.13
32H-5, 70-70	300.10	3.0	8.9	2.97
32H-5, 120-120	300.60	3.0	9.4	3.13
32H-6, 20-20	301.10	3.0	9.8	3.27
32H-6, 70-70	301.60	3.0	9.9	3.30
32H-6, 120-120	302.10	3.0	8.7	2.90

Table 10. Vane shear strength, Site 818.

Core, section, interval (cm)	Depth (mbsf)	Spring number	Torque (degrees)	Strain (degrees)	Shear strength (kPa)
133-818B-					
1H-1, 94-95	0.94	1	16	20	3.4
1H-2, 94-95	2.44	1	8	11	1.7
1H-3, 94-95	3.94	1	19	9	4.0
1H-4, 94-95	5.44	1	19	12	4.0
1H-5, 94-95	6.94	1	16	14	3.4
1H-6, 67-68	8.17	1	16	11	3.4
2H-2, 91-92	10.20	1	34	18	7.2
2H-3, 91-92	11.70	1	30	13	6.4
2H-4, 91-92	13.20	1	24	13	5.1
2H-5, 91-92	14.70	1	18	11	3.8
2H-6, 91-92	16.20	1	27	14	5.7
2H-7, 91-92	17.70	1	26	11	5.5
3H-1, 91-92	18.81	1	27	13	5.7
3H-2, 91-92	20.31	1	24	13	5.1
3H-3, 91-92	21.81	1	28	17	5.9
3H-4, 91-92	23.31	1	15	11	3.2
3H-5, 91-92	24.81	1	31	18	6.6
3H-6, 91-92	26.31	1	24	10	5.1
4H-1, 91-92	28.31	1	9	5	1.9
4H-2, 91-92	29.81	1	27	12	5.7
4H-3, 91-92	31.31	1	16	12	3.4
4H-4, 91-92	32.81	1	14	10	3.0
4H-5, 91-92	34.31	1	14	13	3.0
4H-6, 100-101	35.90	1	15	11	3.2
4H-7, 50-51	36.90	1	14	15	3.0
5H-1, 100-101	37.90	1	22	15	4.7
5H-2, 100-101	39.40	1	17	13	3.6
5H-3, 100-101	40.90	1	36	15	7.6
5H-4, 100-101	42.40	1	29	13	6.2
5H-5, 100-101	43.90	1	30	11	6.4
5H-6, 100-101	45.40	1	20	15	4.2
6H-1, 100-101	47.40	1	39	15	8.3
6H-2, 100-101	48.90	1	7	9	1.5
6H-3, 100-101	50.40	1	38	13	8.1
6H-4, 100-101	51.90	1	44	10	9.3
6H-5, 100-101	53.40	1	41	15	8.7
6H-6, 100-101	54.90	1	34	14	7.2
7H-1, 99-100	56.89	1	31	16	6.6
7H-2, 99-100	58.39	1	52	8	11.0
7H-3, 100-101	59.90	1	21	13	4.5
7H-5, 100-101	62.90	1	37	20	7.9
7H-6, 100-101	64.40	1	29	14	6.2
8H-1, 95-96	66.35	1	40	15	8.5
8H-2, 95-96	67.85	1	32	15	6.8
8H-3, 95-96	69.35	1	24	10	5.1
8H-4, 95-96	70.85	1	36	17	7.6
8H-5, 95-96	72.35	1	42	13	8.9
8H-6, 95-96	73.85	1	37	13	7.9
9H-1, 95-96	75.85	1	50	10	10.6
9H-2, 95-96	77.35	1	44	10	9.3
9H-3, 95-96	78.85	1	36	14	7.6
9H-4, 95-96	80.35	1	48	12	10.2
9H-5, 95-96	81.85	1	28	14	5.9
9H-6, 95-96	83.35	1	39	15	8.3
10H-1, 95-96	85.35	1	47	16	10.0

Table 10 (continued).

Core, section, interval (cm)	Depth (mbsf)	Spring number	Torque (degrees)	Strain (degrees)	Shear strength (kPa)
10H-2, 95-96	86.85	1	55	15	11.7
10H-3, 95-96	88.35	1	33	10	7.0
10H-4, 95-96	89.85	1	29	12	6.2
10H-5, 95-96	91.35	1	30	14	6.4
10H-6, 95-96	92.85	1	35	15	7.4
11H-1, 95-96	94.85	1	37	17	7.9
11H-2, 95-96	96.35	1	47	21	10.0
11H-3, 95-96	97.85	1	50	13	10.6
11H-4, 95-96	99.35	1	36	14	7.6
11H-5, 95-96	100.85	1	39	13	8.3
11H-6, 95-96	102.35	1	44	12	9.3
12H-1, 95-96	104.35	1	55	10	11.7
12H-2, 95-96	105.85	1	60	19	12.7
12H-3, 95-96	107.35	1	46	20	9.8
12H-4, 95-96	108.85	1	35	12	7.4
12H-5, 95-96	110.35	1	39	16	8.3
12H-6, 95-96	111.85	1	33	12	7.0
13H-1, 95-96	113.85	1	67	15	14.2
13H-2, 95-96	115.40	1	50	20	10.6
13H-3, 95-96	116.95	1	58	11	12.3
13H-4, 95-96	118.48	1	54	15	11.5
13H-5, 95-96	119.98	1	72	10	15.3
13H-6, 95-96	121.48	1	34	11	7.2
14H-1, 93-94	123.33	1	30	11	6.4
14H-2, 95-96	124.85	1	40	14	8.5
14H-3, 105-106	126.45	1	57	10	12.1
14H-4, 105-106	127.95	1	45	13	9.5
14H-5, 95-96	129.35	1	51	15	10.8
14H-6, 95-96	130.85	1	52	15	11.0
15H-1, 70-71	132.60	1	44	10	9.3
15H-2, 95-96	134.35	1	49	12	10.4
15H-3, 90-91	135.80	1	43	20	9.1
15H-4, 95-96	137.35	1	30	17	6.4
15H-5, 82-83	138.72	1	29	11	6.2
15H-6, 85-86	140.25	1	60	22	12.7
16H-1, 97-98	142.37	1	72	15	15.3
16H-2, 104-105	143.94	1	61	13	12.9
16H-3, 95-96	145.35	1	69	10	14.6
16H-4, 93-94	146.83	1	76	17	16.1
16H-5, 94-95	148.34	1	61	17	12.9
16H-6, 94-95	149.84	1	39	13	8.3
17H-1, 94-95	151.84	1	42	21	8.9
17H-2, 94-95	153.34	1	34	28	7.2
17H-3, 94-95	154.84	1	47	14	10.0
17H-5, 94-95	157.84	1	57	11	12.1
17H-6, 95-96	159.35	1	30	14	6.4
18H-1, 94-95	161.34	1	48	12	10.2
18H-3, 94-95	164.34	1	51	16	10.8
19H-1, 94-95	170.84	1	51	13	10.8
19H-2, 94-95	172.34	1	42	10	8.9
19H-3, 94-95	173.84	1	45	13	9.5
20H-1, 94-95	180.34	1	44	22	9.3
20H-2, 94-95	181.84	1	15	17	3.2
20H-3, 94-95	183.34	1	79	12	16.8
20H-4, 94-95	184.84	1	41	15	8.7
21H-1, 81-82	189.71	1	79	25	16.8

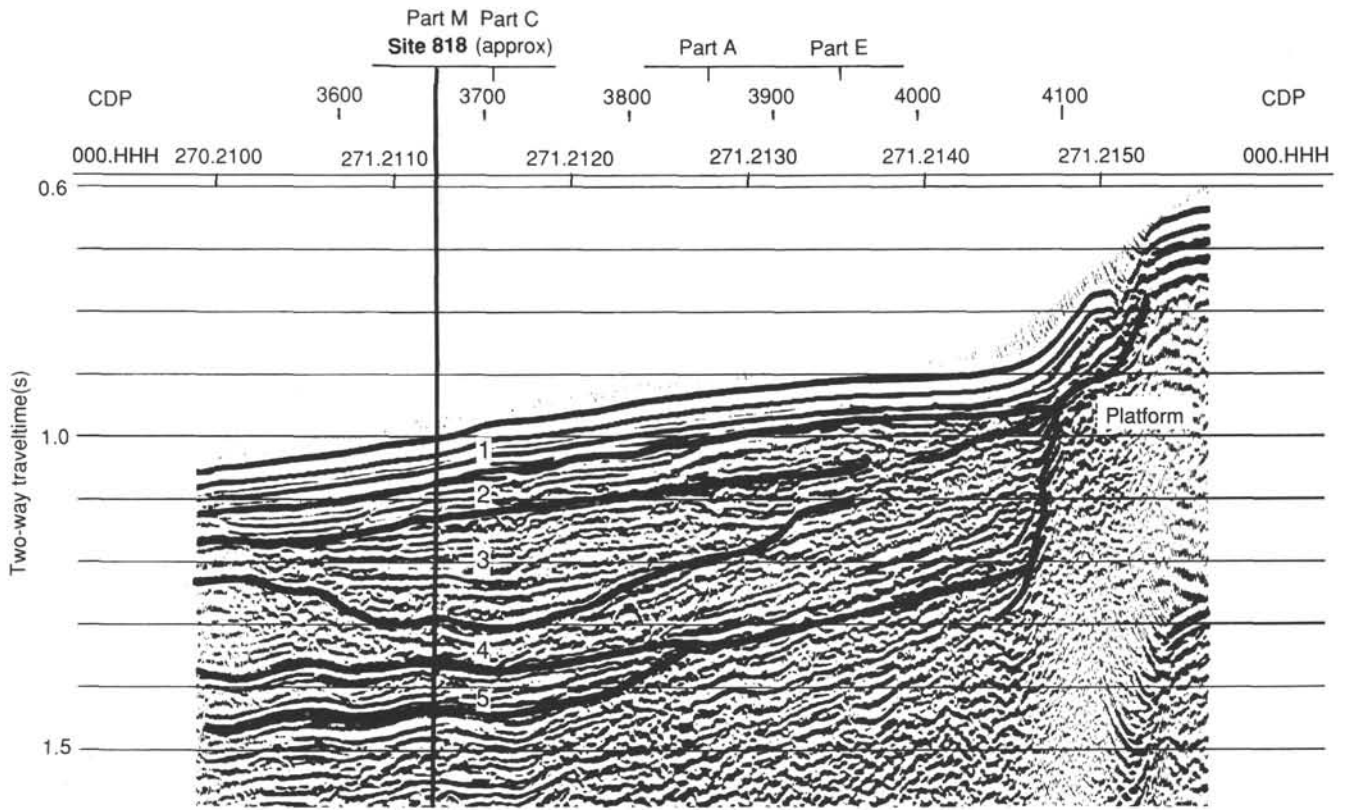


Figure 21. Part of seismic line 75/59 showing the seismic character of the sequences at Site 818 and their relationship to the carbonate platform that is represented by the nonreflecting zone at the right hand side of the section.

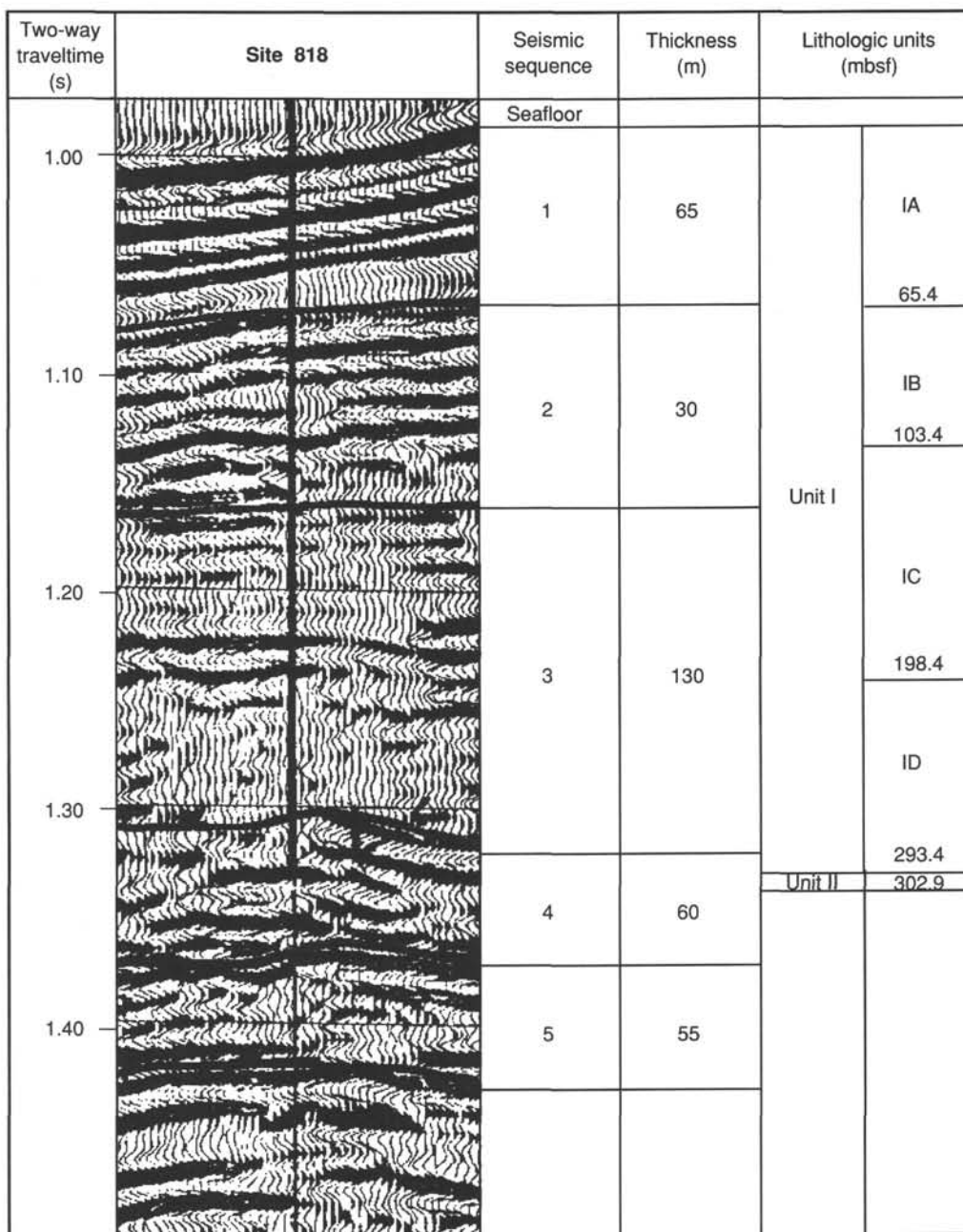


Figure 22. Correlation chart of seismic sequences (as in Fig. 21) with lithostratigraphy for Site 818.